A SERIES SOLUTION FOR SOME PERIODIC ORBITS IN THE RESTRICTED THREE-BODY PROBLEM ACCORDING TO THE PERTURBATION METHOD*

SU-SHU HUANG†

A series is obtained for those periodic orbits surrounding the more massive of the two finite bodies in the restricted three-body problem. The expansion is in terms of the mass of the less massive finite body. The initial conditions predicted by the series for several periodic orbits are compared with those obtained by purely numerical processes. They are in good agreement for the case corresponding to the earth-moon system. Also, a simple theory of nearly periodic orbits in the neighborhood of a periodic orbit is developed and numerically verified by examples. Finally, it is suggested that, if asteroids avoid places where their orbits would be commeasurable with the period of Jupiter, then artificial satellites and dust particles may avoid certain areas around the earth as a result of the presence of the moon.

INTRODUCTION

A periodic solution may be regarded as a solution of the differential equations of motion that satisfies, in addition to the initial conditions, the condition that after a lapse of one period, P, both coordinates and velocities return to their initial values. Thus, the problem of finding a periodic orbit in celestial mechanics resembles the problem of finding the eigen function for an eigen value in quantum mechanics, since the eigen value is determined by boundary conditions. Indeed, it is this basic concept that led to the derivation of a series solution for those periodic orbits in the restricted three-body problem that are revolving around the more massive of the two finite mass points. The recent papers by Szebehely give a detailed discussion of the restricted three-body problem (References 1 and 2).

The mathematical method used here follows the standard technique employed in classical mechanics under these circumstances. Indeed, it is very similar to the method Hill used in his lunar theory (References 3 and 4; also see Reference 5). Actually, the present analysis is somewhat parallel to the analysis that led Hill to his variation orbit, for both his and the present method depend upon some series expansions. However, in his lunar theory Hill expanded the solution in terms of the ratio of the mean motion of the sun to that of the moon in the rotating coordinate system. In this present theory for artificial satellites orbiting the earth in the earth-moon system the solution is expanded in terms of the mass of the moon. The mathematical simplicity in terms of the lunar mass is obvious; however, the result cannot be applied to the study of the motion of the moon because the moon is revolving around a relatively much less massive body (i.e., the earth) in the earth-sun system; consequently, it is senseless to expand the solution in terms of the solar mass.

EQUATIONS OF MOTION

The total mass of the two finite bodies is considered the unit of mass, and their separation the unit of length. The unit of time is such that the gravitational constant is unity. If we adopt the line joining the two finite mass points as the x-axis and the location of the greater of these masses as the origin, the equations of motion of the third,

*Published as *NASA Technical Note* D-2488, September 1964.

†*Goddard Space Flight Center* and Catholic University, Washington, D.C.

infinitesimal body in this rotating system of reference become:

$$\frac{d^2x}{dt^2} - 2\frac{dy}{dt} = x - \mu - (1-\mu)\frac{x}{(r_1')^3} - \mu\frac{x-1}{(r_2')^3}, \quad (1)$$

$$\frac{d^2y}{dt^2} + 2\frac{dx}{dt} = y - (1-\mu)\frac{y}{(r_1')^3} - \mu\frac{y}{(r_2')^3}, \quad (2)$$

where it is assumed that the mass $1-\mu$ is at the origin. Consequently the mass μ is at point (1, 0). Also, r_1' and r_2' are the distances of the third body from the $1-\mu$ and μ components, respectively. It is obvious that r_1' is also the distance of the third body from the origin; so

$$r_1' = r. \quad (3)$$

We are interested in the periodic orbits revolving around the $1-\mu$ component. Therefore, we make the transformations

$$x = r\cos\theta, \quad (4)$$

$$y = r\sin\theta. \quad (5)$$

This brings Equations 1 and 2 into the forms

$$\frac{d^2r}{dt^2} - r\left(\frac{d\theta}{dt}\right)^2 - 2r\frac{d\theta}{dt} = r - (1-\mu)\frac{1}{r^2} - \mu\frac{r}{(r_2')^3} + \mu\left[\frac{1}{(r_2')^3} - 1\right]\cos\theta, \quad (6)$$

$$r\frac{d^2\theta}{dt^2} + 2\frac{dr}{dt}\frac{d\theta}{dt} + 2\frac{dr}{dt} = -\mu\left[\frac{1}{(r_2')^3} - 1\right]\sin\theta. \quad (7)$$

EQUATIONS OF PERTURBATION

When μ equals zero all circles with their center at the origin are the periodic solutions of the problem. We can now argue that if μ is small, the periodic orbit deviates only slightly from a circular one. The deviation obviously depends upon μ. Therefore, the periodic solutions may be written as

$$r = r_0 + \mu r_1(t) + \mu^2 r_2(t) + \cdots, \quad (8)$$

$$\theta = \lambda t + \mu\theta_1(t) + \mu^2\theta_2(t) + \cdots, \quad (9)$$

where r_0 and λ are to be determined and are independent of time. Substituting Equations 8 and 9 into Equations 6 and 7 gives equations of different orders of approximation after a series of long but straightforward calculations.

The zeroth order (μ^0) approximation gives

$$(\lambda+1)^2 = \frac{1-\mu}{r_0^3}, \quad (10)$$

which is simply Kepler's third law in the problem of two bodies, the $1-\mu$ component and the third, infinitesimal body. The term is $\lambda+1$ instead of λ because the equations are expressed in the rotating coordinate system. Also, λ may have positive or negative values, corresponding respectively to the direct and retrograde motion of the third body.

The first order (μ^1) approximation yields

$$\frac{d^2r_1}{dt^2} - 2(\lambda+1)r_0\frac{d\theta_1}{dt} - 3(\lambda+1)^2 r_1 = \frac{1}{2}r_0 + \frac{3}{2}r_0\cos 2\lambda t + \frac{1}{8}r_0^2(9\cos\lambda t + 15\cos 3\lambda t), \quad (11)$$

$$r_0\frac{d^2\theta_1}{dt^2} + 2(\lambda+1)\frac{dr_1}{dt} = -\frac{3}{2}r_0\sin 2\lambda t - \frac{3}{8}r_0^2(\sin\lambda t + 5\sin 3\lambda t), \quad (12)$$

if the terms involving third and higher orders of r_0 are neglected.

With the same degree of approximation in regard to the series in r_0, the second order (μ^2)

equations are:

$$\frac{d^2 r_2}{dt^2} - 2(\lambda+1) r_0 \frac{d\theta_2}{dt} - 3(\lambda+1)^2 r_2 = r_0 \left(\frac{d\theta_1}{dt}\right)^2 + 2(\lambda+1) r_1 \frac{d\theta_1}{dt} - 3(\lambda+1)^2 \frac{r_1^2}{r_0}$$

$$+ \frac{1}{2} r_1 (1 + 3\cos 2\lambda t) + \frac{1}{4} r_0 r_1 (9\cos \lambda t + 15 \cos 3\lambda t)$$

$$- 3 r_0 \theta_1 \sin 2\lambda t - \frac{r_0^2 \theta_1}{8} (45 \sin 3\lambda t + 9 \sin \lambda t) , \qquad (13)$$

and

$$r_0 \frac{d^2 \theta_2}{dt^2} + 2(\lambda+1) \frac{dr_2}{dt}$$

$$= - 2 \frac{dr_1}{dt} \frac{d\theta_1}{dt} - r_1 \frac{d^2 \theta_1}{dt^2} - \frac{3}{2} r_1 \sin 2\lambda t - 3 r_0 \theta_1 \cos 2\lambda t$$

$$- \frac{1}{4} r_0 r_1 (3 \sin \lambda t + 15 \sin 3\lambda t) - \frac{1}{8} r_0^2 \theta_1 (3 \cos \lambda t + 45 \cos 3\lambda t) . \qquad (14)$$

In a similar way equations of higher orders can be derived in terms of the solutions of the equations of lower orders.

THE FIRST ORDER EQUATIONS

The solutions of Equations 11 and 12 can be easily found:

$$r_1 = - \frac{r_0}{6(\lambda+1)^2} + A_1' \cos(\lambda+1)t + A_2' \sin(\lambda+1)t - \frac{2B_1'}{3(\lambda+1)} + k_1 \cos \lambda t + k_2 \cos 2\lambda t + k_3 \cos 3\lambda t , \qquad (15)$$

$$r_0 \theta_1 = l_1 \sin \lambda t + l_2 \sin 2\lambda t + l_3 \sin 3\lambda t + B_1' t + B_2' - 2A_1' \sin(\lambda+1)t + 2A_2' \cos(\lambda+1)t . \qquad (16)$$

A_1', A_2', B_1', and B_2' are arbitrary constants which make Equations 15 and 16 the most general solution, k_n and l_n are defined by

$$k_1 = \frac{15+6}{8\lambda(2\lambda+1)} r_0^2 , \qquad (17)$$

$$k_2 = - \frac{3(2\lambda+1)}{2\lambda(3\lambda^2 - 2\lambda - 1)} r_0 , \qquad (18)$$

$$k_3 = - \frac{5(5\lambda+2)}{8\lambda(8\lambda^2 - 2\lambda - 1)} r_0^2 , \qquad (19)$$

$$l_1 = - \frac{3(10\lambda^2 + 12\lambda + 3)}{8\lambda^2(2\lambda+1)} r_0^2 , \qquad (20)$$

$$l_2 = \frac{3(11\lambda^2 + 10\lambda + 3)}{8\lambda^2(3\lambda^2 - 2\lambda - 1)} r_0 , \qquad (21)$$

$$l_3 = \frac{5(6\lambda^2 + 4\lambda + 1)}{8\lambda^2(8\lambda^2 - 2\lambda - 1)} r_0^2 . \qquad (22)$$

It should be observed that λ (or, equivalently, r_0), which appears in Equation 10, is not an integration constant in the perturbed case, although it is in the unperturbed case. Indeed, in the unperturbed case λ is the only integration constant that does not vanish under the assumed initial conditions. The integration constants in the perturbed case are A_1', A_2', B_1', and B_2'. In general, if higher orders of μ are considered, A_1, A_2, B_1, and B_2 are defined by

$$A_1 = A_1' \mu + A_1'' \mu^2 + \cdots , \quad \text{etc.},$$

because, as we shall see later, the complementary

functions in different orders of approximation are of the same form. Consequently, the integration constants in different orders of μ can be combined into four arbitrary constants A_1, A_2, B_1, and B_2 to agree with the expected number of four that occur in the solution of two second order differential equations (Equations 6 and 7).

The integration constants A_1, A_2, and B_2 are not particularly relevant, but it is important to note the dynamical meaning of B_1. If λ' is the mean angular velocity in the perturbed case, we have, from Equations 9 and 16,

$$\lambda' = \lambda + \frac{B_1' \mu}{r_0}$$

or in general

$$\lambda' = \lambda + \frac{B_1}{r_0} .$$

Therefore, $B_1'\mu/r_0$ (or B_1/r_0) is the change in the mean angular velocity from the unperturbed case to the perturbed case. Hence the four integration constants for the perturbed case may be taken as A_1, A_2, λ', and B_2 (or A_1', A_2', λ', and B_2' in the first approximation), and λ, or equivalently r_0, acts in the perturbed case as a standard for comparison with the perturbed orbits and is consequently a parameter.

We can set $\lambda' = \lambda$ for the sake of simplicity because both the perturbed and unperturbed periodic orbits form a continuous family. This leaves $B_1' = 0$.

Even with $B_1' = 0$, the general solution does not give the periodic orbits because there are two fundamental periods $2\pi/(\lambda+1)$ and $2\pi/\lambda$, with several harmonics of the latter. However, since the existence of some periodic solutions has been proved (see for example Reference 1), these periodic orbits must correspond to the particular integral obtained from Equations 15 and 16 by setting $A_1' = A_2' = B_1' = 0$. Then the solutions contain only terms with period $2\pi/\lambda$ of the fundamental oscillation, and shorter periods corresponding to its harmonics. Thus the periodic orbits around the $1-\mu$ component may be given, to the first order of μ and the second order of r_0, by

$$r = r_0 + \mu r_1 , \tag{23}$$

$$\theta = \lambda t + \mu \theta_1 , \tag{24}$$

where

$$r_1 = -\frac{r_0}{6(\lambda+1)^2} + k_1 \cos \lambda t + k_2 \cos 2\lambda t + k_3 \cos 3\lambda t , \tag{25}$$

$$r_0 \theta_1 = l_1 \sin \lambda t + l_2 \sin 2\lambda t + l_3 \sin 3\lambda t . \tag{26}$$

It follows from the solution given by Equations 15 and 16 that, in general, a periodic solution can be obtained for any given value of λ only by setting A_1, A_2, B_1, and B_2 equal to zero. Thus, one periodic orbit is associated with one value of the period. However, if λ is a ratio of two integers, periodic orbits may exist for arbitrary (small) values of these constants. If they do, a large number of periodic orbits would be found for some particular values of the period.

THE SECOND ORDER EQUATIONS

When the solutions of r_1 and $r_0\theta_1$ given by Equations 25 and 26 are substituted into the second order equations (13 and 14) and the resulting equations are simplified, we obtain:

$$\frac{d^2 r_2}{dt^2} - 2(\lambda+1) r_0 \frac{d\theta_2}{dt} - 3(\lambda+1)^2 r_2 = \beta_0 + \sum_{n=1} \beta_n \cos n\lambda t , \tag{27}$$

$$r_0 \frac{d^2 \theta_2}{dt^2} + 2(\lambda+1) \frac{dr_2}{dt} = \sum_{n=1} \rho_n \sin n\lambda t . \tag{28}$$

These equations have the same form as Equations 11 and 12, except for more terms on the right-hand side. Therefore, the solution can be derived in the same manner as in the case of the first order equations, although finding the explicit expressions of the solutions is much more tedious because of the lengthy equations that define β_n and ρ_n. The author has evaluated only β_0. From this the average radius of the periodic orbit may be derived:

$$\langle r \rangle = r_0 \left\{ 1 - \frac{\mu}{6(\lambda+1)^2} + \mu^2 \left[\frac{1}{18(\lambda+1)^4} + \frac{3(19\lambda^2+14\lambda+3)}{32\lambda^2(\lambda+1)^2(3\lambda^2-2\lambda-1)} + \frac{9(2\lambda+1)^2}{8\lambda^2(3\lambda^2-2\lambda-1)^2} \right] \right\}, \quad (29)$$

correct to the second order both in μ and r_0.

It follows from Equation 29 that for a given value of λ the average radius of the periodic orbit around the earth in the presence of the moon is slightly less than that given by Equation 10, which is for the case of the absence of the moon. This fact may be easily understood because the overall long-range effect of the moon on a satellite that is revolving around the earth is to reduce the central attractive force of the earth on the satellite. The argument becomes physically apparent if we imagine the moon and its orbit to be replaced by an annular ring of the same mass as the moon, with this mass uniformly distributed. From this reasoning the presence of the sun may be expected to further reduce, by a small amount, the average value of the radius of the satellite's orbit. The prediction has been verified by actual calculations.

The similarity between the present calculation and the perturbation theory in quantum mechanics is apparent. In neither case is the convergence of the series solution proven. But, it will be shown in the following sections that the periodic orbits derived in this way agree perfectly with those obtained by the trial and error method, just as the effectiveness of the perturbation method in quantum mechanics is based on its ability to predict empirical results.

On the other hand, the present perturbation method differs in many ways from that in quantum mechanics. For example, the main purpose of the perturbation theory in quantum mechanics is to find the new eigen value as a result of perturbation, whereas here we are interested in the variation in the orbital nature for a given value of λ.

Although the approach parallels Hill's determination of the variation orbit, differences do exist. In the first place, Hill started with a set of differential equations already approximated by the neglecting of terms involving the ratio of the mean distance of the moon to that of the sun. The present investigation uses the equations in the restricted three-body problem. Secondly, Hill was concerned only in obtaining a particular solution but we are interested in the general solution that involves four aribtrary constants, A_1, A_2, B_1, and B_2, which determine, as shall be seen later, those nearly periodic orbits in the neighborhood of the exact periodic solution. Consequently, the present solution gives an entire family of orbits in the neighborhood of any periodic solution that we can determine. Needless to say, for orbits that depart greatly from the periodic one, the approximation employed in this analysis breaks down. Consequently, those orbits can no longer be represented by the equations derived.

The differences between Hill's analysis and the present one clearly reflect divergent problems faced in different times. Indeed, the present solution of periodic and nearly periodic orbits around a more massive component, expanded in terms of the mass of the less massive component, would have had little practical significance in Hill's time.

NUMERICAL APPLICATIONS

In a previous paper (Reference 6), by a numerical method (Reference 7) a synchronous orbit around the earth was derived, under the idealization of the restricted three-body problem with $\mu = 0.012149$. Now we are able to derive it from Equations 23–26.

In the XY coordinate system with the origin at the mass point $1-\mu$, the initial conditions of

the synchronous orbit, derived by successive approximations, are

$$\left.\begin{aligned} x_0 &= 0.1095908\upsilon\ , \\ y_0 &= 0\ , \\ \dot{x}_0 &= 0\ , \\ \dot{y}_0 &= 2.8927303\ , \end{aligned}\right\} \qquad (30)$$

which yield

$$P=0.23802754 \qquad (31)$$

for the period.

We can now calculate for this case the values of k_n and l_n from Equations 17–22, with

$$\lambda=\frac{2\pi}{P}=26.396884, \qquad (32)$$

which gives $r_0=0.10958800$ from Equation 10.

Table 1

Values of k_n and l_n for $\mu = 0.012149$ and $\lambda = 26.396884$.

n	k_n	l_n
1	4.249394×10^{-4}	8.756117×10^{-4}
2	-1.644862×10^{-4}	2.296898×10^{-4}
3	-6.901187×10^{-6}	8.365787×10^{-6}

The computed values are listed in Table 1. Substituting these values of k_n and l_n in the solution given by Equations 23–26 and transforming variables from r and θ to x and y, in accordance with Equations 4 and 5, shows that the values $x(t)$,$y(t)$,$\dot{x}(t)$, and $\dot{y}(t)$ derived from the present formulas agree to seven significant figures with those obtained from direct integration under the initial conditions given by Equations 30. In particular, at $t=0$ our formulas predict the initial conditions

$$\left.\begin{aligned} x_0 &= 0.10959080\ , \\ y_0 &= 0\ , \\ \dot{x}_0 &= 0\ , \\ \dot{y}_0 &= 2.8927300\ , \end{aligned}\right\} \qquad (33)$$

for the periodic orbit with P given by Equation 31. The agreement between Equations 30 and 33 must be regarded as satisfactory.

As would be expected, the prediction of periodic orbits by Equations 23 and 24 becomes less and less accurate as the period increases. A few cases are given in Table 2 to show the progressive worsening of the prediction. However, it should be noted that even at $P=1.6$, the two sets of calculations—one from the numerical approach and the other from the present formulas—still give results that agree to the fourth significant figure.

ORBITS IN THE NEIGHBORHOODS OF THE PERIODIC ONES

It is obvious that for orbits which are not exactly periodic, the general solution given by

Table 2

Initial Conditions Derived by the Series Solution Compared with those Obtained by the Method of Successive Approximation ($\mu = 0.012149$, $y_0 = \dot{x}_0 = 0$).

P	Series Solution		Successive Approximation		
	x_0	$\dot{y}_0$	x_0	$\dot{y}_0$	Jacobian Constant
0.23802754	0.10959080	2.8927300	0.10959080	2.8927303	9.6968861
0.39999890	0.15239388	2.3936373	0.15239410	2.3936354	7.2832706
0.59999666	0.19580805	2.0503747	0.19580870	2.0503734	5.9498741
0.79999290	0.23271671	1.8277779	0.23271790	1.8277824	5.2292161
0.99999026	0.26506832	1.6657674	0.26506980	1.6657871	4.7756998
1.1999940	0.29394940	1.5398118	0.29395020	1.5398618	4.4638648
1.4000154	0.32005211	1.4376335	0.32005020	1.4377350	4.2365564
1.6000716	0.34385494	1.3522620	0.34384680	1.3524439	4.0638285

Equations 23 and 24 together with Equations 15 and 16 should be applied instead of the particular integral given by Equations 23–26. Let us now consider the behavior of these orbits when we make the initial values of x_0 and $\dot{y}_0$ only slightly different from those corresponding to the periodic orbit, while maintaining $y_0 = x_0 = 0$.

The initial values of r, θ, $\dot{r}$, $\dot{\theta}$ will be denoted by r_i, θ_i, $\dot{r}_i$, $\dot{\theta}_i$. Thus, by setting $t=0$ in Equations 15 and 23

$$r_i = r_0 + \mu\left[-\frac{r_0}{6(\lambda+1)^2} - \frac{2B_1}{3(\lambda+1)} + k_1 + k_2 + k_3 + A_1\right]. \tag{34}$$

By assuming $\theta_i = 0$ as usual

$$B_2 = -2A_2 \tag{35}$$

from Equations 16 and 24. We have assumed $\dot{x}_0 = 0$ which is equivalent to $\dot{r}_i = 0$; hence

$$A_2 = B_2 = 0. \tag{36}$$

Finally, it is easy to obtain

$$\theta_i = \lambda + \frac{\mu}{r_0}\left[l_1\lambda + 2l_2\lambda + 3l_3\lambda - 2A_1(\lambda+1) + B_1\right]. \tag{37}$$

The initial values of r and $\dot{\theta}$ for the true periodic orbit will be denoted by $r_{i,p}$ and $\dot{\theta}_{i,p}$. They are given by

$$r_{i,p} = r_0 + \mu\left[-\frac{r_0}{6(\lambda+1)^2} + k_1 + k_2 + k_3\right]. \tag{38}$$

$$\dot{\theta}_{i,p} = \lambda + \frac{\mu\lambda}{r_0}\left(l_1 + 2l_2 + 3l_3\right). \tag{39}$$

From

$$\Delta r_i = r_i - r_{i,p}. \tag{40}$$

$$\Delta\dot{\theta}_i = \dot{\theta}_i - \dot{\theta}_{i,p}, \tag{41}$$

we derive

$$A_1 = -\frac{\Delta r_i}{\mu} - \frac{2r_0\Delta\dot{\theta}_i}{(\lambda+1)\mu}, \tag{42}$$

$$B_1 = -6(\lambda+1)\frac{\Delta r_i}{\mu} - \frac{3r_0\Delta\dot{\theta}_i}{\mu}. \tag{43}$$

We can now examine the behavior of orbits close to the periodic ones. The explicit expression for θ is, from Equations 16 and 24,

$$\vartheta = \left(\lambda + \frac{\mu}{r_0}B_1\right)t + \frac{\mu}{r_0}\left[\sum_{i=1}^{3} l_i \sin i\lambda t - 2A_1 \sin(\lambda+1)t\right]. \tag{44}$$

Let us define time as $t=t_n$ when $\theta = 2\pi n$, and $t=t_{n-1}$ when $\theta = 2\pi(n-1)$, where n is an integer. Therefore P_n, defined by,

$$P_n = t_n - t_{n-1}. \tag{45}$$

is the period of the n^{th} cycle of a nearly periodic orbit. It follows from Equation 44 that

$$P_n = \frac{2\pi r_0}{\lambda r_0 + \mu B_1} - \frac{\mu}{\lambda r_0 + \mu B_1}\left[\sum_{i=1}^{3} 2l_i \sin\frac{i\lambda P_n}{2}\cos\frac{i\lambda\left(t_n + t_{n-1}\right)}{2} - 4A_1 \sin\frac{(\lambda+1)P_n}{2}\cos\frac{(\lambda+1)\left(t_n + t_{n-1}\right)}{2}\right]. \tag{46}$$

from which we note immediately that the mean period of the nearly periodic orbit is

$$\langle P_n\rangle = \frac{2\pi r_0}{\lambda r_0 + \mu B_1}. \tag{47}$$

So the first term on the right-hand side of Equation 46 is associated with the mean period, but the rest denotes small oscillations of the P_n value around its mean value for various values of n.

Since the amplitudes of various oscillating terms in Equation 46 are small, λP_n may be set equal to 2π in the argument of the sine function. All terms involving l_i vanish as a result of this approximation and Equation 46 can be reduced to:

$$P_n = \langle P_n \rangle + \frac{4\mu A_1}{\lambda r_0 + \mu B_1} \sin\frac{\pi}{\lambda} \cos\left[(\lambda+1)\, t_n - \frac{\pi}{\lambda}\right]. \tag{48}$$

where A_1 and B_1 are given by Equations 42 and 43, respectively, and t_n may be considered to be

$$t_n = n\langle P_n \rangle. \tag{49}$$

Since there is a periodic orbit for each value of λ in the range of interest, we can compare a nearly periodic orbit with any periodic orbit in the former's neighborhood. In our calculation we have fixed a single value of λ for both the periodic and nearly periodic orbit in order to derive A_1 and B_1 from Equations 42 and 43. Obviously a slightly different choice of the value of λ will give different values to these two constants for the same nearly periodic orbit.

As a simple example the two orbits may be compared by starting with the same r_i, i.e., $\Delta r_i = 0$. Then A_1 and B_1 are functions of $\Delta\theta_i$ alone and $\Delta\theta_i$ is related to the difference Δy_0, between the initial value, y_0, of the nearly periodic orbit and that of the exactly periodic orbit. If, furthermore,

$$n \ll \frac{\lambda}{20\Delta\dot{\theta}_i}, \tag{50}$$

Equation 48 reduces to

$$P_n = \frac{2\pi}{\lambda - 3\Delta\dot{\theta}_i} - \frac{8\Delta\dot{\theta}_i}{\lambda(\lambda+1)} \sin\frac{\pi}{\lambda} \cos\frac{(2n-1)\pi}{\lambda}. \tag{51}$$

From Equation 51 values of P_n have been computed up to $n = 28$ for two cases, with λ given by Equation 32. The results are given in the second and fourth columns of Table 3. In both cases $\lambda/\Delta\theta_i$ is of the order of several thousand. Therefore, the use of Equation 51 is justified. For comparison P_n has also been computed by direct integration. This was done by computing successive times, t_n, when the orbit crossed the positive axis. A four point interpolation has been used for obtaining t_n from the integrated tables. In this way, from the initial conditions corresponding respectively to two values of y_0 in Table 3, t_n, and consequently P_n, have been computed and the latter has been tabulated in the third and fifth columns of Table 3. The agreement between the second and third columns as well as that between the fourth and fifth columns may be regarded as satisfactory.

Table 3

Time Intervals for Successive Cycles of Nearly Periodic Orbits ($\mu = 0.012149$, $\lambda = 26.396884$).*

n	Time for $\dot{y}_0 = 2.8920000$		Time for $\dot{y}_0 = 2.8930000$	
	Equation 51*	Direct Integration	Equation 51*	Direct Integration
1	0.2378562	0.2378561	0.2380910	0.2380909
2	0.2378557	0.2378556	0.2380912	0.2380911
3	0.2378547	0.2378546	0.2380915	0.2380915
4	0.2378534	0.2378533	0.2380920	0.2380920
5	0.2378517	0.2378516	0.2380927	0.2380926
6	0.2378497	0.2378497	0.2380934	0.2380933
7	0.2378477	0.2378476	0.2380941	0.2380941
8	0.2378456	0.2378456	0.2380949	0.2380948
9	0.2378437	0.2378435	0.2380956	0.2380956
10	0.2378419	0.2378420	0.2380963	0.2380962
11	0.2378405	0.2378404	0.2380968	0.2380967
12	0.2378394	0.2378394	0.2380972	0.2380971
13	0.2378389	0.2378388	0.2380974	0.2380973
14	0.2378388	0.2378388	0.2380974	0.2380974
15	0.2378392	0.2378391	0.2380973	0.2380973
16	0.2378400	0.2378399	0.2380970	0.2380968
17	0.2378413	0.2378411	0.2380965	0.2380965
18	0.2378429	0.2378428	0.2380959	0.2380958
19	0.2378448	0.2378447	0.2380952	0.2380951
20	0.2378469	0.2378467	0.2380944	0.2380944
21	0.2378489	0.2378488	0.2380937	0.2380937
22	0.2378509	0.2378506	0.2380929	0.2380928
23	0.2378527	0.2378528	0.2380923	0.2380923
24	0.2378542	0.2378540	0.2380917	0.2380916
25	0.2378554	0.2378553	0.2380913	0.2380912
26	0.2378560	0.2378558	0.2380910	0.2380908
27	0.2378562	0.2378562	0.2380910	0.2380911
28	0.2378559	0.2378559	0.2380911	0.2380910

* In computing $\Delta\dot{\theta}_i$ the initial condition given by Equation 33 is considered to correspond to the exact periodic orbit used as the reference for comparison.

SOME REMARKS ON RELATED PROBLEMS

Although the present calculation was performed in order to understand the general effect of the

moon on the motion of the earth's satellites, it will serve equally well in understanding the general behavior of the motion of inner planets and asteroids as a result of the perturbation by the major planets, especially Jupiter. Indeed, the smallness of μ in such cases ($\mu = 9.539 \times 10^{-4}$ for the sun-Jupiter system) will make the result derived with the first order equations a good approximation to the problem. However, because of the relatively large sizes of the orbits of the inner planets, it may be necessary to include in the solution terms involving the third and perhaps higher powers of r_0.

The coefficients k_n and l_n contain in their denominators a factor $(n\lambda)^2-(\lambda+1)^2$ where n is an integer. Thus if

$$n\lambda = \lambda + 1$$

the coefficients k_n and l_n diverge. Therefore, periodic orbits cannot be obtained in this way.

However, the Kirkwood gaps in the asteroid belt concide with positions where asteroids, if present, would have periods commeasurable with the period of Jupiter's orbit. Recently, this problem was investigated theoretically by Brouwer (Reference 8).

The presence of the Kirkwood gaps are obviously due to the perturbation by Jupiter. Since perturbation increases with μ, it follows that stronger gaps would be present in systems of two revolving bodies of increasing values of μ. Hence, we may immediately predict stronger gaps around the earth in the earth-moon system than those around the sun in the asteroid belt in the sun-Jupiter system. Such gaps around the earth can be computed easily from the condition of commeasurability of the moon's period and the period of any satellite in such a zone. Of course, a result of this argument is that these zones should be avoided in launching satellites that are intended to stay in orbit for a long time. Being short, the period of the synchronous orbit is not near any strongly commeasurable gap.

Another interesting consequence of the commeasurable gaps around the earth may be found in the distribution of dust particles in the earth-moon system. It is not now known whether dust particles all move at random or partially revolve around the earth. If the latter should be the case, the presence of zones around the earth void of dust particles like the Kirkwood gaps in the asteroid belt around the sun, would be inevitable. Consequently, their detection may be an interesting subject of investigation in the field of space research.

ACKNOWLEDGMENTS

It is the author's pleasure to express his sincere thanks to Dr. D. Brouwer, Dr. G. Hori, Dr. V. Szebehely, and Dr. T. Y. Wu for their valuable discussions.

REFERENCES

1. Szebehely, V. G., "The Restricted Problem of Three Bodies," paper given at the Summer Institute in Dynamical Astronomy, Yale Univ., 1961.
2. Szebehely, V. G., "Zero Velocity Curves and Orbits in the Restricted Problem of Three Bodies," *Astronom. J.* 68(3):147–151, April 1963.
3. Hill, G. W., "Researches in the Lunar Theory, Chapter II," *Amer. J. Math.* 1:5,129–147, and 245–260, 1878.
4. Hill, G. W., "On the Part of the Motion of the Lunar Perigee Which is a Function of the Mean Motions of the Sun and Moon," *Acta Math.* 8:1–36, 1886.
5. Brouwer, D., and Clemence, G. M., "Methods of Celestial Mechanics," New York: Academic Press, 1961, Chapter 12.
6. Huang, S.-S., "The Hypothetical Four-Body Problem," *Astronom. J.* to be published, 1964.
7. Huang, S.-S., and Wade, C., Jr., "Preliminary Study of Periodic Orbits of Interest for Moon Probes. II," *Astronom. J.* 68(6):388–391, August 1963.
8. Brouwer, D., "The Problem of the Kirkwood Gaps in the Asteroid Belt," *Astronom. J.* 68(3):152–159, April 1963.

ON THE APPLICATION OF PFAFF'S METHOD IN THE THEORY OF VARIATION OF ASTRONOMICAL CONSTANTS*

PETER MUSEN

Cartan's integral invariant is taken as a foundation of the theory of variation of astronomical parameters. The differential equations for the general perturbations are obtained as the first system of Pfaffian equations associated with the linear differential form appearing in the intergral invariant.

The equations for general perturbations of the Gibbsian unit vectors, of the Gibbsian rotation vector and of Euler's parameters are derived. The utilization of the Gibbsian rotation vector represents an extension of Strömgren's and of the author's ideas on special perturbations to the problems of general perturbations. Euler's parameters find their application in Hansen's lunar theory.

The case of redundant elements is treated by introducing constraints and Lagrangian multipliers. Cartan's integral invariant expressed in terms of vectorial kinematic elements represents a powerful tool in the search for new sets of elements and it leads to differential equations having a compact form, which is convenient for the programming and use of electronic machines.

NOTATIONS

m_i = the mass of the i-th point in the system of points
$\mathbf{r}_i$ = the position vector of the i-th point
$\mathbf{v}_i$ = the velocity of the i-th point in the system of points
T = the kinetic energy
U = the force function
F = U − T
Ω = the disturbing function
$[\Omega]$ = the disturbing function averaged over the orbit of the disturbed body
$\text{grad}_{\mathbf{s}}\ \phi$—the gradient of ϕ with respect $\mathbf{s}$; $\text{grad}_i\ \phi$—the gradient of ϕ with respect to $\mathbf{s}_i$
k = the Gaussian constant
M = the mass of the sun
m = the mass of the disturbed body
$\mu = k^2(M+m)$
$\mathbf{r}$ = the position vector of the disturbed body
$r = |\mathbf{r}|$
$\mathbf{v}$ = the heliocentric velocity of the disturbed body
$\ell, \omega, i, \Omega, e, a, n$ = the standard elliptic elements of the disturbed body
u = the eccentric anomaly of the disturbed body
$\mathbf{c} = \mathbf{r} \times \mathbf{v}$ = the vector of the angular momentum
$\mathbf{P}, \mathbf{Q}, \mathbf{R}$ = the Gibbsian vectorial elements of the disturbed body
$\mathbf{e} = \mu e \mathbf{P}$ = the Laplacian vector

*Published as *NASA Technical Note* D-2301, April 1964

$\mathbf{g}$ = the Gibbsian rotation vector
$\ell', \omega', \Omega', \cdots, \mathbf{P}', \mathbf{Q}', \mathbf{R}', \cdots$
$\ell'', \omega'', \Omega'', \cdots, \mathbf{P}'', \mathbf{Q}'', \mathbf{R}'', \cdots$
the elements of disturbing bodies
$\mathbf{r}'^0$ = the unit vector in the direction from the sun to the disturbing body
$p = a(1-e^2)$

INTRODUCTION

In treating the problem of general perturbations of planets and satellites it is felt that a general and flexible method is needed which would permit an easy transformation from one system to another and would also facilitate a proper choice of elements under the different circumstances.

The standard way to develop the equations for the general perturbations in elements is based on the computation of the matrix either of Lagrangian or of Poissonian brackets. This computation is relatively simple for the classical elliptic elements, but it can become cumbersome if some algebraic combinations of the classical elements are taken as a new set of elements.

An additional difficulty may arise if, for the sake of the symmetry of the development of the disturbing function, some redundant elements are introduced. As a result, additional constraints appear in the problem. It is necessary to point out, that the presence of these constraints does not necessarily mean that the problem of the determination of the constants of integration will become more complicated. Sometimes the presence of constraints makes this determination easier. Hill's method of general perturbations is a well known example in celestial mechanics where a redundant constant of integration is present.

However, the difficulties associated with the presence of a redundant constant in this particular case should not be generalized to all problems in celestial mechanics. One should not be hesitant to make use of redundant elements if the problem of the determination of constants of integration for all orders of perturbations can be made symmetrical and if the programming can be made more efficient.

In order to have a more general view and to facilitate the search for new types of elements, an application of Pfaff's method is made in this article to the problems of celestial mechanics. This method permits the formation of the equations for the variation of elements in a straightforward manner if these elements are obtained from the classical elements by any type of functional transformation.

Surprisingly, such a direct method has not found wider applications in the theory of variation of astronomical constants. The pioneering work of Bilimovich (Reference 1) stands rather apart from the main stream. Bilimovich succeeded in deducing Milankovich's equations (Reference 2) for the variation of the Laplacian and momentum vectors in a rather simple way. He also deduced the classical equations for the variation of the elliptic elements in a very simple manner.

The existence of Cartan's (Reference 3) integral invariant for dynamical systems is the foundation of the Pfaffian method. Using a hydrodynamical analogy we can say that the theorem of the circulation for an ideal fluid in the phase space is taken as a basis for the theory of perturbations presented herein. The equations for the variation of the elements represent the first system of Pfaffian equations associated with the differential form appearing under the integral sign in the expression for circulation.

In this work we suggest the use of a slightly more general form of Pfaffian equations than in Bilimovich's work by permitting the constraints to be present and by forming the equations with Lagrangian multipliers.

We shall develop the equations for the general perturbations of Gibbsian vectors $\mathbf{P}$ and $\mathbf{Q}$ and also of the elements the author has suggested in his article on Strömgren's (Reference 4) perturbations (Reference 5) and in the articles on Hansen's (Reference 6) lunar theory (References 7 and 16).

In recent times electronic equipment is being used more and more for the purpose of developing general perturbations. We might expect that in the near future the utilization of machines in this domain will become even wider. This fact will have an increasingly greater impact on the theoretical thought and thus the search for different types of new elements is in order now.

PFAFFIAN EQUATIONS OF MOTION WITH REDUNDANT COORDINATES

Let us consider the material system of N points having the position vectors $\mathbf{r}_i$ and the velocity vectors $\mathbf{v}_i$ $(i=1, 2, \cdots, N)$. The Pfaffian linear form associated with this system is

$$\phi = \sum_{i=1}^{N} m_i \mathbf{v}_i \cdot d\mathbf{r}_i - (T - U)\, dt \,. \quad (1)$$

A functional transformation,

$$\mathbf{v}_i = \mathbf{v}_i(\mathbf{x}_1, \mathbf{x}_2, \cdots, \mathbf{x}_n; q_1, q_2, \cdots, q_m) \,,$$

$$\mathbf{r}_i = \mathbf{r}_i(\mathbf{x}_1, \mathbf{x}_2, \cdots, \mathbf{x}_n; q_1, q_2, \cdots, q_m) \,,$$

with the imposed conditions

$$f_p(\mathbf{x}_1, \mathbf{x}_2, \cdots, \mathbf{x}_n; q_1, q_2, \cdots, q_m) = a_p$$

brings Equation 1 to the form

$$\phi \quad \sum_{i=1}^{n} \mathbf{X}_i(\mathbf{x}_1, \mathbf{x}_2, \cdots, \mathbf{x}_n; q_1, q_2, \cdots, q_m) \cdot d\mathbf{x}_i$$

$$+ \sum_{j=1}^{m} Q_j(\mathbf{x}_1, \mathbf{x}_2, \cdots, \mathbf{x}_n; q_1, q_2, \cdots, q_m) dq_j + F dt \,, \quad (2)$$

where $\mathbf{x}_1, \mathbf{x}_2, \cdots, \mathbf{x}_n$ are vectors in k-dimensional Euclidean space and $q_1, q_2, \cdots, q_m$ are scalars.

The condition

$$kn + m - s = 6N$$

must be satisfied. In the process of transformation from Equation 1 to Equation 2 any additive total differential can be neglected

For present purposes we can assume that all constraints are scleronomic. We write the first system of Pfaffian equations, using the notations suggested by Bilimovich, in the form:

$$\sum_{i=1}^{n} (\mathrm{grad}_i \phi - d\mathbf{X}_i) \cdot \delta\mathbf{x}_i + \sum_{j=1}^{m} \left(\frac{\partial \phi}{\partial q_j} - dQ_j\right) \delta q_j + \left(\frac{\partial \phi}{\partial t} - dF\right) \delta t = 0$$

with the additional conditions

$$\sum_{i=1}^{n} \mathrm{grad}_i f_p \cdot \delta\mathbf{x}_i + \sum_{j=1}^{m} \frac{\partial f_p}{\partial q_j} \delta q_j = 0 \quad (i = 1, 2, \cdots, n;\ j = 1, 2, \cdots, m;\ p = 1, 2, \cdots s)$$

imposed on the variations by the constraints. Introducing Lagrangian multipliers, we have

$$\mathrm{grad}_i \phi - d\mathbf{X}_i + \sum_{p=1}^{s} \lambda_p\, dt\, \mathrm{grad}_i f_p = 0 \quad (3)$$

$$\frac{\partial \phi}{\partial q_j} - dQ_j + \sum_{p=1}^{s} \lambda_p\, dt\, \frac{\partial f_p}{\partial q_j} = 0 \,, \quad (4)$$

$$\frac{\partial F}{\partial t} dt - dF = 0 \,. \quad (5)$$

The Lagrangian multipliers $\lambda_p (p=1, 2, \cdots, s)$ can be determined with the help of the equations

$$\sum_{i=1}^{n} \mathrm{grad}_i f_p \cdot d\mathbf{x}_i + \sum_{j=1}^{m} \frac{\partial f_p}{\partial q_j} dq_j = 0, \ (p = 1, 2, \cdots, s). \quad (6)$$

The existence of a Cartan integral invariant on the hypersurface

$$f_p = a_p \quad (p = 1, 2, \cdots, s)$$

defined in (kn+m) -dimensional space serves as a basis for deducing the Pfaffian equations.

Sometimes, for the sake of the symmetry, it might be advantageous to increase beyond six the number of the osculating elements. This is done, for example, by Milankovich (Reference 2), by Herrick (Reference 8) and by the author (Reference 9). Then the relations containing the redundant elements can be understood as the scleronomic constraints and Equations 3–6 can be applied.

PFAFFIAN EXPRESSION FOR PLANETARY MOTION

In this article we deduce Bilimovich's expression for ϕ for disturbed planetary motion using the Eckert-Brouwer (Reference 10) expression for the variation of the position vector of a planet.

Originally the Eckert-Brouwer formula was designed for the purpose of orbit correction. However, experience has shown that this elegant formula can also be used in the vectorial theory of general perturbations as in the present article and in the article published recently by Musen and Carpenter (Reference 11).

We also suggest herein some new sets of elements, canonical and uncanonical, which follow directly from the form of ϕ.

The differential form (Equation 1) in the case of disturbed planetary motion is

$$\phi = v \cdot dr - \left(\frac{v^2}{2} - \frac{\mu}{r} - \Omega\right) dt \ .$$

Making use of the expression for dr as obtained by Eckert and Brouwer,

$$dr = d\psi \times r + \frac{v}{n} dl + \frac{r}{a} da + \left(\frac{r + p - 2a}{ep} r + \frac{r + p}{ep} \cdot \frac{r \cdot v}{a^2 n^2} v\right) de \ ,$$

we deduce

$$v \cdot dr = r \times v \cdot d\psi + \frac{v^2}{n} dl + r \cdot v \frac{da}{a} + \frac{r \cdot v}{ep}\left[(r + p)\left(1 + \frac{v^2}{a^2 n^2}\right) - 2a\right] de \ . \qquad (7)$$

Substituting

$$\begin{aligned} r \cdot v &= \sqrt{\mu a}\, e \sin u \ , \\ r \times v &= R\sqrt{\mu a\left(1 - e^2\right)} \ , \end{aligned} \qquad (8)$$

$$\begin{aligned} v^2 &= \mu\left(\frac{2}{r} - \frac{1}{a}\right) \ , \\ n &= \frac{\sqrt{\mu}}{a^{3/2}} \ , \end{aligned} \qquad (9)$$

into Equation 7 we obtain

$$v \cdot dr = \frac{\mu}{n}\left(\frac{2}{r} - \frac{1}{a}\right) dl + \left(\sqrt{\frac{\mu}{a}}\, e\, da + \sqrt{\mu a}\, 2\frac{a}{r} de\right) \sin u + \sqrt{\mu a\left(1 - e^2\right)}\, R \cdot d\Psi \ . \qquad (10)$$

Differentiating Equation 8 and taking

$$\frac{r}{a} = 1 - e \cos u$$

into account, we have

$$2d(r \cdot v) = \left(e\sqrt{\frac{\mu}{a}} da + 2\sqrt{\mu a}\, de\right) \sin u + 2\sqrt{\mu a}\left(1 - \frac{r}{a}\right) du \ . \qquad (11)$$

Differentiating Kepler's equation we have

$$du = \frac{a}{r} \sin u \, de + \frac{a}{r} \, dl \ . \tag{12}$$

Eliminating du from Equation 11 by means of Equation 12 we obtain

$$2d(r \cdot v) = \left(e \sqrt{\frac{\mu}{a}} \, da + 2 \sqrt{\mu a} \, \frac{a}{r} \, de \right) \sin u + 2 \sqrt{\mu a} \left(\frac{a}{r} - 1 \right) dl$$

Taking Equation 9 into account we deduce

$$2d(r \cdot v) = \left(\frac{v^2}{n} - \sqrt{\mu a} \right) dl + \left(e \sqrt{\frac{\mu}{a}} \, da + 2 \frac{a}{r} \sqrt{\mu a} \, de \right) \sin u \ .$$

Comparing the last equation with Equation 10 we conclude that

$$v \cdot dr = \sqrt{\mu a} \, dl + \sqrt{\mu a (1 - e^2)} \, R \cdot d\psi + 2d(r \cdot v) \ . \tag{13}$$

Decomposing the infinitesimal rotation $d\Psi$ along the axes **P**, **Q**, and **R** we have

$$d\psi = dP \cdot QR + dQ \cdot RP + dR \cdot PQ$$

and Equation 13 becomes

$$v \cdot dr = \sqrt{\mu a} \, dl + \sqrt{\mu a (1 - e^2)} \, Q \cdot dP + 2d(r \cdot v) \ . \tag{14}$$

Neglecting the total differential 2d (**r**·**v**) we have

$$\phi = \sqrt{\mu a} \, dl + \sqrt{\mu a (1 - e^2)} \, Q \cdot dP + F \, dt \tag{15}$$

with $F = \mu/2a + \Omega$. Equation 15 was deduced by Bilimovich on the basis of a different consideration.

EQUATIONS FOR VARIATION OF VECTORIAL ELEMENTS

Milankovich has deduced the vectorial equations for the determination of general perturbations of vectors **c** and **e**.

The vectors **P** and **Q** constitute a better choice for the development of the disturbing function and the computation of the position and velocity vectors.

The elements we choose are

$$l, \ a, \ e, \ P \text{ and } Q$$

For reasons of symmetry we take the expression for ϕ in the form

$$\phi = \sqrt{\mu a} \, dl + \frac{1}{2} \sqrt{\mu a (1 - e^2)} \, (Q \cdot dP - P \cdot dQ) + r \, dt$$

with the three additional conditions

$$P \cdot P = 1, \quad Q \cdot Q = 1, \quad P \cdot Q = 0 \ . \tag{16}$$

The Pfaffian equations (Equations 3–6) for the variation of constants in this particular case become:

$$\text{grad}_P \, \phi - d \left[\frac{1}{2} \sqrt{\mu a (1 - e^2)} \, Q \right] + (uP + wQ) \, dt = 0 \ , \tag{17}$$

$$\mathrm{grad}_{\mathbf{Q}}\,\phi + d\left[\frac{1}{2}\ \sqrt{\mu a\left(1-e^2\right)}\ \mathbf{P}\right] + (v\mathbf{Q} + w\mathbf{P})\,dt = 0\,, \tag{18}$$

$$\frac{\partial \phi}{\partial a} = 0\,, \tag{19}$$

$$\frac{\partial \phi}{\partial e} = 0\,, \tag{20}$$

$$\frac{\partial \phi}{\partial l} - d\sqrt{\mu a} = 0\,, \tag{21}$$

where u, v and w here are the Lagrangian multipliers associated with the constraints (Equation 16).

After some easy transformations we deduce from Equations 17–21:

$$na^2\sqrt{1-e^2}\,\frac{d\mathbf{P}}{dt} + (A + w)\,\mathbf{P} + v\mathbf{Q} + \mathrm{grad}_{\mathbf{Q}}\,F = 0\,, \tag{22}$$

$$na^2\sqrt{1-e^2}\,\frac{d\mathbf{Q}}{dt} + (A - w)\,\mathbf{Q} - u\mathbf{P} - \mathrm{grad}_{\mathbf{P}}\,F = 0\,, \tag{23}$$

$$\frac{1}{2}\,na\,\frac{dl}{dt} + \frac{1}{2}\,na\,\sqrt{1-e^2}\,\mathbf{Q}\cdot\frac{d\mathbf{P}}{dt} + \frac{\partial F}{\partial a} = 0\,, \tag{24}$$

$$\mathbf{Q}\cdot\frac{d\mathbf{P}}{dt} = -\,\mathbf{P}\cdot\frac{d\mathbf{Q}}{dt} = +\,\frac{\sqrt{1-e^2}}{na^2\,e}\,\frac{\partial F}{\partial e}\,, \tag{25}$$

$$\frac{\partial F}{\partial l} - \frac{1}{2}\,na\,\frac{da}{dt} = 0\,, \tag{26}$$

where

$$A = \frac{1}{4}\left(na\sqrt{1-e^2}\,\frac{da}{dt} - \frac{2na^2\,e}{\sqrt{1-e^2}}\,\frac{de}{dt}\right). \tag{27}$$

By multiplying Equation 22 by $\mathbf{P}$ and Equation 23 by $\mathbf{Q}$ we deduce:

$$A + w = -\mathbf{P}\cdot\mathrm{grad}_{\mathbf{Q}}\,F\,,$$

$$A - w = +\mathbf{Q}\cdot\mathrm{grad}_{\mathbf{P}}\,F\,,$$

$$A = +\frac{1}{2}\,\mathbf{Q}\cdot\mathrm{grad}_{\mathbf{P}}\,F - \frac{1}{2}\,\mathbf{P}\cdot\mathrm{grad}_{\mathbf{Q}}\,F\,, \tag{28}$$

$$w = -\frac{1}{2}\,\mathbf{Q}\cdot\mathrm{grad}_{\mathbf{P}}\,F - \frac{1}{2}\,\mathbf{P}\cdot\mathrm{grad}_{\mathbf{Q}}\,F\,. \tag{29}$$

Multiplying Equation 22 by $\mathbf{Q}$ and Equation 23 by $\mathbf{P}$ and taking Equation 25 into account, we have

$$v = -\mathbf{Q}\cdot\mathrm{grad}_{\mathbf{Q}}\,F - \frac{1-e^2}{e}\,\frac{\partial F}{\partial e}\,, \tag{30}$$

$$u = -\mathbf{P}\cdot\mathrm{grad}_{\mathbf{P}}\,F - \frac{1-e^2}{e}\,\frac{\partial F}{\partial e}\,. \tag{31}$$

Substituting Equations 29–31 into Equations 22 and 23 and taking the identity

$$\mathbf{I} = \mathbf{PP} + \mathbf{QQ} + \mathbf{RR}$$

into account, we obtain

$$\frac{d\mathbf{P}}{dt} = -\frac{1}{na^2\sqrt{1-e^2}}\,\mathbf{RR}\cdot\operatorname{grad}_{\mathbf{Q}} F + \frac{\sqrt{1-e^2}}{na^2 e}\frac{\partial F}{\partial e}\,\mathbf{Q}\,, \tag{32}$$

$$\frac{d\mathbf{Q}}{dt} = +\frac{1}{na^2\sqrt{1-e^2}}\,\mathbf{RR}\cdot\operatorname{grad}_{\mathbf{P}} F - \frac{\sqrt{1-e^2}}{na^2 e}\frac{\partial F}{\partial e}\,\mathbf{P}\,. \tag{33}$$

These two last equations are new. Equations 24 and 26 can be written in the classical form:

$$\frac{da}{dt} = \frac{2}{na}\frac{\partial F}{\partial l}\,, \tag{34}$$

$$\frac{dl}{dt} = -\frac{1-e^2}{na^2 e}\frac{\partial F}{\partial e} - \frac{2}{na}\frac{\partial F}{\partial a}\,. \tag{35}$$

From Equations 27, 28, and 34 we deduce

$$\frac{de}{dt} = +\frac{1-e^2}{na^2 e}\frac{\partial F}{\partial l} + \frac{\sqrt{1-e^2}}{na^2 e}\left(\mathbf{P}\cdot\operatorname{grad}_{\mathbf{Q}} F - \mathbf{Q}\cdot\operatorname{grad}_{\mathbf{P}} F\right). \tag{36}$$

The system Equations 32–36 forms a complete set to be used in the development of perturbations.

From Equations 32 and 33 we see that the constraints (Equation 16) are satisfied. Because of the existence of these constraints the determination of the additive constants of integration associated with Equations 32 and 33 becomes extremely simple. This simplicity justifies in part the choice of $\mathbf{P}$ and $\mathbf{Q}$ as the basic elements. Changing the notation, we shall designate any disturbed element E as a series

$$E + E_1 + E_2 + E_3 + \cdots\,,$$

where E now means the undisturbed value and E_k are the perturbations of k-th order. We deduce from Equation 16:

$$\begin{aligned}
&\mathbf{P}\cdot\mathbf{P}_1 = 0\,,\\
&\mathbf{P}\cdot\mathbf{P}_2 + \tfrac{1}{2}\mathbf{P}_1^2 = 0\,, \qquad (37)\\
&\mathbf{P}\cdot\mathbf{P}_3 + \mathbf{P}_1\cdot\mathbf{P}_2 = 0\,,\\
&\qquad\cdots\cdots\cdots\cdots\cdots
\end{aligned}$$

$$\begin{aligned}
&\mathbf{Q}\cdot\mathbf{Q}_1 = 0\,,\\
&\mathbf{Q}\cdot\mathbf{Q}_2 + \tfrac{1}{2}\mathbf{Q}_1^2 = 0\,, \qquad (38)\\
&\mathbf{Q}\cdot\mathbf{Q}_3 + \mathbf{Q}_1\cdot\mathbf{Q}_2 = 0\,,\\
&\qquad\cdots\cdots\cdots\cdots\cdots
\end{aligned}$$

$$\begin{aligned}
&\mathbf{Q}\cdot\mathbf{P}_1 + \mathbf{P}\cdot\mathbf{Q}_1 = 0\,,\\
&\mathbf{Q}\cdot\mathbf{P}_2 + \mathbf{P}\cdot\mathbf{Q}_2 + \mathbf{P}_1\cdot\mathbf{Q}_1 = 0\,, \qquad (39)\\
&\mathbf{Q}\cdot\mathbf{P}_3 + \mathbf{P}\cdot\mathbf{Q}_3 + \mathbf{P}_1\cdot\mathbf{Q}_2 + \mathbf{P}_2\cdot\mathbf{Q}_1 = 0\,.\\
&\qquad\cdots\cdots\cdots\cdots\cdots
\end{aligned}$$

For $\mathbf{P}_k$, $\mathbf{Q}_k$ ($k=1, 2, \cdots$) we obtain from Equations 32 and 33 equations of the form:

$$\frac{d\mathbf{P}_k}{dt} = f_k\left(\mathbf{P}, \mathbf{Q}, a, l, e; \mathbf{P}_1, \mathbf{Q}_1, a_1, l_1, e_1; \cdots; \mathbf{P}_{k-1}, \mathbf{Q}_{k-1}, a_{k-1}, l_{k-1}, e_{k-1}\right),$$

$$\frac{d\mathbf{Q}_k}{dt} = \phi_k\left(\mathbf{P}, \mathbf{Q}, a, l, e; \mathbf{P}_1, \mathbf{Q}_1, a_1, l_1, e_1; \cdots; \mathbf{P}_{k-1}, \mathbf{Q}_{k-1}, a_{k-1}, l_{k-1}, e_{k-1}\right).$$

Let

$$(\mathbf{P}_k) = \int \mathbf{f}_k \, dt \, ,$$

$$(\mathbf{Q}_k) = \int \boldsymbol{\phi}_k \, dt \, ,$$

where the integration is performed in a formal manner. We can write

$$\mathbf{P}_k = (\mathbf{P}_k) + p_{k1}\,\mathbf{P} + p_{k2}\,\mathbf{Q} + p_{k3}\,\mathbf{R} \, ,$$

$$\mathbf{Q}_k = (\mathbf{Q}_k) + q_{k1}\,\mathbf{P} + q_{k2}\,\mathbf{Q} + q_{k3}\,\mathbf{R} \, ,$$

where p_{k1}, q_{k1} are the constants of integration. The expressions $(\mathbf{P}_k)$, $(\mathbf{Q}_k)$ contain the secular, the mixed and the purely periodic terms, but there are no constant terms.

Let [f] designate the constant part in the multiple Fourier series of some function $f(l, l', l'', \cdots)$. Taking into account

$$[(\mathbf{P}_k)] = [(\mathbf{Q}_k)] = 0 \, ,$$

we deduce from Equations 37–39:

$$\begin{aligned} p_{11} &= 0 \, , \\ p_{21} &= -\tfrac{1}{2}[\mathbf{P}_1^2] \, , \\ p_{31} &= -[\mathbf{P}_1 \cdot \mathbf{P}_2] \, , \\ &\cdots\cdots\cdots\cdots \end{aligned} \tag{40}$$

$$\begin{aligned} q_{12} &= 0 \, , \\ q_{22} &= -\tfrac{1}{2}[\mathbf{Q}_1^2] \, , \\ q_{32} &= -[\mathbf{Q}_1 \cdot \mathbf{Q}_2] \, , \\ &\cdots\cdots\cdots\cdots \end{aligned} \tag{41}$$

$$\begin{aligned} q_{11} &= -p_{12} \\ q_{21} &= -p_{22} - [\mathbf{P}_1 \cdot \mathbf{Q}_1] \, , \\ q_{31} &= -p_{32} - [\mathbf{P}_1 \cdot \mathbf{Q}_2] - [\mathbf{P}_2 \cdot \mathbf{Q}_1] \, . \\ &\cdots\cdots\cdots\cdots \end{aligned} \tag{42}$$

We see from Equations 40–42 that in the process of the determination of the perturbations of k-th order in $\mathbf{P}$ and $\mathbf{Q}$ the three constants p_{k2}, p_{k3}, q_{k3} can be considered as independent. The constants q_{k1} are determined in terms of p_{k2} and of the constants of the lower orders. The constants p_{k1} and q_{k2} are also functions of the constants of the lower orders. Although there are redundant elements there are no redundant constants which cannot be determined easily. For the disturbed position vector $\mathbf{r}$ we have the standard expression

$$r = Pa(\cos u - e) + Qa\sqrt{1 - e^2}\sin u \, ,$$

$$u - e\sin u = l \, ,$$

where all symbols now designate the disturbed elements.

In order to verify the correctness of Equations 32, 33, and 36 we shall deduce them from the corresponding classical equations. From

$$\mathbf{P} = \begin{Bmatrix} +\cos\omega\cos\Omega - \sin\omega\sin\Omega\cos i \\ +\cos\omega\sin\Omega + \sin\omega\cos\Omega\cos i \\ +\sin\omega\sin i \end{Bmatrix} ,$$

$$\mathbf{Q} = \begin{Bmatrix} -\sin\omega\cos\Omega - \cos\omega\sin\Omega\cos i \\ -\sin\omega\sin\Omega + \cos\omega\cos\Omega\cos i \\ +\cos\omega\sin i \end{Bmatrix} ,$$

$$\mathbf{R} = \begin{Bmatrix} +\sin\Omega\sin i \\ -\cos\Omega\sin i \\ +\cos i \end{Bmatrix} ,$$

we have

$$\frac{dP}{dt} = Q\frac{d\omega}{dt} + R\sin\omega\frac{di}{dt} + k \times P\frac{d\Omega}{dt} , \quad (43)$$

$$\frac{dQ}{dt} = -P\frac{d\omega}{dt} + R\cos\omega\frac{di}{dt} + k \times Q\frac{d\Omega}{dt} , \quad (44)$$

and as a consequence of the two last equations:

$$\sin i\frac{d\Omega}{dt} = R \cdot \left(-\frac{dP}{dt}\cos\omega + \frac{dQ}{dt}\sin\omega\right) , \quad (45)$$

$$\frac{di}{dt} = R \cdot \left(+\frac{dP}{dt}\sin\omega + \frac{dQ}{dt}\cos\omega\right) , \quad (46)$$

$$\frac{d\omega}{dt} + \cos i\frac{d\Omega}{dt} = Q \cdot \frac{dP}{dt} = -P \cdot \frac{dQ}{dt} . \quad (47)$$

From

$$\frac{\partial F}{\partial E} = \frac{\partial P}{\partial E} \cdot \mathrm{grad}_P F + \frac{\partial Q}{\partial E} \cdot \mathrm{grad}_Q F ,$$

where

$$E = \omega, \Omega, i ,$$

and Equations 43 and 44, we deduce

$$\frac{\partial F}{\partial \omega} = Q \cdot \mathrm{grad}_P F - P \cdot \mathrm{grad}_Q F , \quad (48)$$

$$\frac{\partial F}{\partial i} = \sin\omega\left(R \cdot \mathrm{grad}_P F\right) + \cos\omega\left(R \cdot \mathrm{grad}_Q F\right) , \quad (49)$$

$$\frac{\partial F}{\partial \Omega} = k \times P \cdot \mathrm{grad}_P F + k \times Q \cdot \mathrm{grad}_Q F . \quad (50)$$

Substituting

$$k = (P\sin\omega + Q\cos\omega)\sin i + R\cos i$$

into Equation 50, we obtain

$$-\sin\omega\left(R \cdot \mathrm{grad}_Q F\right) + \cos\omega\left(R \cdot \mathrm{grad}_P F\right) = -\frac{1}{\sin i}\frac{\partial F}{\partial \Omega} + \mathrm{ctg}\, i\frac{\partial F}{\partial \omega} .$$

From Equations 36, 45–47 and Equations 32, 33, 48–50 we obtain the classical equations:

$$\frac{d\Omega}{dt} = \frac{1}{na^2\sqrt{1-e^2}\sin i}\frac{\partial F}{\partial i} ,$$

$$\frac{di}{dt} = -\frac{1}{na^2\sqrt{1-e^2}\sin i}\frac{\partial F}{\partial \Omega} + \frac{\cos i}{na^2\sqrt{1-e^2}\sin i}\frac{\partial F}{\partial \omega} ,$$

$$\frac{d\omega}{dt} = +\frac{\sqrt{1-e^2}}{na^2 e}\frac{\partial F}{\partial e} - \cos i\frac{d\Omega}{dt} ,$$

$$\frac{de}{dt} = +\frac{1-e^2}{na^2 e}\frac{\partial F}{\partial l} - \frac{\sqrt{1-e^2}}{na^2 e}\frac{\partial F}{\partial \omega} .$$

Let the matrix of direction-cosines between (**P**, **Q**, **R**) and (**P′**, **Q′**, **R′**) be:

$$\mathbf{P}\cdot\mathbf{P}' = \alpha_1 , \quad \mathbf{P}\cdot\mathbf{Q}' = \alpha_2 , \quad \mathbf{P}\cdot\mathbf{R}' = \alpha_3 ,$$

$$\mathbf{Q}\cdot\mathbf{P}' = \beta_1 , \quad \mathbf{Q}\cdot\mathbf{Q}' = \beta_2 , \quad \mathbf{Q}\cdot\mathbf{R}' = \beta_3 ,$$

$$\mathbf{R}\cdot\mathbf{P}' = \gamma_1 , \quad \mathbf{R}\cdot\mathbf{Q}' = \gamma_2 , \quad \mathbf{R}\cdot\mathbf{R}' = \gamma_3 .$$

The disturbing function depends upon α_1, α_2, β_1 and β_2. Taking into account

$$\mathrm{grad}_{\mathbf{P}}\,\alpha_1 = \mathrm{grad}_{\mathbf{Q}}\,\beta_1 = \mathbf{P}' ,$$

$$\mathrm{grad}_{\mathbf{Q}}\,\beta_2 = \mathrm{grad}_{\mathbf{P}}\,\alpha_2 = \mathbf{Q}' ,$$

$$\mathrm{grad}_{\mathbf{Q}}\,\alpha_1 = \mathrm{grad}_{\mathbf{Q}}\,\alpha_2 = \mathrm{grad}_{\mathbf{P}}\,\beta_1 = \mathrm{grad}_{\mathbf{P}}\,\beta_2 = 0 ,$$

we obtain:

$$\mathrm{grad}_{\mathbf{P}}\,F = \frac{\partial F}{\partial \alpha_1}\,\mathbf{P}' + \frac{\partial F}{\partial \alpha_2}\,\mathbf{Q}' , \qquad (51)$$

$$\mathrm{grad}_{\mathbf{Q}}\,F = \frac{\partial F}{\partial \beta_1}\,\mathbf{P}' + \frac{\partial F}{\partial \beta_2}\,\mathbf{Q}' , \qquad (52)$$

$$\mathbf{R}\cdot\mathrm{grad}_{\mathbf{P}}\,F = \frac{\partial F}{\partial \alpha_1}\,\gamma_1 + \frac{\partial F}{\partial \alpha_2}\,\gamma_2 ,$$

$$\mathbf{R}\cdot\mathrm{grad}_{\mathbf{Q}}\,F = \frac{\partial F}{\partial \beta_1}\,\gamma_1 + \frac{\partial F}{\partial \beta_2}\,\gamma_2 ;$$

and the Equations 32 and 33 become

$$\frac{d\mathbf{P}}{dt} = -\frac{1}{na^2\sqrt{1-e^2}}\left(\frac{\partial F}{\partial \beta_1}\,\gamma_1 + \frac{\partial F}{\partial \beta_2}\,\gamma_2\right)\mathbf{R} + \frac{\sqrt{1-e^2}}{na^2\,e}\,\frac{\partial F}{\partial e}\,\mathbf{Q} ,$$

$$\frac{d\mathbf{Q}}{dt} = +\frac{1}{na^2\sqrt{1-e^2}}\left(\frac{\partial F}{\partial \alpha_1}\,\gamma_1 + \frac{\partial F}{\partial \alpha_2}\,\gamma_2\right)\mathbf{R} - \frac{\sqrt{1-e^2}}{na^2\,e}\,\frac{\partial F}{\partial e}\,\mathbf{P} .$$

If the frame (**P′**, **Q′**, **R′**) is a basic reference frame, then the last two equations become:

$$\frac{d\mathbf{P}}{dt} = -\frac{1}{na^2\sqrt{1-e^2}}\left(\frac{\partial F}{\partial \beta_1}\,\gamma_1 + \frac{\partial F}{\partial \beta_2}\,\gamma_2\right)\mathbf{R} + \frac{\sqrt{1-e^2}}{na^2\,e}\,\frac{\partial F}{\partial e}\,\mathbf{Q} + \mathbf{P}\times\boldsymbol{\psi}' , \qquad (53)$$

$$\frac{d\mathbf{Q}}{dt} = +\frac{1}{na^2\sqrt{1-e^2}}\left(\frac{\partial F}{\partial \alpha_1}\,\gamma_1 + \frac{\partial F}{\partial \alpha_2}\,\gamma_2\right)\mathbf{R} - \frac{\sqrt{1-e^2}}{na^2\,e}\,\frac{\partial F}{\partial e}\,\mathbf{P} + \mathbf{Q}\times\boldsymbol{\psi}' , \qquad (54)$$

where

$$\boldsymbol{\psi}' = \psi_1'\,\mathbf{P}' + \psi_2'\,\mathbf{Q}' + \psi_3'\,\mathbf{R}'$$

is the absolute angular velocity of rotation of the frame (**P′**, **Q′**, **R′**), and

$$\psi_1' = +\sin\omega'\sin i'\,\frac{d\Omega'}{dt} + \cos\omega'\,\frac{di'}{dt} ,$$

$$\psi_2' = +\cos\omega'\sin i'\,\frac{d\Omega'}{dt} - \sin\omega'\,\frac{di'}{dt} ,$$

$$\psi_3' = \cos i'\,\frac{d\Omega'}{dt} + \frac{d\omega'}{dt} .$$

From Equations 53 and 54 we deduce the following system of scalar equations for the variation of

the direction-cosines:

$$\frac{d\alpha_1}{dt} = -\frac{1}{na^2\sqrt{1-e^2}}\gamma_1\left(\frac{\partial F}{\partial \beta_1}\gamma_1 + \frac{\partial F}{\partial \beta_2}\gamma_2\right) + \frac{\sqrt{1-e^2}}{na^2 e}\frac{\partial F}{\partial e}\beta_1 + (\alpha_2\psi_3' - \alpha_3\psi_2') ,$$

$$\frac{d\alpha_2}{dt} = -\frac{1}{na^2\sqrt{1-e^2}}\gamma_2\left(\frac{\partial F}{\partial \beta_1}\gamma_1 + \frac{\partial F}{\partial \beta_2}\gamma_2\right) + \frac{\sqrt{1-e^2}}{na^2 e}\frac{\partial F}{\partial e}\beta_2 + (\alpha_3\psi_1' - \alpha_1\psi_3') ,$$

$$\frac{d\alpha_3}{dt} = -\frac{1}{na^2\sqrt{1-e^2}}\gamma_3\left(\frac{\partial F}{\partial \beta_1}\gamma_1 + \frac{\partial F}{\partial \beta_2}\gamma_2\right) + \frac{\sqrt{1-e^2}}{na^2 e}\frac{\partial F}{\partial e}\beta_3 + (\alpha_1\psi_2' - \alpha_2\psi_1') ,$$

and

$$\frac{d\beta_1}{dt} = +\frac{1}{na^2\sqrt{1-e^2}}\gamma_1\left(\frac{\partial F}{\partial \alpha_1}\gamma_1 + \frac{\partial F}{\partial \alpha_2}\gamma_2\right) - \frac{\sqrt{1-e^2}}{na^2 e}\frac{\partial F}{\partial e}\alpha_1 + (\beta_2\psi_3' - \beta_3\psi_2') ,$$

$$\frac{d\beta_2}{dt} = +\frac{1}{na^2\sqrt{1-e^2}}\gamma_2\left(\frac{\partial F}{\partial \alpha_1}\gamma_1 + \frac{\partial F}{\partial \alpha_2}\gamma_2\right) - \frac{\sqrt{1-e^2}}{na^2 e}\frac{\partial F}{\partial e}\alpha_2 + (\beta_3\psi_1' - \beta_1\psi_3') ,$$

$$\frac{d\beta_3}{dt} = +\frac{1}{na^2\sqrt{1-e^2}}\gamma_3\left(\frac{\partial F}{\partial \alpha_1}\gamma_1 + \frac{\partial F}{\partial \alpha_2}\gamma_2\right) - \frac{\sqrt{1-e^2}}{na^2 e}\frac{\partial F}{\partial e}\alpha_3 + (\beta_1\psi_2' - \beta_2\psi_1') .$$

Substituting Equations 51 and 52 into Equation 36 we obtain

$$\frac{de}{dt} = +\frac{1-e^2}{na^2 e}\frac{\partial F}{\partial l} + \frac{\sqrt{1-e^2}}{na^2 e}\left(\alpha_1\frac{\partial F}{\partial \beta_1} - \beta_1\frac{\partial F}{\partial \alpha_1} + \alpha_2\frac{\partial F}{\partial \beta_2} - \beta_2\frac{\partial F}{\partial \alpha_2}\right) .$$

Equations 32, 33, and 36 can be applied to the determination of the lunar and solar long period effects in the motion of close satellites. In the case of close satellites the short period terms, depending upon the mean anomaly of the satellite, can be neglected and the remaining portion $[\Omega]$ of the disturbing function can be developed (References 12 and 13) into the series of polynomials in e and in

$$\alpha = \alpha_1 \cos f' + \alpha_2 \sin f' ,$$

$$\beta = \beta_1 \cos f' + \beta_2 \sin f' ,$$

$$\gamma = \gamma_1 \cos f' + \gamma_2 \sin f' .$$

Taking into account

$$\mathrm{grad}_P\,\alpha = \mathrm{grad}_Q\,\beta = 1 ,$$

$$\mathrm{grad}_Q\,\alpha = \mathrm{grad}_P\,\beta = 0 ,$$

we obtain from Equations 32, 33 and 36

$$\frac{dP}{dt} = -\frac{\gamma R}{na^2\sqrt{1-e^2}}\frac{\partial[\Omega]}{\partial \beta} + \frac{\sqrt{1-e^2}}{na^2 e}\frac{\partial[\Omega]}{\partial e}Q ,$$

$$\frac{dQ}{dt} = +\frac{\gamma R}{na^2\sqrt{1-e^2}}\frac{\partial[\Omega]}{\partial \alpha} - \frac{\sqrt{1-e^2}}{na^2 e}\frac{\partial[\Omega]}{\partial e}P ,$$

and

$$\frac{de}{dt} = + \frac{\sqrt{1 - e^2}}{na^2 e} \left(a \frac{\partial [\Omega]}{\partial \beta} - \beta \frac{\partial [\Omega]}{\partial i} \right) .$$

A very elegant and convenient development of the disturbing function for close satellites was given by Kaula (Reference 14). The use of the Gibbsian rotation vector $\mathbf{g}$ (Reference 15) was suggested in an article (Reference 5) on the improvement of Strömgren's theory (Reference 4).

The basic vectors $\mathbf{P}$ and $\mathbf{Q}$ can be represented as relatively simple functions of $\mathbf{g}$ and the introduction of $\mathbf{g}$ removes the necessity of keeping constraints (Equation 16) as the additional conditions. The components of $\mathbf{g}$ in the inertial system are

$$g_1 = + \frac{\cos \frac{1}{2} (\omega - \Omega)}{\cos \frac{1}{2} (\omega + \Omega)} \operatorname{tg} \frac{i}{2} ,$$

$$g_2 = - \frac{\sin \frac{1}{2} (\omega - \Omega)}{\cos \frac{1}{2} (\omega + \Omega)} \operatorname{tg} \frac{i}{2} ,$$

$$g_3 = + \operatorname{tg} \frac{1}{2} (\omega + \Omega) .$$

Equation 47 shows that the Pfaffian (Equation 15) can be written as

$$\phi = \sqrt{\mu a}\, dl + \sqrt{\mu a (1 - e^2)}\, (d\omega + \cos i\, d\Omega) + F\, dt . \qquad (55)$$

This form was originally used by Bilimovich. Taking

$$\omega - \Omega = - 2 \arctan \frac{g_2}{g_1} ,$$

$$\omega + \Omega = 2 \arctan g_3 ,$$

and

$$\tan^2 \frac{i}{2} = \frac{g_1^2 + g_2^2}{1 + g_3^2}$$

into account, we deduce from Equation 55

$$\phi = \sqrt{\mu a}\, dl + \frac{2 \sqrt{\mu a (1 - e^2)}}{1 + g^2} s \cdot dg + F\, dt , \qquad (56)$$

where we put

$$s = k + g \times k . \qquad (57)$$

The Pfaffian equation corresponding to $\mathbf{g}$ is

$$\operatorname{grad}_g \left\{ \frac{2 \sqrt{\mu a (1 - e^2)}}{1 + g^2} s \cdot dg \right\} - d \left\{ \frac{2 \sqrt{\mu a (1 - e^2)}}{1 + g^2} s \right\} + \operatorname{grad}_g F\, dt = 0$$

or, after the differentiation is performed,

$$\frac{4na^2 \sqrt{1 - e^2}}{1 + g^2} \left(k \times \frac{dg}{dt} + \frac{sg \cdot \frac{dg}{dt} - gs \cdot \frac{dg}{dt}}{1 + g^2} \right)$$

$$- \left(na \sqrt{1 - e^2} \frac{da}{dt} - \frac{2na^2 e}{\sqrt{1 - e^2}} \frac{de}{dt} \right) \frac{s}{1 + g^2} + \operatorname{grad}_g F = 0 . \qquad (58)$$

Taking into account

$$\mathbf{s}\mathbf{g} \cdot \frac{d\mathbf{g}}{dt} - \mathbf{g}\mathbf{s} \cdot \frac{d\mathbf{g}}{dt} = (\mathbf{g} \times \mathbf{s}) \times \frac{d\mathbf{g}}{dt} ,$$

we can write Equation 58 in the form

$$\frac{4na^2\sqrt{1-e^2}}{1+g^2}\,\mathbf{h} \times \frac{d\mathbf{g}}{dt} - \left(na\sqrt{1-e^2}\,\frac{da}{dt} - \frac{2na^2 e}{\sqrt{1-e^2}}\,\frac{de}{dt}\right)\frac{\mathbf{s}}{1+g^2} + \operatorname{grad}_{\mathbf{g}} F = 0 , \quad (59)$$

where

$$\mathbf{h} = \mathbf{k} + \frac{\mathbf{g} \times \mathbf{s}}{1+g^2} = \frac{\mathbf{k} + \mathbf{g} \times \mathbf{k} + \mathbf{g}\mathbf{g} \cdot \mathbf{k}}{1+g^2} . \quad (60)$$

We have from Equation 59:

$$\frac{4na^2\sqrt{1-e^2}}{1+g^2}\,\mathbf{s} \times \left(\mathbf{h} \times \frac{d\mathbf{g}}{dt}\right) + \mathbf{s} \times \operatorname{grad}_{\mathbf{g}} F = 0 ,$$

or, after developing the triple product,

$$\mathbf{h} \cdot \mathbf{s}\,\frac{d\mathbf{g}}{dt} = \mathbf{h}\mathbf{s} \cdot \frac{d\mathbf{g}}{dt} + \frac{1+g^2}{4na^2\sqrt{1-e^2}}\,\mathbf{s} \times \operatorname{grad}_{\mathbf{g}} F . \quad (61)$$

From Equations 57 and 60 we have

$$\mathbf{h} \cdot \mathbf{s} = 1 , \quad (62)$$

and Equation 61 becomes

$$\frac{d\mathbf{g}}{dt} = \mathbf{h}\mathbf{s} \cdot \frac{d\mathbf{g}}{dt} + \frac{1+g^2}{4na^2\sqrt{1-e^2}}\,\mathbf{s} \times \operatorname{grad}_{\mathbf{g}} F . \quad (63)$$

The Pfaffian equation associated with e is simply

$$\frac{\partial \phi}{\partial e} = 0$$

or

$$-\frac{2na^2 e}{\sqrt{1-e^2}}\,\frac{\mathbf{s} \cdot d\mathbf{g}}{1+g^2} + \frac{\partial F}{\partial e}\,dt = 0 . \quad (64)$$

From Equations 63 and 64 we obtain

$$\frac{d\mathbf{g}}{dt} = \mathbf{h}\,\frac{(1+g^2)\sqrt{1-e^2}}{2na^2 e}\,\frac{\partial F}{\partial e} + \frac{1+g^2}{4na^2\sqrt{1-e^2}}\,\mathbf{s} \times \operatorname{grad}_{\mathbf{g}} F . \quad (65)$$

Multiplying Equation 59 by $\mathbf{h}$ and taking Equations 62 and 34 into account, we deduce

$$\frac{de}{dt} = + \frac{1-e^2}{na^2 e}\,\frac{\partial F}{\partial l} - \frac{(1+g^2)\sqrt{1-e^2}}{2na^2 e}\,\mathbf{h} \cdot \operatorname{grad}_{\mathbf{g}} F . \quad (66)$$

The use of the Gibbsian rotation vector represents an application and an extension of Strömgren's and of the author's ideas from the domain of special perturbations to the domain of general perturbations. The use of the vector $\mathbf{g}$ becomes especially convenient if the basic reference plane

nearly coincides with the osculating orbit plane at the initial epoch. Then the components of $\mathbf{g}$ become small—of the order of perturbations.

Now let a, e, l be the disturbed and **P**, **Q** the un-disturbed elements and put

$$r_0 = Pa(\cos u - e) + Qa\sqrt{1 - e^2}\,\sin u \,.$$

$$u - e\sin u = l$$

Writing the matrix of rotation Γ, which transforms $\mathbf{r}_0$ into the disturbed position vector $\mathbf{r}$, in the Gibbsian form

$$\Gamma = I + \frac{2}{1 + g^2}\left[g \times I + g \times (g \times I)\right] \,, \quad (67)$$

we have

$$r = \Gamma \cdot r_0 \,,$$

or, in the developed form,

$$r = r_0 + \frac{2}{1 + g^2}\left[g \times r_0 + g \times (g \times r_0)\right] \,,$$

or

$$r = \frac{1 - g^2}{1 + g^2} r_0 + \frac{2}{1 + g^2}\left[g \times r_0 + g g \cdot r_0\right] .$$

EQUATIONS FOR VARIATION OF EULER'S PARAMETERS

It is also of interest to deduce the equations for the variation of elements in terms of Euler parameters:

$$\begin{aligned} \lambda_1 &= \sin\tfrac{1}{2} i \cos\tfrac{1}{2}(\omega - \Omega) \,, \\ \lambda_2 &= \sin\tfrac{1}{2} i \sin\tfrac{1}{2}(\omega - \Omega) \,, \\ \lambda_3 &= \cos\tfrac{1}{2} i \sin\tfrac{1}{2}(\omega + \Omega) \,, \\ \lambda_4 &= \cos\tfrac{1}{2} i \cos\tfrac{1}{2}(\omega + \Omega) \,. \end{aligned} \quad (68)$$

The additional constraint is

$$\lambda_1^2 + \lambda_2^2 + \lambda_3^2 + \lambda_4^2 = 1 \,. \quad (69)$$

Two of these parameters, namely λ_1 and λ_2, were used by Hansen (Reference 6) in his lunar theory. The author has suggested the use of all four in the theory of artificial satellites (Reference 7) and in a modification of Hansen's lunar theory (Reference 16). Writing the Pfaffian (Equation 55) in the form

$$\phi = \sqrt{\mu a}\, dl + \sqrt{\mu a(1 - e^2)}\,\frac{d(\omega + \Omega) + \tan^2\frac{i}{2}\, d(\omega - \Omega)}{1 + \tan^2\frac{i}{2}} + F\, dt$$

and taking Equation 68 into account, we deduce

$$\phi = \sqrt{\mu a}\, dl + 2\sqrt{\mu a(1 - e^2)}\left(\lambda_1 d\lambda_2 - \lambda_2 d\lambda_1 + \lambda_4 d\lambda_3 - \lambda_3 d\lambda_4\right) + F\, dt \,. \quad (70)$$

The Pfaffian equations associated with the λ-parameters take the form:

$$\frac{\partial\phi}{\partial\lambda_1} + 2d\left[\sqrt{\mu a(1 - e^2)}\,\lambda_2\right] - w\lambda_1\, dt = 0 \quad (71)$$

$$\frac{\partial\phi}{\partial\lambda_2} - 2d\left[\sqrt{\mu a(1 - e^2)}\,\lambda_1\right] - w\lambda_2\, dt = 0 \quad (72)$$

$$\frac{\partial\phi}{\partial\lambda_3} - 2d\left[\sqrt{\mu a(1 - e^2)}\,\lambda_4\right] - w\lambda_3\, dt = 0 \quad (73)$$

$$\frac{\partial\phi}{\partial\lambda_4} + 2d\left[\sqrt{\mu a(1 - e^2)}\,\lambda_3\right] - w\lambda_4\, dt = 0 \,, \quad (74)$$

where w is the Lagrangian multiplier associated with the constraint (Equation 69). Putting

$$A = na\sqrt{1-e^2}\,\frac{da}{dt} - \frac{2na^2 e}{\sqrt{1-e^2}}\,\frac{de}{dt}, \tag{75}$$

we can write Equations 71–74 in the form:

$$-A\lambda_2 - 4na^2\sqrt{1-e^2}\,\frac{d\lambda_2}{dt} - \frac{\partial F}{\partial \lambda_1} + w\lambda_1 = 0, \tag{76}$$

$$+A\lambda_1 + 4na^2\sqrt{1-e^2}\,\frac{d\lambda_1}{dt} - \frac{\partial F}{\partial \lambda_2} + w\lambda_2 = 0, \tag{77}$$

$$+A\lambda_4 + 4na^2\sqrt{1-e^2}\,\frac{d\lambda_4}{dt} - \frac{\partial F}{\partial \lambda_3} + w\lambda_3 = 0, \tag{78}$$

$$-A\lambda_3 - 4na^2\sqrt{1-e^2}\,\frac{d\lambda_3}{dt} - \frac{\partial F}{\partial \lambda_4} + w\lambda_4 = 0. \tag{79}$$

From this last set of equations and Equation 69 we have

$$A = -\lambda_2\frac{\partial F}{\partial \lambda_1} + \lambda_1\frac{\partial F}{\partial \lambda_2} - \lambda_3\frac{\partial F}{\partial \lambda_4} + \lambda_4\frac{\partial F}{\partial \lambda_3}, \tag{80}$$

and

$$w = B - 4na^2\sqrt{1-e^2}\left(-\lambda_1\frac{d\lambda_2}{dt} + \lambda_2\frac{d\lambda_1}{dt} + \lambda_3\frac{d\lambda_4}{dt} - \lambda_4\frac{d\lambda_3}{dt}\right), \tag{81}$$

where, for the sake of brevity, we put

$$B = \lambda_1\frac{\partial F}{\partial \lambda_1} + \lambda_2\frac{\partial F}{\partial \lambda_2} + \lambda_3\frac{\partial F}{\partial \lambda_3} + \lambda_4\frac{\partial F}{\partial \lambda_4}. \tag{82}$$

From the Pfaffian equation

$$\frac{\partial \phi}{\partial e} = 0,$$

we deduce, after some transformations,

$$-\lambda_1\frac{d\lambda_2}{dt} + \lambda_2\frac{d\lambda_1}{dt} + \lambda_3\frac{d\lambda_4}{dt} - \lambda_4\frac{d\lambda_3}{dt} = -\frac{\sqrt{1-e^2}}{2na^2 e}\frac{\partial F}{\partial e}, \tag{83}$$

and Equation 81 becomes

$$w = B + \frac{2(1-e^2)}{e}\frac{\partial F}{\partial e}.$$

Substituting this value of w into Equations 76–79 we obtain:

$$\frac{d\lambda_1}{dt} = + \frac{1}{4na^2\sqrt{1-e^2}}\left(\frac{\partial F}{\partial \lambda_2} - \lambda_1 A - \lambda_2 B\right) - \frac{\sqrt{1-e^2}}{2na^2 e}\lambda_2 \frac{\partial F}{\partial e} ,$$

$$\frac{d\lambda_2}{dt} = - \frac{1}{4na^2\sqrt{1-e^2}}\left(\frac{\partial F}{\partial \lambda_1} + \lambda_2 A - \lambda_1 B\right) + \frac{\sqrt{1-e^2}}{2na^2 e}\lambda_1 \frac{\partial F}{\partial e} ,$$

$$\frac{d\lambda_3}{dt} = - \frac{1}{4na^2\sqrt{1-e^2}}\left(\frac{\partial F}{\partial \lambda_4} + \lambda_3 A - \lambda_4 B\right) + \frac{\sqrt{1-e^2}}{2na^2 e}\lambda_4 \frac{\partial F}{\partial e} ,$$

$$\frac{d\lambda_4}{dt} = + \frac{1}{4na^2\sqrt{1-e^2}}\left(\frac{\partial F}{\partial \lambda_3} - \lambda_4 A - \lambda_3 B\right) - \frac{\sqrt{1-e^2}}{2na^2 e}\lambda_3 \frac{\partial F}{\partial e} .$$

Taking Equations 80 and 82 into account we deduce from the last set of equations:

$$\frac{d\lambda_1}{dt} = \frac{1}{4na^2\sqrt{1-e^2}}\left[+\left(\lambda_4^2 + \lambda_3^2\right)\frac{\partial F}{\partial \lambda_2} - \left(\lambda_1\lambda_4 + \lambda_2\lambda_3\right)\frac{\partial F}{\partial \lambda_3} - \left(\lambda_2\lambda_4 - \lambda_1\lambda_3\right)\frac{\partial F}{\partial \lambda_4}\right] - \frac{\sqrt{1-e^2}}{2na^2 e}\lambda_2\frac{\partial F}{\partial e} ,$$

$$\frac{d\lambda_2}{dt} = \frac{1}{4na^2\sqrt{1-e^2}}\left[-\left(\lambda_3^2 + \lambda_4^2\right)\frac{\partial F}{\partial \lambda_1} - \left(\lambda_2\lambda_4 - \lambda_1\lambda_3\right)\frac{\partial F}{\partial \lambda_3} + \left(\lambda_1\lambda_4 + \lambda_2\lambda_3\right)\frac{\partial F}{\partial \lambda_4}\right] + \frac{\sqrt{1-e^2}}{2na^2 e}\lambda_1\frac{\partial F}{\partial e} ,$$

$$\frac{d\lambda_3}{dt} = \frac{1}{4na^2\sqrt{1-e^2}}\left[+\left(\lambda_1\lambda_4 + \lambda_2\lambda_3\right)\frac{\partial F}{\partial \lambda_1} + \left(\lambda_2\lambda_4 - \lambda_1\lambda_3\right)\frac{\partial F}{\partial \lambda_2} - \left(\lambda_1^2 + \lambda_2^2\right)\frac{\partial F}{\partial \lambda_4}\right] + \frac{\sqrt{1-e^2}}{2na^2 e}\lambda_4\frac{\partial F}{\partial e} ,$$

$$\frac{d\lambda_4}{dt} = \frac{1}{4na^2\sqrt{1-e^2}}\left[+\left(\lambda_2\lambda_4 - \lambda_1\lambda_3\right)\frac{\partial F}{\partial \lambda_1} - \left(\lambda_1\lambda_4 + \lambda_2\lambda_3\right)\frac{\partial F}{\partial \lambda_2} + \left(\lambda_1^2 + \lambda_2^2\right)\frac{\partial F}{\partial \lambda_3}\right] - \frac{\sqrt{1-e^2}}{2na^2 e}\lambda_3\frac{\partial F}{\partial e} .$$

A similar set of equations was recently deduced by the author in less direct manner (Reference 16). From Equations 34, 75 and 80 we obtain

$$\frac{de}{dt} = + \frac{1 - e^2}{na^2 e} \frac{\partial F}{\partial l} + \frac{\sqrt{1 - e^2}}{2na^2 e} \left(\lambda_2 \frac{\partial F}{\partial \lambda_1} - \lambda_1 \frac{\partial F}{\partial \lambda_2} + \lambda_3 \frac{\partial F}{\partial \lambda_4} - \lambda_4 \frac{\partial F}{\partial \lambda_3} \right)$$

The disturbed position vector $\mathbf{r}$ is given by the formula:

$$r = \Gamma \cdot \begin{bmatrix} a(\cos u - e) \\ a\sqrt{1 - e^2} \sin u \\ 0 \end{bmatrix},$$

where

$$u - e \sin u = l ,$$

where a, e, l are the disturbed elements. The expression for the matrix Γ in terms of λ_1, λ_2, λ_3, λ_4 is given in Reference 7. We repeat it here for the sake of completeness:

$$\Gamma = [\lambda_{ij}] ,$$

$$\lambda_{11} = + \lambda_1^2 - \lambda_2^2 - \lambda_3^2 + \lambda_4^2 ,$$

$$\lambda_{12} = - 2(\lambda_1 \lambda_2 + \lambda_3 \lambda_4) ,$$

$$\lambda_{13} = + 2(\lambda_1 \lambda_3 - \lambda_2 \lambda_4) ,$$

$$\lambda_{21} = + 2(\lambda_3 \lambda_4 - \lambda_1 \lambda_2) ,$$

$$\lambda_{31} = + 2(\lambda_1 \lambda_3 + \lambda_2 \lambda_4) ,$$

$$\lambda_{22} = - \lambda_1^2 + \lambda_2^2 - \lambda_3^2 + \lambda_4^2 ,$$

$$\lambda_{32} = + 2(\lambda_1 \lambda_4 - \lambda_2 \lambda_3) ,$$

$$\lambda_{23} = - 2(\lambda_1 \lambda_4 + \lambda_2 \lambda_3) ,$$

$$\lambda_{33} = - \lambda_1^2 - \lambda_2^2 + \lambda_3^2 + \lambda_4^2 .$$

We can also form different sets of purely vectorial elements by taking Equation 15 as a basis. Writing Equation 15 in an equivalent form

$$\phi = - \sqrt{\mu a}\, dl + \sqrt{\mu a(1 - e^2)}\, \mathbf{P} \cdot d\mathbf{Q} - F\, dt \tag{84}$$

and putting

$$\mathbf{p} = \sqrt{\mu a}\, \mathbf{P} ,$$

$$\mathbf{q} = \sqrt{1 - e^2}\, \mathbf{Q} - l\mathbf{P} ,$$

we deduce from Equation 84

$$\phi = \mathbf{p} \cdot d\mathbf{q} - F\, dt .$$

Thus $\mathbf{p}$ and $\mathbf{q}$ represent a purely vectorial canonical set of elements. We have

$$\frac{d\mathbf{q}}{dt} = + \operatorname{grad}_{\mathbf{p}} F ,$$

$$\frac{d\mathbf{p}}{dt} = - \operatorname{grad}_{\mathbf{q}} F .$$

CONCLUSION

The Pfaffian method is suggested for use in the search for new sets of elements and in the formation of equations for their variations. The application of vector analysis permits the formation of Pfaffian equations in a very compact and elegant form. A method of integration similar to von Zeipel's method (Reference 17) can be based on the expansion of the Pfaffian differential form in powers of a small parameter.

REFERENCES

1. Bilimovich, A., "Über die Anwendungen der Pfaffschen Methode in der Störungstheorie," *Astr. Nachr.* 273:161–178, 1943.
2. Milankovich, M., "On Application of Vectorial Elements in the Computation of the Planetary Perturbations," *Bull. Acad. Math. Natur.* (A), Belgrade, No. 6, 1939 (In Serbian).
3. Cartan, E., "Leçons sur les Invariants Intégraux," Paris; A. Hermann et Fils, 1922.

4. STRÖMGREN, B., *Pub. Med. Kobenhavns Obs.* No. 65, p. 5, 1929.
5. MUSEN, P., "Om Strömgren's Method of Special Perturbations," *J. Astronaut. Sci.* 8:48–51, Summer 1961.
6. HANSEN, P. A., "Fundamenta," Gotha: Carolum Glasser, p. 331, 1838.
7. MUSEN, P., "Application of Hansen's Theory to the Motion of an Artificial Satellite in the Gravitational Field of the Earth," *Journ. Geophys. Res.* 64(12): 2271–2279, December 1959.
8. Herrick, S., "A Modification of the Variation of Constants Method for Special Perturbations," Astron. Soc. Pacific Pub. 60:321–323, October 1948.
9. MUSEN, P., "Special Perturbations of the Vectorial Elements," *Astron. J.* 59(7):262–267, August 1954.
10. ECKERT, W. J., and BROUWER, D., "The Use of Rectangular Coordinates in the Differential Corrections of Orbits," *Astron. J.* 46(13):125–132, August 16, 1937.
11. MUSEN, P., and CARPENTER, L., "On the General Planetary Perturbations in Rectangular Coordinates," *J. Geophys. Res.* 68(9):2727–2734, May 1, 1963.
12. MUSEN, P., "On the Long-Period Lunar and Solar Effects in the Motion of an Artificial Satellite, 2," *J. Geophys. Res.* 66(9):2797–2805, September 1961.
13. COOK, G. E., "Luni-Solar Perturbations of the Orbit of an Earth Satellite," Royal Aeronautical Establishment Report, Farnborough, 1961.
14. KAULA, W. M., "Development of the Lunar and Solar Disturbing Functions for a Close Satellite," *Astron. J.* 67(5):300–303, June 1962; also NASA Technical Note D-1126, January 1962.
15. GIBBS, J. W., "Vector Analysis," New York: Charles Scribner's Sons, 1901, pp. 343-345.
16. MUSEN, P., "On a Modification of Hansen's Lunar Theory," *J. Geophys. Res.* 68(5):1439–1456, March 1, 1963; also NASA Technical Note D-1745, June 1963.
17. VON ZEIPEL, H., "Recherches sur le Mouvement des Petites Planètes," *Arkiv Matem. Astron. o Fysik*, 11(1):1–58, 1916–1917.

ON THE SIMULTANEOUS COMPUTATION OF THE SECULAR AND RESONANCE EFFECTS IN THE MOTION OF CELESTIAL BODIES*

PETER MUSEN

The stability of the orbit of a celestial body depends predominantly upon the long period perturbations in its elements. The long period effects produced by the sun and the moon can prolong or shorten the lifetime of a satellite considerably. In every attempt to solve the problem of stability of the asteroidal ring the long period effects must be taken into account. Unfortunately, no convenient expansion of the disturbing function exists for large values of the eccentricity, large values of the inclinations, or large values of the ratio of the semimajor axes of the disturbed and disturbing body. Thus numerical integration must be used.

In the problem of determining orbital stability the disturbing function cannot be used in its standard form, because it contains the combined effects of the long and short period terms. If the short period terms are not removed, then the integration step will be too short, and the accumulation of the errors from rounding off will be too great over a long time interval. Thus, before integration all short period effects were removed from the disturbing function by a numerical process which avoids the development into series. In a previous article by the author the suggestion was made to use Halphen's method to compute the effects caused by the secular terms.

However, the author feels that the results of computation cannot be considered complete if they do not include the near resonance effects. As a result, Halphen's method is extended by inclusion of the near resonance effects caused by the commensurability of the mean motions of the disturbed and disturbing bodies. Liouville's method reduces the problem to a single harmonic analysis. The introduction of a nonsingular set of elements permits the extension of the method to the cause of near circular orbits and to the case of low inclinations of the orbital planes.

LIST OF SYMBOLS

k = the Gaussian constant

ϵ = the angle between the equatorial and the ecliptical planes 1950.0

$\mathbf{r}$ = the position vector of the disturbed body

u = the eccentric anomaly of the disturbed body

f = the true anomaly of the disturbed body

$\ell, \omega, \Omega, \pi, i, e, a,$ = the standard elliptic elements of the disturbed body

$\mathbf{P}, \mathbf{Q},$ = Gibbs' vectorial elements of the disturbed body

σ = the angular distance of the departure point in the orbit plane of the disturbed body from the ascending node

χ = the orbital true longitude of the perigee

$$\xi = e \cos \chi$$

$$\eta = e \sin \chi$$

*Published as *NASA Technical Note* D-2152, June 1964.

L = the mean longitude of the disturbed body
$L_1 = \ell + \chi$ = the orbital mean longitude of the disturbing body

$$X = r \cos(f + \chi)$$

$$Y = r \sin(f + \chi)$$

$$p = \frac{\cos \frac{\Omega + \sigma}{2}}{\cos \frac{\Omega - \sigma}{2}} \tan \frac{i}{2}$$

$$q = \frac{\sin \frac{\Omega + \sigma}{2}}{\cos \frac{\Omega - \sigma}{2}} \tan \frac{i}{2}$$

$$s = \tan \frac{\Omega - \sigma}{2}$$

$\mathbf{r}'$ = the position vector of the disturbing body
u' = the eccentric anomaly of the disturbing body
ℓ', ω', Ω', π', i', e', a', n' = the standard elliptic elements of the disturbing body
$\mathbf{P}'$, $\mathbf{Q}'$, $\mathbf{R}'$ = Gibbs' vectorial elements of the disturbing body
ρ = the distance between the disturbed and the disturbing body
S = the component of the disturbing force in the direction of the radius vector of the disturbed body
T = the component of the disturbing force lying in the orbital plane and normal to the radius vector
W = the component of the disturbing force normal to the orbital plane.

INTRODUCTION

The problem of determining the long period effects in the motions of celestial bodies is a central problem in the determination of orbital stability over a long time interval. Two types of long period perturbations are of primary importance in treating the problem of stability:

1. The effects produced by the secular terms in the disturbing function. The arguments of the secular terms contain neither the mean anomaly of the disturbing body nor the mean anomaly of the disturbed body.

2. The effects produced by the commensurability of mean motions. If the ratio of the mean motions of the disturbed and the disturbing bodies can be approximated by a rational number, then a small divisor will appear when the integration is performed analytically. The terms producing such small divisors are named "the critical terms."

The long period effects as well as their interactions can be determined analytically, but only under the restrictions that the eccentricities or inclinations are small and that only one critical term is present.

The secular effects have been treated numerically with Halphen-Goriachev theory (References 1–4). The only restriction imposed on the elements by this method is that a very close approach between the disturbed and the disturbing bodies cannot be considered. The secular effects of the first and second order were computed by means of numerical integration over an interval of 10–20 years for artificial satellites, and over an interval of many thousands of years for minor planets.

Several unexpected features and large variations of the elements affecting their stability have been discovered (References 4 and 5).

However, the scheme previously used becomes incomplete if there are critical terms in the development of the disturbing function. The effects produced by the critical terms in the elements might become comparable with those produced by the secular terms, and in addition, the problem of the mutual influence of terms of both types arises.

COMPUTATION OF THE SYSTEM OF FORMULAS FOR SECULAR AND RESONANCE EFFECTS

The system of formulas given in this article is based on the application of the method of Liouville (Reference 6) and on Halphen's method. It takes into account the secular as well as the critical effects. The equations for variations of the elements are also given in the form which includes the cases of small eccentricity and small inclination. Let F(u, u′) be a function of the form

$$F(u, u') = \sum_{j=0}^{+\infty} \sum_{j'=-\infty}^{+\infty} \left[A_{j,j'} \cos(jl - j'l') + B_{j,j'} \sin(jl - j'l') \right]. \quad (1)$$

where

$$l = u - e \sin u ,$$

$$l' = u' - e' \sin u' ,$$

and the coefficients $A_{j,j'}$, $B_{j,j'}$ are functions of all the remaining elements. If it is assumed that

$$\frac{n'}{n} \approx \frac{i}{i'}$$

where i and i′ are relative primes, then the critica arguments have the form

$$k(il - i'l') .$$

By using the Liouville substitution (Reference 6),

$$l = i'\sigma' ,$$

$$l' = i\sigma' - \frac{\theta}{i'} ,$$

Equation 1 can be written in the form:

$$F(u, u') = \sum_{j=0}^{+\infty} \sum_{j'=-\infty}^{+\infty} \left\{ A_{j,j'} \cos\left[(ji' - j'i)\sigma' + \frac{j'}{i'}\theta \right] + B_{j,j'} \sin\left[(ji' - j'i)\sigma' + \frac{j'}{i'}\theta \right] \right\}. \quad (2)$$

The angle σ' is not contained in the argument if

$$ji' - j'i = 0 ,$$

or, consequently, if

$$\left.\begin{aligned} j &= pi , \\ j' &= pi' , \end{aligned}\right\} \quad (3)$$

where p=0, 1, 2,⋯. Let us designate the combination of all terms in F(u, u′) which do not contain σ' by $\Psi(\theta)$:

$$\Psi(\theta) = \sum_{p=0}^{+\infty} \left(A_{pi,pi'} \cos p\theta + B_{pi,pi'} \sin p\theta \right) .$$

By taking Equation 3 into account, it may be deduced from Equation 2 that

$$\Psi(\theta) = \frac{1}{2\pi} \int_0^{2\pi} F(u, u')\, d\sigma'$$

$$= \sum_{p=0}^{+\infty} \left(A_{pi,pi'} \cos p\theta + B_{pi,pi'} \sin p\theta \right) . \quad (4)$$

Putting $\theta = 0, \pi, \pi/2, 3\pi/2, \pi/4$, in Equation 4 yields:

$$\Psi(0) = A_{0,0} + A_{i,i'} + A_{2i,2i'} + A_{3i,3i'} + \cdots ,$$

$$\Psi(\pi) = A_{0,0} - A_{i,i'} + A_{2i,2i'} - A_{3i,3i'} + \cdots ,$$

$$\Psi\left(\frac{\pi}{2}\right) = A_{0,0} + B_{i,i'} - A_{2i,2i'} - B_{3i,3i'} + \cdots ,$$

$$\Psi\left(\frac{3\pi}{2}\right) = A_{0,0} - B_{i,i'} - A_{2i,2i'} + B_{3i,3i'} + \cdots ,$$

$$\Psi\left(\frac{\pi}{4}\right) = A_{0,0} + \frac{\sqrt{2}}{2}\left(A_{i,i'} + B_{i,i'}\right) + B_{2i,2i'} + \cdots .$$

It is rarely necessary to go beyond the critical term with the argument $2il - 2i'l'$. Thus, the coefficients $A_{2i,2i'}$, $B_{2i,2i'}$, etc. can be neglected and a set of simple formulas results:

$$A_{i,i'} = \frac{\Psi(0) - \Psi(\pi)}{2} , \quad (5)$$

$$B_{i,i'} = \frac{\Psi\left(\frac{\pi}{2}\right) - \Psi\left(\frac{3\pi}{2}\right)}{2} , \quad (6)$$

$$A_{2i,2i'} = \frac{\Psi(0) - \Psi\left(\frac{\pi}{2}\right) + \Psi(\pi) - \Psi\left(\frac{3\pi}{2}\right)}{4}, \tag{7}$$

$$B_{2i,2i'} = \Psi\left(\frac{\pi}{4}\right) - \frac{\sqrt{2}+1}{4}\left[\Psi(0) + \Psi\left(\frac{\pi}{2}\right)\right] + \frac{\sqrt{2}-1}{4}\left[\Psi(\pi) + \Psi\left(\frac{3\pi}{2}\right)\right]. \tag{8}$$

In the case of a large or moderate eccentricity set

$$u = i'\phi ;$$

then

$$l' = u' - e'\sin u'$$

$$= i\phi - \frac{ie}{i'}\sin i'\phi - \frac{\theta}{i'}, \tag{9}$$

and Equation 4 takes a form more convenient for numerical computations:

$$\Psi(\theta) = \frac{1}{2\pi}\int_0^{2\pi} F(u, u')\,\frac{r}{a}\,d\phi . \tag{10}$$

This last integral is computed as a simple arithmetical mean of the integrands of equidistant values of the angle ϕ. Now a collection of formulas can be established for the actual computation of the effect of resonance in the elements on the basis of the Liouville equations (Equations 5–8). Setting

$$A_1(\alpha) = \begin{bmatrix} +1 & 0 & 0 \\ 0 & +\cos\alpha & -\sin\alpha \\ 0 & +\sin\alpha & +\cos\alpha \end{bmatrix},$$

$$A_3(\alpha) = \begin{bmatrix} +\cos\alpha & -\sin\alpha & 0 \\ +\sin\alpha & +\cos\alpha & 0 \\ 0 & 0 & +1 \end{bmatrix},$$

we can deduce the Gibbs vectorial elements **P**, **Q**, **R** and **P′**, **Q′**, **R′** by means of the formulas:

$$[\mathbf{P}, \mathbf{Q}, \mathbf{R}] = A_1(\epsilon) \cdot A_3(\Omega) \cdot A_1(i) \cdot A_3(\omega) ,$$

$$[\mathbf{P}', \mathbf{Q}', \mathbf{R}'] = A_1(\epsilon) \cdot A_3(\Omega') \cdot A_1(i') \cdot A_3(\omega') .$$

In the case of an artificial satellite the elements ω and Ω are referred to the equator and

$$[\mathbf{P}, \mathbf{Q}, \mathbf{R}] = A_3(u) \cdot A_1(i) \cdot A_3(\omega) .$$

The coordinates of the disturbed body are

$$\left.\begin{aligned} x &= a\mathbf{P}_x(\cos u - e) + a\sqrt{1-e^2}\,\mathbf{Q}_x \sin u , \\ y &= a\mathbf{P}_y(\cos u - e) + a\sqrt{1-e^2}\,\mathbf{Q}_y \sin u , \\ z &= a\mathbf{P}_z(\cos u - e) + a\sqrt{1-e^2}\,\mathbf{Q}_z \sin u , \end{aligned}\right\} \tag{11}$$

and the coordinates of the disturbing body are

$$\left.\begin{aligned} x' &= a'P_x'(\cos u' - e') + a'\sqrt{1-e'^2}\,Q_x'\sin u' \ , \\ y' &= a'P_y'(\cos u' - e') + a'\sqrt{1-e'^2}\,Q_y'\sin u' \ , \\ z' &= a'P_z'(\cos u' - e') + a'\sqrt{1-e'^2}\,Q_z'\sin u' \ . \end{aligned}\right\} \tag{12}$$

The square of the mutual distance is

$$\rho^2 = r^2 + r'^2 - 2\mathbf{r}\cdot\mathbf{r}' \ . \tag{13}$$

Let the critical argument be

$$\theta = il - i'l' \ .$$

Set

$$u = i'\phi \ ,$$

$$u' - e'\sin u' = i\phi - \frac{\theta}{i'} - \frac{ie}{i'}\sin i'\phi \ .$$

The radial component S, the orthogonal component T, and the normal component W of the disturbing force can be considered functions of the angle ϕ and the critical argument θ. Thus

$$rS = km'\left(\frac{1}{\rho^3} - \frac{1}{r'^3}\right)\mathbf{r}\cdot\mathbf{r}' - km'\frac{r^2}{\rho^3} = rS(\phi, \theta) \ , \tag{14}$$

$$rT = km'\left(\frac{1}{\rho^3} - \frac{1}{r'^3}\right)(\mathbf{R}\cdot\mathbf{r}\times\mathbf{r}') = rT(\phi, \theta) \ , \tag{15}$$

$$W = km'\left(\frac{1}{\rho^3} - \frac{1}{r'^3}\right)\mathbf{R}\cdot\mathbf{r}' = W(\phi, \theta) \ . \tag{16}$$

From the following standard equations for variations of the elements

$$\frac{dn}{dt} = -\frac{3k}{a^2}\left(S\frac{ae\sin f}{\sqrt{1-e^2}} + T\frac{a^2}{r}\sqrt{1-e^2}\right) \ ,$$

$$\frac{de}{dt} = \frac{na(1-e^2)}{ke}\left(S\frac{ae\sin f}{\sqrt{1-e^2}} + T\frac{a^2}{r}\sqrt{1-e^2}\right) - \frac{na\sqrt{1-e^2}}{ke}Tr \ ,$$

$$\frac{d\pi}{dt} = \frac{na\sqrt{1-e^2}}{ke}\left[-S\cos f + T\left(1 + \frac{1}{1-e^2}\frac{r}{a}\right)\sin f\right] + 2\sin^2\frac{i}{2}\frac{d\Omega}{dt} \ ,$$

$$\frac{dL}{dt} = -\frac{2nar}{k}S + \left(1 - \sqrt{1-e^2}\right)\frac{d\pi}{dt} + 2\sqrt{1-e^2}\sin^2\frac{i}{2}\frac{d\Omega}{dt} \ ,$$

$$\sin i\frac{d\Omega}{dt} = \frac{nar}{k\sqrt{1-e^2}}W\sin(f+\omega) \ ,$$

$$\frac{di}{dt} = \frac{nar}{k\sqrt{1-e^2}}W\cos(f+\omega) \ .$$

the short period and the secular terms may be eliminated by using the process described above, and the transformed equations will contain only the effect of the critical terms. By designating

$$A_{1,1}' = K_1 , \qquad B_{1,1}' = K_2 , \qquad A_{2i,2i}' = K_3 , \qquad B_{2i,2i}' = K_4 ,$$

the derivative of an element E becomes

$$\frac{dE}{dt} = K_1 \cos\theta + K_2 \sin\theta + K_3 \cos 2\theta + K_4 \sin 2\theta . \tag{17}$$

Let us introduce the following notations:

$$\frac{f(\phi, 0) - f(\phi, \pi)}{2} = f_1(\phi) ,$$

$$\frac{f\left(\phi, \frac{\pi}{2}\right) - f\left(\phi, \frac{3\pi}{2}\right)}{2} = f_2(\phi) ,$$

$$\frac{f(\phi, 0) - f\left(\phi, \frac{\pi}{2}\right) + f(\phi, \pi) - f\left(\phi, \frac{3\pi}{2}\right)}{4} = f_3(\phi) ,$$

$$f\left(\phi, \frac{\pi}{4}\right) - \frac{\sqrt{2}+1}{4}\left[f(\phi, 0) + f\left(\phi, \frac{\pi}{2}\right)\right] + \frac{\sqrt{2}-1}{4}\left[f(\phi, \pi) + f\left(\phi, \frac{3\pi}{2}\right)\right] = f_4(\phi) .$$

These values of the coefficients K_j (j = 1, 2, 3, 4) are deduced:

in dn/dt

$$K_j^{(n)} = -\frac{3k}{2\pi a}\int_0^{2\pi}\left(S_j\, e \sin u + T_j \sqrt{1-e^2}\right) d\phi ; \tag{18}$$

in de/dt

$$K_j^{(e)} = \frac{\sqrt{a(1-e^2)}}{2\pi}\int_0^{2\pi}\left[\sqrt{1-e^2}\ S_j \sin u + T_j\left(-\frac{3}{2}\, e + 2\cos u - \frac{1}{2}\, e\cos 2u\right)\right] d\phi ; \tag{19}$$

in dπ/dt

$$K_j^{(\pi)} = \frac{\sqrt{a(1-e^2)}}{2\pi e}\int_0^{2\pi}\left[-S_j(\cos u - e) + T_j\left(1 + \frac{r}{a}\,\frac{1}{1-e^2}\right)\sqrt{1-e^2}\ \sin u\right] d\phi + 2\sin^2\frac{i}{2}\, K_j^{(\Omega)} ; \tag{20}$$

in dL/dt

$$K_j^{(L)} = \frac{e^2}{1+\sqrt{1-e^2}}\, K_j^{(\pi)} + \sqrt{1-e^2}\, K_j^{(\Omega)}\, 2\sin^2\frac{i}{2} - \frac{2\sqrt{a}}{2\pi}\int_0^{2\pi} S_j\,\frac{r^2}{a^2}\, d\phi ; \tag{21}$$

in dΩ/dt

$$K_j^{(\Omega)} = \frac{1}{2\pi \sin i}\sqrt{\frac{a}{1-e^2}}\int_0^{2\pi} W_j\,\frac{r}{a}\left[(\cos u - e)\sin\omega + \sqrt{1-e^2}\ \sin u\cos\omega\right] d\phi ; \tag{22}$$

in di/dt

$$K_j^{(i)} = \frac{1}{2\pi}\sqrt{\frac{a}{1-e^2}}\int_0^{2\pi} W_j \frac{r}{a}\left[(\cos u - e)\cos\omega - \sqrt{1-e^2}\,\sin u \sin\omega\right] d\phi \,. \tag{23}$$

It is interesting to note that Equations 18–23 are similar in form to the equations for the computation of secular effects. The cases of small inclination and small eccentricity deserve special attention. Equations 20 and 22 contain a "small divisor" if i or e is very small. Instead of the standard orbital elements, a nonsingular set of elements can be introduced. The set of elements

$$\left.\begin{aligned} p &= \frac{\cos\frac{\Omega+\sigma}{2}}{\cos\frac{\Omega-\sigma}{2}}\tan\frac{i}{2}\,, \\ q &= \frac{\sin\frac{\Omega+\sigma}{2}}{\cos\frac{\Omega-\sigma}{2}}\tan\frac{i}{2}\,, \\ s &= \tan\frac{\Omega-\sigma}{2}\,, \end{aligned}\right\} \tag{24}$$

$$\left.\begin{aligned} \xi &= e\cos\chi\,, \\ \eta &= e\sin\chi\,, \end{aligned}\right\} \tag{25}$$

determines the position of the osculating ellipse without the introduction of a singularity for $i=0$ or $e=0$. The use of Equations 25 for the computation of perturbations was suggested by the author in his article on Strömgren's perturbations (Reference 7). In fact, p, q, and s are the components of Gibbs' rotation vector (Reference 8). From the equations

$$\sin i\,\frac{d\Omega}{dt} = \frac{rW}{\sqrt{a(1-e^2)}}\sin(f+\omega)\,,$$

$$\frac{di}{dt} = \frac{rW}{\sqrt{a(1-e^2)}}\cos(f+\omega)\,,$$

$$\frac{d\sigma}{dt} = \cos i\,\frac{d\Omega}{dt}\,,$$

it is deduced that

$$\left.\begin{aligned} \frac{dp}{dt} &= \frac{W}{2\sqrt{a(1-e^2)}}\left[(1+p^2)X + (pq-s)Y\right], \\ \frac{dq}{dt} &= \frac{W}{2\sqrt{a(1-e^2)}}\left[(pq+s)X + (1+q^2)Y\right], \\ \frac{ds}{dt} &= \frac{W}{2\sqrt{a(1-e^2)}}\left[(ps-q)X + (qs+p)Y\right]. \end{aligned}\right\} \tag{26}$$

It can be seen that no small divisor is present, even if the inclination is small. X and Y are the coordinates of the disturbing body in an ideal system of coordinates with the X- and Y-axes in the orbital plane. They can be written in the form:

$$\begin{aligned} X &= r\cos(f+\chi) \\ &= a\left[\left(\frac{1+\sqrt{1-e^2}}{2} + \frac{\xi^2-\eta^2}{2}\,\frac{1}{1+\sqrt{1-e^2}}\right)\cos\lambda + \frac{\xi\eta}{1+\sqrt{1-e^2}}\sin\lambda - \xi\right], \end{aligned} \tag{27}$$

$$\begin{aligned} Y &= r\sin(f+\chi) \\ &= a\left[\left(\frac{1+\sqrt{1-e^2}}{2} - \frac{\xi^2-\eta^2}{2}\,\frac{1}{1+\sqrt{1-e^2}}\right)\sin\lambda + \frac{\xi\eta}{1+\sqrt{1-e^2}}\cos\lambda - \eta\right], \end{aligned} \tag{28}$$

where λ is the eccentric orbital longitude,

$$\lambda = u + \chi \,. \tag{29}$$

Also (Reference 9)

$$\frac{d\xi}{dt} = \sqrt{a(1-e^2)}\left[S\sin(f+\chi) + T\left(1+\frac{r}{a}\frac{1}{1-e^2}\right)\cos(f+\chi) + \frac{r}{a}\frac{1}{1-e^2}\,T\xi\right], \tag{30}$$

$$\frac{d\eta}{dt} = \sqrt{a(1-e^2)}\left[-S\cos(f+\chi) + T\left(1+\frac{r}{a}\frac{1}{1-e^2}\right)\sin(f+\chi) + \frac{r}{a}\frac{1}{1-e^2}\,T\eta\right]. \tag{31}$$

We write the critical argument in the form:

$$\alpha = iL_1 - i'l' \,.$$

Then the Liouville substitution becomes

$$L_1 = i'\sigma' \,,$$

$$l' = i\sigma' - \frac{\alpha}{i'} \,.$$

Considering the disturbing force as a function of σ' and α, set

$$\frac{f(\sigma', 0) - f(\sigma', \pi)}{2} = f_1(\sigma'), \text{ etc.}$$

From Equations 26, 30, and 31 the following expressions are deduced for the coefficients of the critical terms:

$$K_j^{(p)} = \frac{1}{4\pi\sqrt{a(1-e^2)}}\int_0^{2\pi} W_j\left[(1+p^2)\,X + (pq-s)\,Y\right]d\sigma' \,, \tag{32}$$

$$K_j^{(q)} = \frac{1}{4\pi\sqrt{a(1-e^2)}}\int_0^{2\pi} W_j\left[(pq+s)\,X + (1+q^2)\,Y\right]d\sigma' \,, \tag{33}$$

$$K_j^{(s)} = \frac{1}{4\pi\sqrt{a(1-e^2)}}\int_0^{2\pi} W_j\left[(ps-q)\,X + (qs+p)\,Y\right]d\sigma' \,, \tag{34}$$

$$K_j^{(\xi)} = \frac{1}{2\pi}\sqrt{\frac{1-e^2}{a}}\int_0^{2\pi}\left[+S_jY + T_j\left(1+\frac{r}{a}\frac{1}{1-e^2}\right)X + \frac{r^2}{a^2}\frac{1}{1-e^2}\,T_j\xi\right]\frac{a}{r}\,d\sigma' \,, \tag{35}$$

$$K_j^{(\eta)} = \frac{1}{2\pi}\sqrt{\frac{1-e^2}{a}}\int_0^{2\pi}\left[-S_jX + T_j\left(1+\frac{r}{a}\frac{1}{1-e^2}\right)Y + \frac{r^2}{a^2}\frac{1}{1-e^2}\,T_j\xi\right]\frac{a}{r}\,d\sigma' \,. \tag{36}$$

The expression for the position vector of the disturbed body to be used in the computations of the integrands is:

$$r = \frac{A_3(\epsilon)\cdot\Gamma}{1+p^2+q^2+s^2}\begin{bmatrix}X\\Y\\0\end{bmatrix}, \tag{37}$$

where the elements γ_{ij} (i is the row ind· x and j is the column index) of the matrix Γ are determined from the formulas (Reference 10):

$$\left.\begin{aligned}
\gamma_{11} &= +p^2 - q^2 - s^2 + 1 , & \gamma_{21} &= +2(s+pq) , & \gamma_{31} &= +2(sp-q) ,\\
\gamma_{12} &= -2(s-pq) , & \gamma_{22} &= -p^2 + q^2 - s^2 + 1 , & \gamma_{32} &= +2(p+sq) ,\\
\gamma_{13} &= +2(q+ps) , & \gamma_{23} &= -2(p-sq) , & \gamma_{33} &= -p^2 - q^2 + s^2 - 1 .
\end{aligned}\right\} \quad (38)$$

X and Y are given by Equations 27–29. Kepler's equation is replaced by

$$\lambda - \xi \sin\lambda + \eta \cos\lambda = L_1 \qquad (39)$$

in a way similar to Herget's method of writing Kepler's equation for small eccentricities (Reference 11). Similar systems of equations can be established for numerical integration of the secular effects for the case of a small eccentricity or a small inclination.

The effects of the secular and critical terms must be integrated together. Again Halphen's method may be used for the computations of the secular effects. A complete collection of formulas is given in the author's previous article (Reference 3). However, if i or e, or both, are small, the system requires some modification.

For the values, say, $\lambda = 0°, 10°, \cdots, 350°$, compute:

$$\begin{bmatrix} x \\ y \\ z \end{bmatrix} = \frac{1}{1+p^2+q^2+s^2} \begin{bmatrix} P_x' & P_y' & P_z' \\ Q_x' & Q_y' & Q_z' \\ R_x' & R_y' & R_z' \end{bmatrix} \cdot \Gamma \cdot \begin{bmatrix} X \\ Y \\ 0 \end{bmatrix} . \qquad (40)$$

X and Y are defined by Equations 27 and 28. Kepler's equation is taken in the form of Equation 39. Then, as in the previous article, put

$$\alpha = x' + e'a ,$$

$$\beta = y ,$$

$$\gamma = z .$$

Equations 4–9 of Reference 3 remain unchanged, but Equation 10, p. 121, for the variations of the elements must be replaced by:

$$\frac{dn}{dt} = -\frac{3k}{a}\frac{1}{2\pi}\int_0^{2\pi}\left[\frac{S_0(Y\xi - X\eta)}{\sqrt{1-e^2}} + T_0\sqrt{1-e^2}\right]d\lambda , \qquad (41)$$

$$\frac{d\xi}{dt} = \sqrt{\frac{1-e^2}{a}}\frac{1}{2\pi}\int_0^{2\pi}\left[S_0 Y + T_0\left(1+\frac{r}{a}\frac{1}{1-e^2}\right)X + \left(\frac{r}{a}\right)^2\frac{a}{1-e^2}T_0\xi\right]d\lambda , \qquad (42)$$

$$\frac{d\eta}{dt} = \sqrt{\frac{1-e^2}{a}}\frac{1}{2\pi}\int_0^{2\pi}\left[-S_0 X + T_0\left(1+\frac{r}{a}\frac{1}{1-e^2}\right)Y + \left(\frac{r}{a}\right)^2\frac{a}{1-e^2}T_0\eta\right]d\lambda , \qquad (43)$$

$$\frac{dp}{dt} = \frac{1}{2\sqrt{a\left(1-e^2\right)}} \frac{1}{2\pi} \int_0^{2\pi} W_0 \frac{r}{a} \left[\left(1+p^2\right) X + (pq - s) Y\right] d\lambda \ , \tag{44}$$

$$\frac{dq}{dt} = \frac{1}{2\sqrt{a\left(1-e^2\right)}} \frac{1}{2\pi} \int_0^{2\pi} W_0 \frac{r}{a} \left[(pq + s) X + \left(1+q^2\right) Y\right] d\lambda \ , \tag{45}$$

$$\frac{ds}{dt} = \frac{1}{2\sqrt{a\left(1-e^2\right)}} \frac{1}{2\pi} \int_0^{2\pi} W_0 \frac{r}{a} \left[(ps - q) X + (qs + p) Y\right] d\lambda \ , \tag{46}$$

$$\frac{dL_1}{dt} = -\frac{2}{\sqrt{a}} \frac{1}{2\pi} \int_0^{2\pi} \left(\frac{r}{a}\right)^2 S_0 \, d\lambda + \frac{\xi \frac{d\eta}{dt} - \eta \frac{d\xi}{dt}}{1 + \sqrt{1-e^2}} \ . \tag{47}$$

CONCLUSIONS

The combined effects of the secular and critical terms have a deciding influence in determining the orbital stability over a long time interval. Some approximate schemes based on the process of averaging lead to conclusions concerning the stability of the ring of minor planets which definitely require a further check. The proposed scheme will at least give a more accurate answer over an interval of some thousands of years. Our knowledge about the stability of the orbits of artificial satellites is still incomplete. The described method will be programmed in order to investigate these problems. The application of the method of secular effects leads to some conclusions which were not anticipated. It remains to be seen what interesting conclusions will follow from the superposition of all long period terms and from the computations of their direct actions, as well as their interactions, in the problems of orbital stability of the minor planets and artificial satellites.

REFERENCES

1. Halphen, G. H., "Traité des Fonctions Elliptiques et de Leurs Applications," Paris: Gauthier-Villars et Fils, 1888, V.2.
2. Goriachev, N. N., "On the Method of Halphen of the Computation of Secular Perturbations," University of Tomsk, 1937, pp. 1–115.
3. Musen, P., "A Discussion of Halphen's Method, Part 1," *Rev. Geophys* 1 (1):85–122, 1963.
4. Smith, A. J., Jr., "A Discussion of Halphen's Method for Secular Perturbations and its Application to the Determination of Long Range Effects in the Motions of Celestial Bodies. Part II.," NASA Technical Report (in press).
5. Shute, B. E., "A Cislunar Orbit (IMP)" *Astronom. J.* 67(5):283, June 1962 (abstract).
6. Liouville, J., "Note Sur le Calcul des Inégalités Périodiques de Mouvement des Planétes," *J. Math. Pures Appliquées* 1:197–210, 1836.
7. Musen, P., "On Stromgrens Method of Special Perturbations," *J. Astronaut. Sci.* 8(2):48, 1961.
8. Gibbs, J. W., "Vector Analysis," (E. B. Wilson, ed.): New York: Charles Scribner's Sons, 1901, pp. 343–345.
9. Tisserand, F., "Traité de la Mécanique céleste," Paris: Gauthier-Villars et Fils, 1896, V. 4, p. 328.
10. Musen, P. "Application of Hansen's Theory to the Motion of an Artificial Satellite in the Gravitational Field of the Earth," *J. Geophys, Res.* 64(12): 2271–2279, December 1959.

N64-23737

DETERMINATION OF THE TRIAXIALITY OF THE EARTH FROM OBSERVATIONS ON THE DRIFT OF THE SYNCOM II SATELLITE*

C. A. WAGNER

SUMMARY

The near 24-hour Syncom II satellite (with an almost circular orbit) has been under continuous observation by range and range-rate radar and minitrack stations for 7 months since mid-August 1963, when the orbit was relocated, placing its mean longitude at about 55 degrees west of Greenwich. During the first 4 months of this period, the satellite was allowed to drift free in the gravity fields of the earth, sun, and moon. In this first free-drift period, the satellite experienced a mean daily drift acceleration of its ascending node (with respect to Greenwich) of

$$-(1.27\pm.02)\times10^{-3} \text{ degrees/day}^2. \quad (1)$$

The average growth of the semimajor axis for this period was

$$(.0993\pm.0042) \text{ km/day}. \quad (2)$$

These values, checked by a simulated particle trajectory run on the Goddard ITEM program, confirm a significant longitude-dependent earth-gravity potential. The existence of a "triaxial earth" has been a speculation of geodesists since the early years of this century.

During the last 3 months of this 7-month drift period, starting at the end of November 1963, Syncom II was relocated at about 60 degrees west of Greenwich. In this period, the mean daily drift acceleration of the ascending node was

$$-(1.32\pm.02)\times10^{-3} \text{ degrees/day}^2. \quad (3)$$

The average growth of the semimajor axis for this period was

$$(.0994\pm.0080) \text{ km/day}. \quad (4)$$

Combining the results of (1) through (4) above for the two separate drift periods, it is estimated (on the basis of a triaxial geoid only) that the absolute magnitude of the longitude dependent-gravity coefficient J_{22} is

$$J_{22}=-(1.7\pm.05)\times10^{-6}.$$

This value corresponds to a difference in major and minor earth-equatorial radii of

$$(a_e-b_e)=213\pm6 \text{ feet}$$

The best present estimate of the position of the earth's major equatorial axis is

$$\lambda_{22}=19\pm6 \text{ degrees west of Greenwich.}$$

In view of previous estimates of the higher order tesseral harmonics of the earth's field, the true value of J_{22}, separated from the small influence of gravity anomalies of third and higher order on the reduction for a triaxial earth only at "synchronous" altitudes, will probably be somewhat higher than the -1.7×10^{-6} reported herein. The true value of J_{22}, however, is not likely to be greater than -2.2×10^{-6} or smaller than -1.6×10^{-6}. The true location of the earth equator's major axis is not expected to differ significantly from that reported herein, when all higher tesseral harmonics are accounted for. (See Appendix B.)

*Published as *Goddard Space Flight Center Document* X-621-64-90, April 1964.

The reported value of $J_{22} = -1.7 \times 10^{-6}$ implies that a maximum tangential velocity correction of

$$\Delta V_T = 5.36 \text{ ft./sec./year}$$

is required to keep a satellite with a 24-hour circular equatorial orbit continuously "on station" at a longitude midway between the longitudes of the equatorial major and minor axes of the earth. The original "conservative" Syncom I design requirement of $\Delta V_T = 17$ ft./sec./year correction capability was based on the longitude-dependent earth field of Izsak (January 1961), which is now outdated. (See Appendix B and Reference 4.)

INTRODUCTION

SUMMARY OF PREVIOUS INVESTIGATIONS AND DISCUSSION OF RESULTS

The question of the existence and extent of the longitude-dependence of the earth's external gravity field has concerned geodesists since the early years of this century. (See Reference 1 for example.) The existence of a longitude-dependent field implies the existence of inhomogeneities and states of stress within the earth which are of fundamental importance to all dynamical theories of the earth's interior.

In Appendix B, I have summarized 23 reductions of gravimetric, astro-geodetic, and satellite gravity data reporting longitude-dependent terms in the earth's external gravity field represented as a series of spherical harmonics. Ten of these reductions are based on worldwide surface-gravity measurements only. Although surface measurements have the advantage of providing an excellent sampling of the field in latitude and longitude, they are seriously affected by even small uncertainties in station position with respect to the mean earth geoid, as these are of the same order-of-magnitude as the *reported* geoid deviations caused by longitude-dependent gravity.

Of the 12 satellite reduced tesseral gravity fields, those of Kozai (1962), Izsak (July 1963), Kaula (September 1963), and Guier (1963) show good general agreement in the eastern hemisphere when the constants are used as a set. All of these observers are aware, nevertheless, of the high degree of uncertainty in the reported values of the individual coefficients themselves, this uncertainty being due mainly to unresolved station-datum errors and to the limited sampling of the field from observations on a small number of medium-altitude, medium-inclination satellites.

As late as July 1963, Izsak stated (Reference 2): "It might be some time before one can arrive at definite conclusions regarding the longitude dependence of the earth's gravity field." The presence of Syncom II, high over the earth with a nearly stationary, narrow figure-8 ground track centered close to the equator, dramatically alters this gloomy outlook. The 24-hour satellite is high enough to be unaffected by the earth's atmosphere, yet is close enough to the earth to be protected from the solar wind by the "magnetosphere" of the earth, and to remain essentially unaffected by sun or moon gravity.

In theory, as the ground track is nearly stationary, any small earth-gravity anomaly in longitude will in time, cause significant drift of the ground-track configuration. In theory too, only observations of the longitude of the satellite from a single ground station are necessary to reveal this effect of the "tesseral" gravity field over an extended period of time. Long-term observations of the longitude drift of one or more 24-hour satellites should reveal the exact nature of the tesseral-gravity field to at least the third order without essential difficulty. The great height of the 24-hour satellite tends to cancel out the individual contributions to the longitudinal drift of anomalies higher than about the fourth order. It is fortunate that the initial slow westward drift of the ground track of Syncom II (August 1963 to March 1964) appears to have occurred relatively close to a point midway between the triaxial earth's major and minor equatorial axes where the perturbation of the second tesseral-gravity anomaly, for which the reduction was made, is greatest. A weighted average of the longitude-perturbation fields of Kozai (1962), Zhongolovitch (1957), Kaula (September 1963), and Izsak (July 1963), at the altitude and longitude of Syncom II during this period, shows that the second tesseral should be contributing about 80 to 85 percent of the perturbing force. If further observations of this and other 24-hour satellites confirm this estimate, then the magnitude of the dominant J_{22} potential term, separated from higher order effects, will increase by 25 percent at most from the value reported here, which is based on the assumption

that only the triaxial earth-gravity field is being measured by the drift observations. The reported location of the major equatorial axis of the triaxial earth ellipsoid is not expected to change significantly with this later refinement.

In summary, long-term observations on the drift of Syncom II have already established to a high degree of certainty that:

1. The earth must be considered to be a "triaxial ellipsoid" (for example, having a sea-level surface of this form) for the purposes of 24-hour satellite design. (For broader geodetic purposes; a significant longitude dependent gravity field exists, defining:

$$2.2\times10^{-6}<|J_{22}|<1.6\times10^{-6};$$
$$-25^\circ<\lambda_{22}<-13^\circ.)$$

2. The difference between the major and minor equatorial radii of that ellipsoid is not less than 200 feet nor greater than 225 feet.

3. The location of the major equatorial axis of the "triaxial geoid" is between 13 degrees and 25 degrees west of Greenwich.

It may be added that the study of simulated 24-hour satellite drift in a triaxial earth field, influenced also by sun and moon gravity and by sun-radiation pressure perturbations, shows that the theory of longitude drift presented in this report is substantially unaffected by all perturbations except that due to the earth's elliptical equator and possible higher order longitude-dependent earth-gravity anomalies.

1. Basic Theory of this Reduction

(Determination of the Longitude Drift and Orbit Expansion for a 24-Hour Satellite With a Near-Circular Orbit Affected by a Small But Persistent Tangential Perturbing Force.)

The dominant perturbations of a 24-hour equatorial satellite in a higher order earth-gravity field have been derived many times in the literature (References 3, 4, 5, and 6). In these references, the perturbations were found by directly linearizing the equations of motion themselves and displaying the perturbed motion in appropriate geographic coordinates; no attempt was made to treat the drift of the inclined 24-hour satellite.

In this report, I will depart from this rather involved and difficult-to-visualize procedure of linearization-of-the-equations-of-motion. Instead, I will show how simple it is to derive the dominant drift and orbit-expansion equations for the 24-hour satellite by dealing with what can be called "the perturbation of the 2-body energy" of the geographically stationary satellite by the small but persistent longitude-dependent earth-gravity force. This paper will not discuss in detail the limits of validity of the expressions derived. Instead, to assess the accuracy with which these expressions predict the satellite's behavior, simulated trajectories with typical Syncom II orbit elements have been run on Goddard's particle program "ITEM." These trajectories (Appendix A) confirm the validity of the derived drift equations to an accuracy well within the "noise levels" in the orbital elements reported for Syncom II. The equations are essentially the same as those which P. Musen has derived by a more general but more complex "energy perturbation" method (Reference 7).

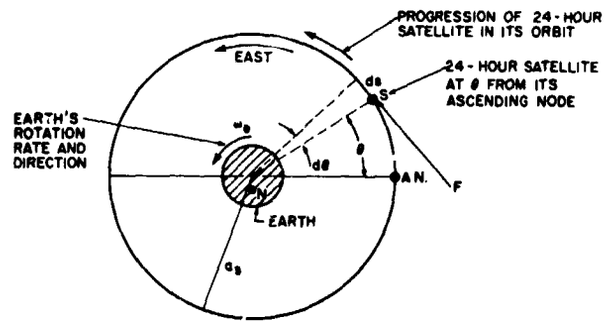

FIGURE 1.—Orbit plane of a 24-hour satellite, looking southerly.

In Figure 1, F is a small earth-gravity perturbation force acting tangentially to an initial circular 24-hour satellite orbit; ds is a small arc length of the satellite's path around the earth. At the beginning of the dynamics, the total energy (the sum of potential and kinetic) of the satellite in a spherical earth-gravity field (Reference 8) is

$$E=-\frac{\mu_E}{2a_s} \qquad (1)$$

where μ_E is the earth's gaussian gravity constant (3.986×10^5 km^3/sec^2). The energy added to the satellite by F per day is

$$\Delta E = \oint F ds = 2\pi a_s \bar{F}, \tag{2}$$

where $\bar{F} = (1/2\pi)\oint F d\theta \cdot F$, in units of force per unit mass, is the orbit averaged energy perturbing force. If the orbit is purely circular, only a tangential perturbation force can cause a change in the total energy. The ITEM simulated trajectories in Appendix A and the real Syncom II orbits both maintain eccentricities of the order of 0.0001 for periods up to 100 days. Equation (2) assumes the eccentricity is zero for the 24-hour satellite of semimajor axis a_s.

From (1), the change in energy of a 24-hour satellite is accompanied by a change in semi-major axis expressed by

$$\Delta E = \frac{\mu_E a_s}{2(a_s)^2}, \quad \text{or}$$

$$\Delta a_s = \frac{2(a_s)^2 \Delta E}{\mu_E}. \tag{3}$$

Substituting (2) into (3), the change in semimajor axis of the 24-hour near-circular orbit, per day, is approximately given by

$$\Delta a_s = \frac{4\pi (a_s)^3 \bar{F}}{\mu_E}. \tag{4}$$

From Kepler's third law, the period of a 24-hour orbit as a function of its semimajor axis is

$$T_s = \frac{2\pi (a_s)^{3/2}}{(\mu_E)^{1/2}}. \tag{5}$$

Thus, if the semimajor axis changes by Δa_s, the period change is given by

$$\Delta T_s = \frac{3\pi (a_s)^{1/2} \nabla a_s}{(\mu_E)^{1/2}}. \tag{6}$$

Substituting (4) into (6), the change in period, per day, of a 24-hour circular orbit is given by

$$\Delta T_s = \frac{12\pi^2 (a_s)^{7/2} \bar{F}}{(\mu_E)^{1/2}}. \tag{7}$$

The apparent net longitudinal drift rate of the 24-hour satellite's ground track with respect to the surface of the earth after the first sidereal day is

$$\dot{\lambda}(t = 1 \text{ sidereal day}) = -\frac{(\Delta T_s) 2\pi}{T_s} (\text{radians/sidereal day}) \tag{8}$$

(See Reference 9 for example). The minus sign is taken in (8) because a gain in period is accompanied by a decrease in net geographic longitude for the initially 24-hour satellite (for example, for the daily geographic position of the ascending node). Combining Equations (7) and (5) in (8) gives

$$\dot{\lambda}(t = 1 \text{ sid. day}) = -\frac{12\pi^2 \bar{F}}{\mu_E/(a_s)^2} \text{ (rad./sid. day)}. \tag{9}$$

As the gain in semimajor axis is small over one day (and, in fact, small compared to a_s, for the entire libration period of the satellite in the triaxial earth field), the drift rate will continue to build up linearly with time initially, adding increments of (9) each day. Thus, the net longitudinal drift acceleration of an initially 24-hour satellite is

$$\ddot{\lambda} = -\frac{12\pi^2 \bar{F}}{\mu_E/(a_s)^2} \text{ (rad./sid. day}^2\text{)} \tag{10}$$

Rewriting (4) as

$$\dot{a} = \frac{4\pi (a_s)^3 F}{\mu_E}, \text{ (length units/sid. day)} \tag{11}$$

gives the expansion rate of the initially 24-hour near-circular satellite orbit due to a small but persistently acting orbit-averaged tangential perturbing force $\bar{F}$.

2. Evaluation of the Perturbing Force

Figure 2 shows the position of the 24-hour satellite with respect to the earth and the celestial sphere. F_r, F_ϕ and F_λ, earth-gravity perturbing forces in the radial, latitude, and longitude directions, are assumed to be acting on the satellite at s. Considering only the earth-gravity perturbation forces arising from the ellipticity of the earth's equator (Reference 10), Appendix B gives these forces as

$$F = \frac{\mu_E (R_0/a_s)^2}{(a_s)^2} \left\{ 9 J_{22} \cos^2 \phi \cos 2(\lambda - \lambda_{2^{2,0}}) \right\} \tag{12}$$

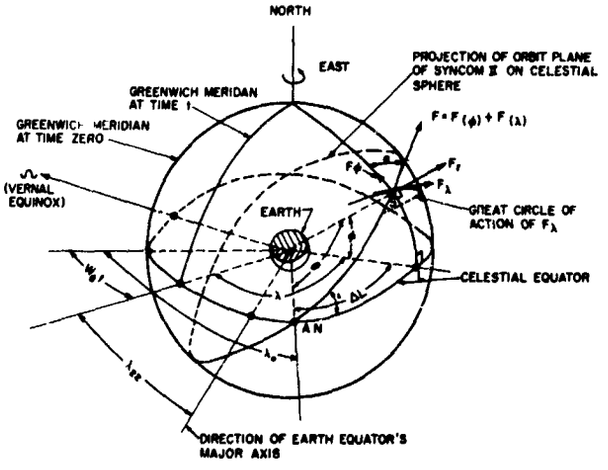

FIGURE 2.—Position of a 24-hour satellite with a near-circular orbit with respect to the earth and the celestial sphere.

$$F_\phi = \frac{\mu_E (R_0/a_s)^2}{(a_s)^2}\{6J_{22}\cos\phi\sin\phi\cos 2(\lambda-\lambda_{22})\}, \tag{12A}$$

$$F_\lambda = \frac{\mu_E (R_0/a_s)^2}{(a_s)^2}\{6J_{22}\cos\phi\sin 2(\lambda-\lambda_{22})\}. \tag{13}$$

As long as the orbit is nearly circular, F_r will have negligible contribution to F. The contribution to F from F_ϕ is:

$$F_{(\phi)} = F_\phi\cos\alpha = K\sin\phi\cos\phi\cos\alpha\cos 2(\lambda-\lambda_{22}) \tag{14}$$

K is a constant for a single orbit.

$$K = 6J_{22}\left(\frac{\mu_E R_0^2}{(a_s)^4}\right). \tag{14A}$$

In the right spherical triangle AN, s, L, note the following trigonometric relations:

$$\cos(i) = \frac{\tan\Delta L}{\tan\theta}, \tag{15A}$$

$$\cos\alpha = \frac{\tan\phi}{\tan\theta}, \tag{15B}$$

$$\sin\phi = \sin(i)\sin\theta, \tag{15C}$$

$$\sin\alpha = \frac{\cos(i)}{\cos\phi}. \tag{15D}$$

From (15A),

$$\Delta L = \tan^{-1}[\tan\theta\cos(i)]. \tag{16}$$

Let the geographic longitude of the satellite at the ascending node (AN) be λ_0. Counting time from this orbital position, the geographic longitude of the 24-hour satellite at s in its near-circular orbit is

$$\lambda = \lambda_0 + \Delta L - \omega_{et} \text{ (Figure 2)}$$

or, using (16),

$$\lambda = \lambda_0 + \tan^{-1}[\tan\theta\cos(i)] - \omega_{et} \tag{17}$$

w_e is the earth's sidereal rotation rate. For the 24-hour satellite (starting the dynamics with S. at A.N., for convenience), $\theta \doteq w_{er}$, so that (17) becomes

$$\lambda = \lambda_0 + \tan^{-1}[\tan\theta\cos(i)] - \theta, \tag{18}$$

approximately. The function $\tan^{-1}[\tan\theta\cos(i)] - \theta$ is even about $\theta=0$ and $\theta=\pi/2$, with a period of π, and behaves like a somewhat distorted sine function (Figure 3 and Appendix C). Call this function $\Delta\lambda$ and note that for $i<33$ degrees, $\Delta\lambda$ is always less than 5°. Thus, using (18) and assuming i is sufficiently small ($i<45°$ proves to be a sufficient restriction on the inclination), $\cos 2(\lambda-\lambda_{22})$ for the 24-hour satellite can be approximated by

$$\cos 2(\lambda-\lambda_{22}) \doteq \cos 2(\lambda_0-\lambda_{22}) - 2\Delta\lambda\sin 2(\lambda_0-\lambda_{22}) = -\cos 2\gamma_0 + 2\Delta\lambda\sin 2\gamma_0. \tag{18A}$$

Similarly, $\sin 2(\lambda-\lambda_{22})$ can be approximated by

$$\sin 2(\lambda_0-\lambda_{22}) + 2\Delta\lambda\cos 2(\lambda_0-\lambda_{22}) = -\sin 2\gamma_0 - 2\Delta\lambda\cos 2\gamma_0 \doteq \sin 2(\lambda-\lambda_{22}) \tag{18B}$$

In Figure 3, γ_0 is the geographic longitude of the node of the 24-hour nearly circular satellite orbit with respect to the minor equatorial axis. With these expansions [(18A) and (18B)], and using (15B), (14) becomes

$$F_{(\phi)} = K\frac{\sin\phi\cos\phi\tan\phi}{\tan\theta}\{-\cos 2\lambda_0 + 2\Delta\lambda\sin 2\lambda_0\}.$$

Using (15C) in the above expression, the contribution to the perturbing force F due to F_φ becomes

$$F_{(\phi)} = K\frac{\sin^2(i)\sin 2\nu}{2}\{-\cos 2\lambda_0 + 2\Delta\lambda\sin 2\lambda_0\}. \tag{19}$$

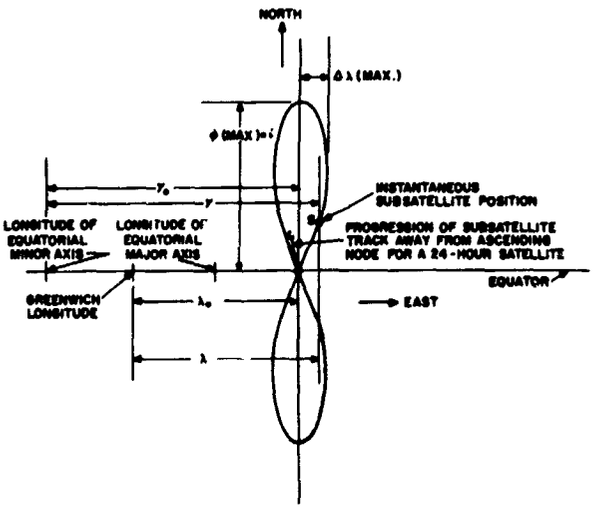

FIGURE 3.—Geographic subsatellite track of 24-hour satellite in a near-circular orbit.

Writing $\Delta\lambda \doteq \Delta\lambda\ (\max) \sin 2\theta$, (19) becomes

$$F_{(\phi)} \doteq K \sin^2 (i)\ [-\cos 2\gamma_0]\ \frac{\sin 2\theta}{2}$$

$$-K \sin^2 (i)\ \Delta\lambda\ (\max)\ [\sin 2\gamma_0 \sin^2 2\theta] \quad (20)$$

Averaging $F_{(\phi)}$ over $0 \leq \theta \leq 2\pi$, (20) gives

$$\bar{F}_{(\phi)} = \frac{1}{2\pi}\int_0^{2\pi} F_{(\phi)} d\theta$$

$$= -\frac{\sin^2 i \Delta\lambda\ (\max)}{2}[K \sin 2\gamma_0] \quad (21)$$

The contribution to F from F_λ is

$$F\omega = F_\lambda \cos (90-\alpha) = F_\lambda \sin \alpha$$
$$= K \sin \alpha \cos \phi \{-\sin 2\gamma_0 - 2\Delta\lambda \cos 2\gamma_0\}, \quad (22)$$

from (13) and (18B). Using (15D) in (22), and noting that $\Delta\lambda \doteq \Delta\lambda\ (\max) \sin 2\theta$, as before, gives the contribution to F from F_λ as

$$F\omega = K \cos (i) \{-\sin 2\gamma_0 - 2\Delta\lambda (\max) \sin 2\theta \cos 2\gamma_0\}. \quad (23)$$

Averaging $F_{(\lambda)}$ over $0 \leq \theta \leq 2\pi$, (23) gives

$$\bar{F}\omega = -K \cos (i) \sin 2\gamma_0. \quad (24)$$

Thus, combining the contributions of the latitude and longitude perturbations to the average perturbation force over a single 24-hour orbit, (21) and (24) sum to produce

$$\bar{F}\ (\text{total}) = -\bar{F}_{(\phi)} + \bar{F}_{(\gamma)}$$
$$= -K \sin 2\gamma_0 \left\{\cos (i) + \frac{\sin^2 (i)\ \Delta\lambda(\max)}{2}\right\}. \quad (25)$$

3. Completion of the Derivation of the Drift Equations

Appendix C shows that

$$\Delta\lambda(\max) = \tan^{-1}[\sec (i)] - 45°.$$

It is also shown there that, to a high degree of accuracy for $i < 50°$,

$$\cos (i) + \frac{\sin^2 \Delta\lambda\ (\max)}{2} \doteq \frac{1+\cos^2 (i)}{2}.$$

Numerically integrated orbits have shown that the drift theory for a 24-hour satellite stemming from (25) is in error by more than 2 percent for $i > 45°$. With this restriction on orbit inclination, using the above approximation for the inclination factor, we can rewrite the longitude drift and orbit expansion equations (10) and (11), evaluating $\bar{F}$ by (25), giving

$$\dot{\gamma} = \frac{12\pi^2 K}{\mu_E/(a_s)^3}\left[\frac{\cos^2 (i)+1}{2}\right] \sin 2\gamma_0,$$
(rad./sid. day²) (26)

$$\dot{a} = -\frac{4\pi (a_s)^2 K}{\mu_E}\left[\frac{\cos^2 (i)+1}{2}\right] \sin 2\gamma_0,$$
(length units/sid. day). (27)

Substituting (14A) into (26) and (27) reduces these expressions to

$$\dot{\gamma} = 72\pi^2 J_{22}(R_0/a_s)^2\left[\frac{\cos^2(i)+1}{2}\right] \sin 2\gamma_0,$$
(rad./sid. day²) (28)

$$\dot{a} = -24\pi J_{22}(R_0/a_s) R_0\left[\frac{\cos^2(i)+1}{2}\right] \sin 2\gamma_0,$$
(length unit/sids. day). (29)

Define a nondimensional change of semimajor axis from a_s during the drift as

$$a_1 = \frac{a - a_s}{a_s} = \frac{\Delta a}{a_s} \text{ so that, } \dot{a}_1 = \frac{\dot{a}}{a_s}. \quad (29A)$$

With (29A), (29) becomes

$$\dot{a}_1 = -24\pi J_{22}(R_0/a_s)^2\left\{\frac{\cos^2(i)+1}{2}\right\}\sin 2\gamma_0, \quad (1/\text{sid. day}) \quad (30)$$

Define:

$$A_{22} = -72\pi^2 J_{22}(R_0/a_s)^2\left\{\frac{\cos^2(i)+1}{2}\right\}, \quad (\text{rad./sid. day}^2). \quad (30A)$$

With (30A), (28) and (30) become;

$$\ddot{\gamma} + A_{22}\sin 2\gamma_0 = 0, \ (\text{rad./sid. day}^2) \quad (31)$$

$$\dot{a}_1 - \frac{A_{22}\sin 2\gamma_0}{3\pi} = 0, \ (1/\text{sid. day}). \quad (32)$$

Note that π in (32) has dimensions of rad./sid. day. It must be understood that (31) describes the *net* daily geographic acceleration of the initially 24-hour satellite with respect to the earth's minor equatorial axis. Stated another way, (31) describes the geographic drift of the entire originally stationary, figure-8 ground track (Figure 3). Similarly, (32) describes the net daily orbit-expansion rate of the 24-hour satellite. In particular, it it convenient to treat the motion of the ascending node of the orbit in geographic longitude as a reference for the entire configuration. In what follows, therefore, γ will refer always to the geographic longitude of the ascending node east of the equatorial minor axis; γ_0 will refer to the initial geographic longitude of the A.N. east of the minor axis, at the start of the dynamics under consideration. (31) and (32) can thus be rewritten in terms of the general nodal longitude position γ, to give the relevant partially uncoupled long-term drift and orbit-expansion differential equations for the near-24-hour near-circular orbit satellite:

$$\ddot{\gamma} + A_{22}\sin 2\gamma = 0, \ (\text{rad./sid. day}^2) \quad (33)$$

$$\dot{a}_1 - \frac{A_{22}\sin 2\gamma}{3\pi} = 0, \ (1/\text{sid. day}). \quad (34)$$

4. General Considerations of the Solutions of the Drift Equation

Equation (33) can be integrated directly for the geographic drift rate by noting that

$$\ddot{\gamma} = \frac{d\dot{\gamma}}{dt} = \frac{d(\dot{\gamma})^2}{2\dot{\gamma}dt} = \frac{d(\dot{\gamma})^2}{2d\gamma}.$$

Thus (33) can be separated to

$$d(\dot{\gamma})^2 = -2A_{22}\sin 2\gamma d\gamma. \quad (35)$$

Since the variables $(\dot{\gamma})^2$ and γ are separated in (35), (35) integrates to

$$(\dot{\gamma})^2 = A_{22}\cos 2\gamma + C_1. \quad (36)$$

With the initial condition that $\dot{\gamma} = \dot{\gamma}_0$ at $\gamma = \gamma_0$, (36) becomes

$$\dot{\gamma} = [(\dot{\gamma}_0)^2 + A_{22}(\cos 2\gamma - \cos 2\gamma_0)]^{1/2}, \quad (37)$$

giving the drift rate of the 24-hour satellite as a function of the initial drift rate $\dot{\gamma}_0$, the earth gravity constant A_{22}, the initial longitude east of the minor axis γ_0, and the instantaneous longitude γ. Returning to the semicoupled system of equations (33) and (34), the explicit dependence of the equations on the location from the minor axis and the magnitude of the equatorial ellipticity may be eliminated by multiplying (33) by $\frac{1}{3}\pi$ and adding the resulting equation to (34), giving

$$\ddot{\gamma} + 3\pi\dot{a}_1 = 0. \quad (38)$$

(38) can be rewritten as

$$\frac{d(\dot{\gamma})}{dt} + 3\pi\dot{a}_1 = 0 = d(\dot{\gamma}) + 3\pi\dot{a}_1 dt = d(\dot{\gamma}) + 3\pi d(a_1) \quad (39)$$

Separation of the variables $\dot{\gamma}$ and a_1 is thus achieved in (39). (39) integrates directly to

$$3\pi a_1 + \dot{\gamma} = C_2. \quad (40)$$

With the initial conditions: $a_1 = 0$, when $\dot{\gamma} = 0$ (the satellite is in the momentarily stationary ground-track configuration); $C_2 = 0$. If γ_0 in (37) is also the longitude of this initially stationary orbit, $(\dot{\gamma}_0)^2 = 0$ there, and (37) in (40) yields for a_1, the semimajor axis change from "synchronism" in the drift motion,

$$a_1 = \pm\frac{(A_{22})^{1/2}(\cos 2\gamma - \cos 2\gamma_0)^{1/2}}{3\pi}, \quad (41)$$

(41) shows explicitly that the semimajor axis is bounded in long-term drift from a stationary orbit. From (33), since $A_{22} > 0$, if $0 < \gamma_0 < 90°$, drift proceeds *towards* the nearest longitude of the earth's equatorial minor axis (in $a-\gamma$ direction). If $-90° < \gamma_0 < 0°$, (33) shows that drift

again proceeds *toward* the nearest minor axis longitude (in $a+\gamma$ direction). Thus, in all cases of drift from a stationary geographic configuration, $\cos 2\gamma - \cos 2\gamma_0$ is a positive function which has a maximum when $\gamma=0$ (when the satellite has drifted over the longitude of the minor axis). Thus (41) gives (for the librations of a 24-hour satellite)

$$a_1 \text{ (max)} = \left| \frac{(A_{22})^{1/2}(1-\cos 2\gamma_0)^{1/2}}{3\pi} \right|. \qquad (42)$$

Again it is noted that π in (42) has units of rad/sid. day. An absolute maximum semimajor axis change in the drift occurs when the "synchronous" condition is established near the longitude of the major equatorial axis. Here, $\gamma_0 = -90°$, $\cos 2\gamma_0 = -1$, and

$$a_1 \text{ (absolute maximum for a librating 24-hour satellite)} = \frac{(2A_{22})^{1/2}}{3\pi} \qquad (43)$$

For the constant $J_{22} = -1.7\times10^{-6}$ (derived in this study from long-term observations on the drift of the Syncom II satellite) and using the additional constants from this study: $i=33°$, $a_s \doteq 42166$ km, $R_0 = 6368.388$ km; (30A) gives

$$A_{22} = 23.2\times10^{-6} \text{ (rad./sid. day}^2\text{)}.$$

(43) then gives

a_1 (absolute max.) $= .72\times10^{-3}$, from which, by (29A),

Δa (absolute max. from a "synchronous" condition near the equatorial major axis, for a satellite of $i=33°$) $= 30.7$ km.

Thus the assumption made in (10) and (11), to approximate the slightly varying semimajor axis by a_s (a constant) throughout the drift motion, appears amply justified.

Figure 4 is a graph of (41) for a_1 vs. γ (the longitude with respect to the nearest minor axis location) as a function of γ_0, the longitude in the initially stationary configuration.

Note that (41) allows equal $\pm$values for a_1 for each γ. Suppose the satellite is initially at $+\gamma_0$ (position 1 in Figure 4) from the nearest location

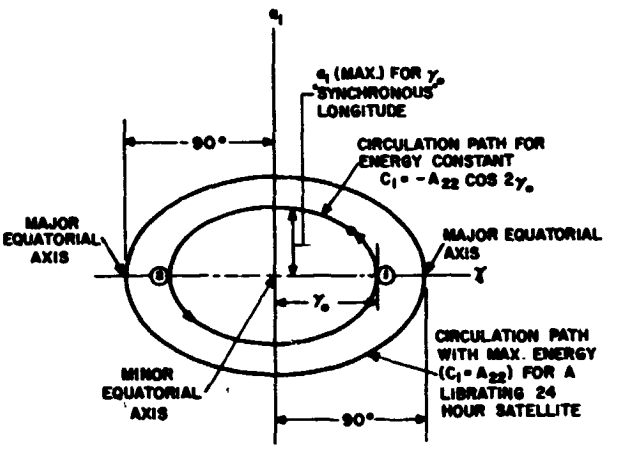

FIGURE 4.—Libration with longitude of the semimajor axis of a 24-hour satellite as a function of the longitude of the initially stationary configuration.

of the minor axis: From (33), $\sin 2\gamma_0$ being positive, the satellite begins to drift west (attaining a negative drift rate) towards the minor axis. But, from (40), since $C_2=0$, $a_1 = -(\gamma)/3\pi > 0$; the drift therefore proceeds counterclockwise in Figure 4, around the central point of the minor axis and $a_1=0$, along the upper portion of the two-valued arc determined from (41).

The same situation holds for the motion beginning or stemming away from the "synchronous" longitude at $-\gamma_0$, position 2 in Figure 4. Here $\sin 2\gamma_0$ is negative, and the drift proceeds at a positive rate to the east. Again from (40), as soon as the satellite leaves position 2, $a_1 = -(\gamma)/3\pi < 0$, and the circulation continues in a counterclockwise direction. Every trajectory in the phase plane $a_1 \leftrightarrow \gamma$ may be conveniently defined by the constant C_1 of the "energy integral" of the drift motion (36). Since (33) is the equation-of-motion defining the large-angle oscillations of a mathematical pendulum (in the case of the 24-hour-orbit satellite, the point of symmetry is the minor axis where $2\gamma=0$), it can be expected that the general solutions in that theory apply to the long-term librations of the "synchronous satellite" (Appendix D). For example, in (36), with a momentarily "synchronous" condition at γ_0 being given by $\gamma_0=0$, the "energy constant" is evaluated as

$$C_1 = -A_{22} \cos 2\gamma_0.$$

With this evaluation, (36) becomes

$$(\dot{\gamma})^2 - A_{22}\cos 2\gamma = -A_{22}\cos 2\gamma_0. \qquad (44)$$

Solving for the initially "synchronous" longitude as a function of any longitude in the drift and the corresponding longitude rate, (44) gives

$$\gamma_0 = \frac{1}{2}\cos^{-1}\left[\cos 2\gamma - \frac{(\dot{\gamma})^2}{A_{22}}\right]. \qquad (45)$$

Since $(\dot{\gamma})^2/A_{22} \geq 0$, the argument of $\cos^{-1}$ in (45) is always less than or equal to 1. Thus, as long as $\cos 2\gamma - (\dot{\gamma})^2/A_{22} \geq -1$, (45) will give a real solution for the momentarily "synchronous" longitude with respect to the minor axis. But, if $\cos 2\gamma - (\dot{\gamma})^2/A_{22} < -1$, there will be no real momentarily "synchronous" configuration for the near-24-hour satellite. With this energy, the world-circulation regime commences, corresponding to the over-the-top, high-energy regime of the mathematical pendulum (Reference 3). The above inequality implies that, for the commencement of "world circulation" for the near-24-hour satellite,

$$(\dot{\gamma})^2 \geq A_{22}(1+\cos 2\gamma), \text{ or}$$
$$(\dot{\gamma})^2 \geq 2A_{22}\cos^2\gamma. \qquad (46)$$

When $2\gamma = 0$, or the satellite is over the minor axis, (46) allows the maximum possible drift rate for a librating 24-hour satellite:

$$\dot{\gamma}(\max)_{\text{for libration}} = (2A_{22})^{1/2}, \text{ (rad./sid. day)}. \qquad (47)$$

For example, using the reported value of $A_{22} = 23.2\times10^{-6}$ rad./day^2 for the inclination of the Spncom II satellite, (47) gives

$$\dot{\gamma}(\max)_{\text{for libration with } J_{22}=-1.7\times10^{-6},\ i=33^\circ} = (46.4\times10^{-6})^{1/2} = .39 \text{ degrees/day}. \qquad (48)$$

5. Approximations to the Exact Drift Solutions for Periods Very Close to Synchronous

Expanding the drift from the "synchronous" longitude ($\gamma = \gamma_0$ in this section) in a Taylor series, with respect to increments of time Δ_t from the momentarily stationary condition,

$$\gamma(\Delta t) = \gamma_0 + \dot{\gamma}_0\Delta t + \ddot{\gamma}_0\frac{(\Delta t)^2}{2} + \dddot{\gamma}_0\frac{(\Delta t)^3}{6} + \gamma_0^{[4]}\frac{(\Delta t)^4}{24} + \gamma_0^{[5]}\frac{(\Delta t)^5}{120} + \gamma_0^{[6]}\frac{(\Delta t)^6}{720} + \gamma_0^{[7]}\frac{(\Delta t)^7}{5040} + \gamma_0^{[8]}\frac{(\Delta t)^8}{40320} + \cdots \qquad (50)$$

Differentiating (33) six times with respect to time, it is clear that all derivatives in (50) can be written as functions of A_{22}, γ_0 and $\dot{\gamma}_0$. Noting that $\gamma(\Delta_t) - \gamma_0 = \Delta\lambda$ (the geographic longitude with respect to the "synchronous" configuration) and $\dot{\gamma}_0 = 0$, (50) can be shown to reduce to the expansion

$$\Delta\lambda = (-A_{22}\sin 2\gamma_0)\frac{(\Delta t)^2}{2} + [(A_{22})^2\sin 4\gamma_0]\frac{(\Delta t)^4}{24} + [(A_{22})^3\sin 2\gamma_0\,(4\sin^2 2\gamma_0 - 1)]\frac{(\Delta t)^6}{180} - [(A_{22})^4\sin 4\gamma_0(34\sin^2 2\gamma_0 - 1)]\frac{(\Delta t)^8}{10080} + \ldots \qquad (51)$$

It is apparent that, as $\Delta_t \to 0$, the higher order terms of (51) become increasingly more insignificant to the total drift, in comparison to the terms of lower order.

In Appendix D, the exact "elliptic integral" of motion from (33) is calculated from a synchronous longitude of 60° east of the minor axis. This calculation demonstrates that the simple term-inclusion-time criterion below gives an adequately converging series to the "exact" drift. In the actual reduction, all higher order terms in (51) which are less in magnitude than the root mean square (rms) error of the observed Syncom II longitudes, are ignored. Section 7 of this report shows that this rms error of longitude determination for the ascending equator crossings of Syncom II from August 1963 to March 1964 has been of the order of $\pm.025$ degrees. Thus, 0.025° is used below in forming the minimum-time-term-inclusion criterion for each term of (51).

A_{22} is assumed to be 23.2×10^{-6} rad./sid. day^2.

A) For inclusion of the $(\Delta t)^4$ term:

$|\sin 4\gamma_0|$ is maximum when $\gamma_0 = \pm 22.5^\circ$ and $\pm 67.5^\circ$.

Therefore,

$$|\Delta\gamma_{\max} \text{ (from the fourth-order term)}| = (A_{22})^2\frac{(\Delta t)^4}{24}. \qquad (52A)$$

Solving (52A) for Δt, when $|\Delta\lambda_{max}$ (4th order)$|$ $=.025°$,

Δt (min. fourth-order term inclusion)
$=(.025\times24/57.3\times[23.2\times10^{-6}]^2)^{1/4}$
$=66.5$ sid. days from "synchronism".

B) For inclusion of the $(\Delta t)^6$ term:

$|\sin 2\gamma_0\ (4\sin^2 2\gamma_0-1)\ |$ is maximum when γ_0 $=\pm45°$.

Therefore,

$|\Delta\gamma_{max}$ (from the sixth-order term)$|$
$$=(A_{22})^3\frac{(\Delta t)^6}{60}. \qquad (52B)$$

Solving (52B) for Δt, when $|\Delta\lambda_{max}$ (sixth order)$|$ $=.025°$,

Δt (min. for sixth-order term inclusion)
$=(.025\times60/57.3\times[23.2\times10^{-6}]^3)^{1/6}$
$=113.$ sid. days from "synchronism".

C) For inclusion of the $(\Delta t)^8$ term:

$|\sin^4\gamma_0\ (34\sin^2 2\gamma_0-1)\ |$ is maximum wh $=\pm5914°$.

Therefore,

$|\Delta\lambda_{max}$(from the eighth-order term)$|$
$$=21.2(A_{22})^4\frac{(\Delta t)^8}{10080} \qquad (52C)$$

Solving (52C) for Δt, when $|\Delta\lambda_{max}$ (eight order)$|$ $=.025°$,

(min. for eight-order term inclusion)
$=(10080\times.025/21.2\times57.3\times[23.2\times10^{-6}]^4)^{1/8}$
$=171.$ sid. days from "synchronism".

Similarly, expanding $a_1\ (t)$ in a Taylor series about the time of "synchronism", $(t_0,\ \gamma_0)$:

$$a_1(t_0+\Delta t)=(a_1)_0+(\dot a_1)_0(\Delta t)+(\ddot a_1)_0\frac{(\Delta t)^2}{2}+(\dddot a_1)_0\frac{(\Delta t)^3}{6}+\cdots. \qquad (53)$$

But, from (34),

$$(\dot a_1)_0=\frac{A_{22}\sin 2\gamma_0}{3\pi}. \qquad (53A)$$

Differentiating (53A) with respect to time,

$$(\ddot a_1)_0=\frac{2\dot\gamma_0A_{22}\cos 2\gamma_0}{3\pi}=0, \qquad (53B)$$

since $\gamma_0=0$. Differentiating (53B) with respect to time,

$$(\dddot a_1)_0=\frac{-4(\dot\gamma_0)^2A_{22}\sin 2\gamma_0}{3\pi}+\frac{2\ddot\gamma_0A_{22}\cos 2\gamma_0}{3\pi}=\frac{-(A_{22})^2\sin 4\gamma_0}{3\pi}, \qquad (54)$$

using equation (33). From the conventional definition of a_1, $(a_1)_0=0$. (53) then becomes

$$a_1\ (\text{at }\Delta t\text{ from "synchronism"})=\frac{(A_{22}\sin 2\gamma_0)\Delta t}{3\pi}-\frac{(A_{22})^2\sin 4\gamma_0(\Delta t)^3}{18\pi}+\cdots, \qquad (54A)$$

with the results of (53A), (53B), and (54) in (53).

Section 7 shows that the rms error of semimajor axis determination for Syncom II (including sun and moon "noise") is of the order of ±0.5 km. Therefore, the rms error to be expected in a_1 is of the order of $.5/42166.=1.185\times10^{-5}$. Following the procedure for the longitude drift, 1.185×10^{-5} is used below to determine the minimum time for the inclusion of the terms beyond the first on the righthand side of (54A), to ensure adequate convergence of the infinite series for $a_1(\Delta t)$.

A) For inclusion of the $(\Delta t)^3$ term:

$|\sin 4\gamma_0|$ is maximum when γ_0 $=\pm22.5°$ and $\pm67.5°$.

Therefore,

$|a_{1(max)}$ [from the third-order term of (54A)]$|$
$$=\frac{(A_{22})^2(\Delta t)^3}{18\pi}. \qquad (55)$$

Solving (55) for Δt, when $|a_1$ (max)$|$ $=1.185\times10^{-5}$,

Δt [min. for the third-order term inclusion in (54A)] $=\left[\frac{1.185\times10^{-5}\times18\pi}{23.2\times10^{-12}}\right]^{1/3}$
$=$ 108 sid days from synchronism.

From a "synchronous" configuration at 54.8° west of Greenwich, on or about 6 September 1963, Syncom II drifted to 59.2° west of Greenwich on 28 November 1963, where it was "stopped" by the tangential firing of on-board cold-gas jets. A second free-drift period followed from a "synchronous" configuration at 59 2° west on about 29 November 1963, to 66.3° west on 18 March 1964, where the on-board tangential jets were fired to speed up the westward drift. Of the 34 separate orbits calculated by the Goddard Data and Tracking Systems Directorate for these free-drift periods, only 7 fell outside the minimum 66-day period around a condition of "synchronism",

for which the inclusion of higher order terms in (54A) would be necessary in reducing the drift data according to that theory. The data reduction of Section 7 includes only those orbits falling within the minimum 36-day period around "synchronism". Further refinement of this reduction to include the 7 outside-of-synchronous orbits (according to the criterion of this chapter), will be made in the near future. This refinement is not expected to materially affect the results of this report.

6. Determination of Earth-Equatorial Ellipticity from Two Observations of Drift Acceleration At a Given Longitude Separation

Given two independent near-synchronous drifts (in the sense discussed previously), whose momentarily synchronous longitudes $(\gamma_0)_1$ and $(\gamma_0)_2$ are separated by $\nabla\lambda$. Let the two drift accelerations at these two "synchronous" configurations be $(\ddot{\gamma}_0)_1$ and $(\ddot{\gamma}_0)_2$. The drift accelerations may be determined from drift-data reduction according to the theory of (51).

From (33),

$$(\ddot{\gamma}_0)_1 = -(A_{22})_1 \sin 2(\gamma_0)_1 \tag{56}$$

$$(\ddot{\gamma}_0)_2 = -(A_{22})_2 \sin 2[(\gamma_0)_1 + \nabla\lambda], \tag{57}$$

since $(\gamma_0)_2 - (\gamma_0)_1 = \Delta\lambda = (\lambda_0)_2 - (\lambda_0)_1$. Expanding (57) and dividing by (56) gives

$$\left[\frac{(\ddot{\gamma}_0)_2}{(\ddot{\gamma}_0)_1}\right]\left[\frac{(A_{22})_1}{(A_{22})_2}\right] = \cos 2\nabla\lambda + \sin 2\nabla\lambda \cot 2(\gamma_0)_1 \tag{58}$$

Solving (58) for $(\gamma_0)_1$,

$$(\gamma_0)_1 = \frac{1}{2}\tan^{-1}\left\{\frac{\sin(\nabla\lambda)}{\frac{(\ddot{\gamma}_0)_2(A_{22})_1}{(\ddot{\gamma}_0)_1(A_{22})_2} - \cos 2(\nabla\lambda)}\right\}. \tag{59}$$

The quadrant of $(\gamma_0)_1$ is either the first or the fourth, because drift acceleration is always in the direction of the *nearest* longitude extension of the earth's minor equatorial axis. Once the minor axis is located by (59), the absolute value of J_{22} in the earth's triaxial gravity field can be determined through (56) and (30A), for example, as

$$J_{22} = \frac{(A_{22})_1}{72\pi^2[R_0/(a_s)_1]^2\left[\frac{\cos^2(i)_1+1}{2}\right]} = \frac{(\ddot{\gamma}_0)_1}{72\pi^2 \sin 2(\gamma_0)_1[R_0/(a_s)_1]^2\left[\frac{\cos^2(i)_1+1}{2}\right]} \tag{60}$$

Note that the units of $(\ddot{\gamma}_0)_1$ in (60) must be those of radians/sidereal day^2 so that J_{22} will be dimensionless. Note also that in (59), using the result of (30A),

$$\frac{(A_{22})_1}{(A_{22})_2} \simeq \left[\frac{(a_s)_2}{(a_s)_1}\right]^2\left[\frac{\cos^2(i)_1+1}{\cos^2(i)_2+1}\right]. \tag{61}$$

Using (59), since $(\lambda_0)_1$ is known from the data reduction (the geographic longitude of the "synchronous" configuration), the geographic longitude of the nearest minor axis location can be calculated as

$$\gamma_{22} = (\lambda_0)_1 - (\gamma_0)_1. \tag{61A}$$

Similarly, the geographic longitude of the nearest major equatorial axis location can be calculated from

$$\lambda_{22} = (\lambda_0)_1 - (\gamma_0)_1 + 90^\circ \tag{61B}$$

(See figure 3).

Following the theory of Reference 10, the difference in major and minor equatorial radii of the earth's triaxial geoid (a_0-b_0), is related to the gravity constant J_{22} by

$$a_0-b_0=-6R_0J_{22}. \tag{62}$$

7. Reduction of 27 Syncom II Orbits to Determine the Earth's Equatorial Ellipticity

Appendix A tabulates the 27 Syncom II orbits from which the reduction below was made. Table 1 gives the estimated ascending equator crossings nearest to the epoch of these orbits. These were calculated by hand, and therefore are listed only to 0.01 degrees and 0.01 days. The technique used was to locate from the Nautical Almanac, the geographic longitude of the ascending node at epoch through the reported right ascension of the ascending node for the orbit, and the hour-angle of the vernal equinox calculated at epoch. The geographic longitude of the ascending equator crossing was then estimated by turning the earth back through the orbit angle from the ascending node to the satellite at epoch. This latter quantity was estimated as $\omega-M$ for the near-circular orbit of Syncom II. A correction factor to this orbit angle- -the ratio of the satellite's period to the earth's sidereal period—was applied for orbits whose period was sufficiently different from the earth's. The nodal longitude at epoch, minus this reduced nodal excursion angle, is the estimated "ascending equator crossing nearest to epoch" reported in Table 1. (See Appendix E for an example of this calculation.)

Table 2 gives the Goddard-reported semimajor axes for these 27 orbits. Truncating equations (51) and (54A) at their first righthand terms:

$$\Delta\lambda \text{ (longitude drift from "synchronism")} \doteq -(A_{22}\sin 2\gamma_0)\frac{(\Delta t)^2}{2} \tag{63}$$

$$a_1 \text{ (semimajor axis change from "synchronism")} \doteq A_{22}\frac{\sin 2\gamma_0(\Delta t)}{3\pi}. \tag{64}$$

Let the drift time be given from a certain arbitrary base time by T. Let T_0 be the time of "synchronism" from the base time. Let the drift be given from a certain arbitrary geographic longitude by λ. Let λ_0 be the geographic longitude from this base longitude, of the "synchronous" configuration. Then:

$$\Delta_t = T-T_0, \text{ and}$$
$$\Delta\lambda=\lambda-\lambda_0.$$

With these changes, (63) and (64) become (noting that $a_1=\frac{a-a_s}{a_s}$):

$$\lambda=\lambda_0-\frac{(A_{22})(\sin 2\gamma_0)}{2}-(T^2-2TT_0T_0^2), \text{ or}$$

$$\lambda=\left\{\lambda_0-\frac{T_0^2(A_{22}\sin 2\lambda_0)}{2}\right\}+T\left\{T_0A_{22}\sin 2\gamma_0\right\}+T^2\left\{-\frac{A_{22}\sin 2\gamma_0}{2}\right\}. \tag{65}$$

(Note that from (65), $\dot{\lambda}=-A_{22}\sin 2\gamma_0=\gamma_0$ from (33). This result is valid only for orbits sufficiently close to "synchronous," as discussed previously.)

$$a=a_s+a_s\left[\frac{A_{22}\sin 2\gamma_0}{3\pi}\right][T-T_0], \text{ or}$$

$$a=a_s\left(1-\frac{T_0A_{22}\sin 2\gamma_0}{3\pi}\right)+T\left(\frac{a_sA_{22}\sin 2\gamma_0}{3\pi}\right). \tag{66}$$

TABLE 1.—*Estimated Ascending Equator Crossings Nearest the Epoch of 27 Syncom II Orbits.*

First Drift Orbit #	Time from 20.0 Aug. 1963 (days)	Ascending Equator Crossing in Degrees West of 50.0° West	Second Drift Orbit #	Time from 26.0 Nov. 1963 (days)	Ascending Equator Crossing in Degrees West of 50.0° West
1-1	2.12	4.89	2-1	1.86	9.17
1-2	7.11	4.83	2-2	7.84	9.17
1-3	11.09	4.78	2-3	13.83	9.22
1-4	16.08	4.74	2-4	20.81	9.38
1-5	20.07	4.77	2-5	41.75	10.15
1-6	23.06	4.78	2-6	44.74	10.36
1-7	28.05	4.85	2-7	55.71	11.02
1-8	31.04	4.90	2-8	64.69	11.76
1-9	38.02	5.06	2-9	71.67	12.32
1-10	42.01	5.09	2-10	76.66	12.81
1-11	48.09	5.45	2-11	83.64	13.49
1-12	54.97	5.68			
1-13	62.95	6.09			
1-14	70.93	6.60			
1-15	77.91	7.14			
1-16	83.90	7.61			
	~100.0	First free drift period ends at an ascending equator crossing of ~9.15° west of 50.0° west.			

TABLE 2.—*Goddard-Reported Semimajor Axes for 27 Syncom II Orbits.*

First Drift Orbit#	Time from 20.0 Aug. 1963 (days)	Semimajor Axis: (42160.0+Data; km)	Second Drift Orbit#	Time from 26.0 Nov. 1963 (days)	Semimajor Axis: (42160.0+Data; km)
1-1	2.27	4.58	2-1	2.04	5.89
1-2	6.71	4.52	2-2	8.00	7.20
1-3	11.00	6.02	2-3	14.00	7.18
1-4	16.00	6.39	2-4	20.71	8.17
1-5	20.00	6.35	2-5	41.71	8.01
1-6	23.08	6.55	2-6	44.25	9.90
1-7	28.08	7.70	2-7	55.88	11.43
1-8	31.08	7.42	2-8	64.83	11.91
1-9	38.08	7.51	2-9	71.67	12.89
1-10	42.08	8.88	2-10	76.79	13.31
1-11	49.08	9.14	2-11	83.71	14.89
1-12	55.08	9.78			
1-13	63.08	11.51			
1-14	71.00	11.09			
1-15	78.00	12.15			
1-16	84.21	12.51			
	~100.0	First free drift period ends with a semimajor axis of ~42174.5 km.			

(66) and (65) may be written with determinable coefficients as

$$\lambda = d_0 + d_1 T + d_2 T^2, \tag{67}$$

$$a = e_0 + e_1 T, \tag{68}$$

where:

$$d_0 = \lambda_0 - \frac{T^2 A_{22} \sin 2\gamma_0}{2},$$

$$d_1 = (+A_{22} T_0 \sin 2\gamma_0),$$

$$d_2 = -\frac{A_{22} \sin 2\gamma_0}{2}, \tag{69}$$

$$e_0 = a_s\left(1 - \frac{T_0 A_{22} \sin 2\gamma_0}{3\pi}\right),$$

$$e_1 = a_s A_{22} \frac{\sin 2\gamma_0}{3\pi}$$

From (69),

$$T_0 = -d_1/2d_2, \tag{70}$$

$$\lambda_0 = d_0 - \frac{(d_1)^2}{4d_2}, \tag{71}$$

$$\dot{\gamma}_0 = -A_{22} \sin 2\gamma_0 = 2d_2. \tag{72}$$

Alternately, and as an internal check on the theory of the coupling of the drift and orbit expansion,

$$\dot{\gamma}_0 = -A_{22} \sin 2\gamma_0 = \frac{-3\pi e_1}{a_s}, \text{ implying}$$

$$d_2 = 3\pi e_1 / 2a_s. \tag{73}$$

In equation (73), the units of d_2 must be radians/sidereal day^2, and the units of e_1 must be length/sidereal day so that the equation will be dimensionally correct. The semimajor axis at the "synchronous" configuration is calculated from (68) for $T = T_0$:

$$a_s = e_0 + e_1 T_0. \tag{74}$$

For the first drift period (orbits 1–1 through 1–16), the best estimates (in the "least squares" sense) of the coefficients $(d)_1$ and $(e)_1$, obtained by fitting (67) and (68) to the data in Tables 1 and 2, have been found to be:

$$(d_0)_1 = (4.941 \pm .018) \text{ degrees}$$
$$(d_1)_1 = -(.0216 \pm .0010) \text{ degrees/solar day}$$
$$(d_2)_1 = (6.37 \pm .11) \times 10^{-4} \text{ degrees/solar day}^2$$
$$= (6.33 \pm .11) \times 10^{-4} \text{ degrees/sid. day}^2$$

$(e_0)_1 = (4.35 \pm .19)$ km
$(e_1)_1 = (.0993 \pm .0042)$ km/solar day
$(.0990 \pm .0042)$ km/sid. day.

The mean value of the inclination during this period was

$$(i)_1 = 33.018 \pm .005 \text{ degrees.}$$

From (70),

$$(T_0)_1 = \left(16.95 \begin{matrix} +1.09 \\ -1.05 \end{matrix}\right) \text{ days from 29.0 August 1963.}$$

From (71),

$$(\lambda^0)_1 = (4.76 \pm .03) \text{ degrees west of 50.0 degrees west longitude.}$$

From (72),

$$(\dot{\gamma}_0)_1 = -(1.27 \pm .02) \times 10^{-3} \text{ degrees/solar day}^2 = -(2.20 \pm .04) \times 10^{-6} \text{ rad./sid. day}^2.$$

From (74) and the above value of $(T_0)_1$,

$$(a_e)_1 = (42166.0 \pm .2) \text{ km.}$$

For the second drift period (orbits 2-1 through 2-11), the best estimates (in the "least squares" sense) of the coefficients $(d)_2$ and $(e)_2$, obtained by fitting (67) and (68) to the data in Tables 1 and 2, have been found to be:

$(d_0)_2 = (9.156 \pm .017)$ degrees
$(d_1)_2 = -(.0030 \pm .0010)$ degrees/solar day
$(d_2)_2 = (6.59 \pm .11) \times 10^{-4}$ degrees/solar day^2
$= (6.55 \pm .11) \times 10^{-4}$ degrees/sid. day^2

$(e_0)_2 = (5.70 \pm .42)$ km
$(e_1)_2 = (.0994 \pm .0080)$ km/solar day
$= (.0990 \pm .0080)$ km/sid. day.

The mean value of the inclination during this period was

$$(i)_2 = 32.851 \pm .010 \text{ degrees.}$$

From (70),

$$(T_0)_2 = 2.3 \pm .8 \text{ days from 26.0 November 1963.}$$

From (71),

$$(\lambda_0)_2 = 9.15 \pm .02 \text{ degrees west of 50.0 degrees west longitude.}$$

From (72),

$$(\dot{\gamma}_0)_2 = -(1.32 + .02) \times 10^{-3} \text{ degrees/solar day}^2 = -(2.29 \pm .04) \times 10^{-6} \text{ rad./sid. day}^2.$$

From (74) and the above value of $(T_0)_2$,

$$(a_e)_2 = (42165.9 \pm .4) \text{ km.}$$

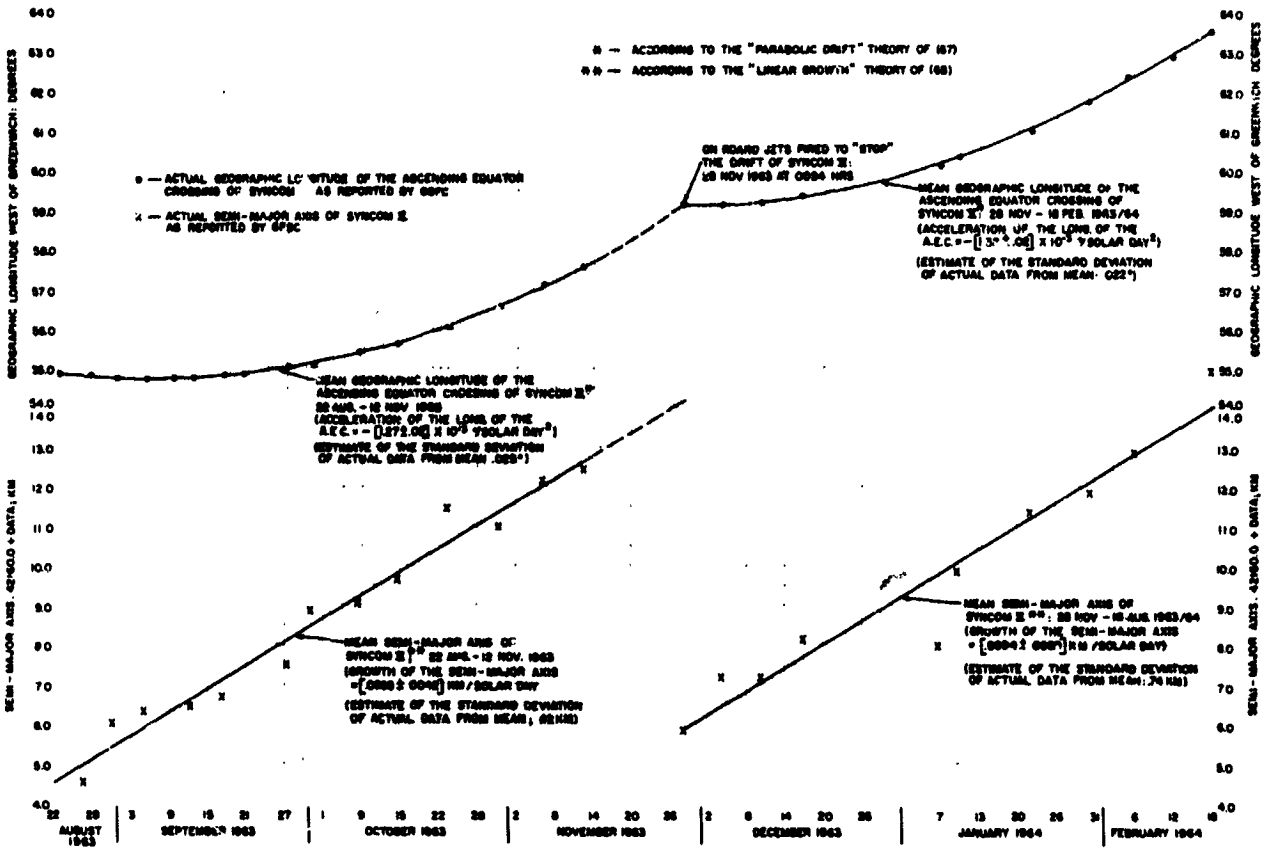

FIGURE 5.—Drift of the ascending equator crossing and growth of the semimajor axis of Syncom II.

(See Figure 5 for a graph of this orbit data and reduction for the two drift periods.) Combining the above results of the two free-drift periods, from (61),

$$\frac{(A_{22})_1}{(A_{22})_2} = (42165.9 \pm .4/42166.0 \pm .2)^2 \frac{[\cos^2 (33.018 \pm .005) + 1]}{[\cos^2 (32.851 \pm .010) + 1]}$$
$$= .99845 \pm .00014.$$

The longitude separation between the two drift periods is given by

$$\nabla\lambda = (\lambda_0)_2 - (\lambda_0)_1 = [-(59.15 \pm .02)] - [-(54.76 \pm .03)] \text{ degrees}$$
$$= -(4.39 \pm .05) \text{ degrees geographic longitude.}$$

Thus

$$2\nabla\lambda = -(8.78 \pm .10) \text{ degrees geographic longitude.}$$

Therefore, from (59), the location of the minor equatorial axis with respect to the "synchronous" longitude during the first free-drift period (54.76 ± .03 degrees west of Greenwich) is

$$(\gamma_0)_1 = \frac{1}{2} \tan^{-1} \left\{ \frac{\sin [-(8.78 \pm .10)]}{\frac{(1.32 \pm .02)}{(1.27 \pm .02)} (.99845 \pm .00014 - \cos [-(8.78 \pm .10)])} \right\}$$

$$= 54 \begin{matrix} +4 \\ -6 \end{matrix} \text{ degrees east of the minor equatorial axis.}$$

From (61B), the best estimate of the location of the major equatorial axis is

$$\lambda_{22} = -55 - \left(54^{+4}_{-6}\right) + 90 = -\left(19^{+4}_{-6}\right) \text{ degrees geographic longitude}$$

From (60), the best estimate of the triaxial gravity coefficient J_{22} is

$$J_{22} = \frac{-(2.20 \pm .04) \times 10^{-6}}{72\pi^2 \left[\sin 2\left(54^{+4^\circ}_{-6^\circ}\right)\right](6378.2/42166.0 \pm .3)^2 \left[\frac{\cos^2(33.018 \pm .005) + 1}{2}\right]}$$

$$= -\left(1.67^{+.07}_{-.03}\right) \times 10^{-6}.$$

The mean equatorial radius, taken as $R_0 = 6378.2$ km, is a compromise between a number of currently used values. It is stated above without error. The likely error in (a_e) has been increased arbitrarily by 0.1 km. to account for the likely uncertainty in R_0.

Using the above estimate of J_{22} from observations on Syncom II drift, the difference between the major and minor equatorial radii of the triaxial geoid is, by (62),

$$a_0 - b_0 = 64^{+3}_{-1} \text{ meters} = 210^{+10}_{-4} \text{ feet.}$$

Comparing the deviation due to earth ellipticity with other higher order earth-gravity deviations (Appendix B and Reference 10), we note that the above figure implies a maximum deviation from the mean earth sphere, due to the ellipticity of the equator, of

$$\Delta R_0 = 105^{+5}_{-2} \text{ feet.}$$

REFERENCES

1. Heiskanen and Meinesz: 1958, *The Earth and Its Gravity Field*, (McGraw-Hill).
2. Izsak: July, 1963, "Tesseral Harmonics In The Geopotential," *Nature* July 13, 1963, pp. 137–139.
3. Blitzer, Boughton, Kang and Page: 1962, "Effect of Ellipticity of the Equator On 24-Hour Nearly Circular Satellite Orbits," *Journal of Geophysica Research*, Vol. 67, pp. 329–335.
4. Frick and Garber: 1962, private communication (Rand Corp. Memo. RM-2296).
5. Barrett: 1962, "The Perturbations of a Synchronous Satellite Resulting From The Gravitational Field of a Triaxial Earth," GSFC Document X-623-62-160, Sept. 10, 1962, NASA.
6. Wagner: 1964, "The Drift of a 24-Hour Equatorial Satellite Due To An Earth Gravity Field Through 4th Order," NASA TN-D-2103, Feb. 1964.
7. Musen: 1962, "On The Motion Of A 24-Hour Satellite," *Journal of Geophysical Research*, Vol. 67 #3, pp. 1123–1132.
8. Thomson: 1961, *Introduction To Space Dynamics*, p. 72 (John Wiley and Sons).
9. Isley: 1962, "A Sommary of Constants Associated With Orbital Analysis of Earth Satellites, Including the Influence Of Their Uncertainties Upon Gravitational Measurements For Synchronous Satellites," GSFC Document X-623-62-169.
10. Wagner: 1962, "The Gravitational Potential of a Triaxial Earth," GSFC Document X-623-62-206, Oct. 62, NASA.
11. Salvadori and Schwarz: 1954, *Differential Equations in Engineering Problems*, Chapter 9 (Prentice Hall).
12. Jahnke and Emde: 1945 ed., *Table Of Functions*, Chapter V (Dover Publications).
13. Kozai: 1961, "The Earth's Gravitational Potential Derived from Motions of Three Satellites," *Astronomical Journal*, Vol. 66, pp. 8–10.
14. O'Keefe, Eckels and Squires: 1959, "The Gravitational Field of the Earth," *Astronomical Journal*, vol. 64, pp. 245–253.

LIST OF SYMBOLS

J_{nm}, λ_{nm} = Spherical harmonic constants (order n, power m) of the earth's gravity potential

F = A gravity force per unit mass acting on a 24-hour satellite

θ = (except in Appendix F) The argument from the ascending node to the satellite position for the 24-hour orbit

a, a_s = The instantaneous semimajor axis, and the "momentarily synchronous" semimajor axis of the orbit of the 24-hour earth satellite. (a_s, estimated to within 2 km, is 42166 km.)

ds = A small arc length of a space trajectory

μ_E = The earth's gaussian gravity constant (3.986×10^5 km^3/sec.^{2})

T_p, T_s = The orbital period for a satellite, and the "momentarily synchronous" period of a 24-hour satellite (i.e., the earth's sidereal rotation period)

λ, r, ϕ = Geographic longitude, geocentric radius, and geocentric latitude of the 24-hour satellites position

$(\dot{}), (\ddot{}), ()^n = \frac{d()}{dt}, \frac{d^2()}{dt^2}, \frac{d^n()}{dt^n}$: time differentials

R_0 = The mean equatorial radius of the earth (6378.2 km)

i = The inclination of the orbit of the 24-hour satellite

λ_0 = The "initial" geographic longitude of the satellite, or the ascending node of the 24-hour satellite's orbit at the start of the dynamics under consideration

ω_e = The earth's sidereal rotation rate ($.7292115 \times 10^{-4}$ rad./sec.)

t = Real time

$\Delta( )$ = A small argument ( )

γ_0 = The geographic longitude (positive to the east) of the ascending node of the 24-hour satellite's orbit with respect to the earth's minor equatorial axis' longitude location, at the start of the dynamics under consideration

γ = The geographic longitude (positive to the east) of the 24-hour satellite, or the ascending node of the satellite's orbit with respect to the longitude of the earth's minor equatorial axis

$a_1 = (a - a_s)/a_s$; a nondimensional semimajor axis change for the 24-hour satellite's orbit, with respect to the "momentarily synchronous" semimajor axis

A_{22} = The driving function causing drift and orbit expansion of a 24-hour satellite in a "triaxial" earth-gravity field; a constant for a given 24-hour orbit inclination

$( )_0$ = The argument ( ) at the start of the dynamics under consideration

$( )_n$ = The argument ( ) at a specified location n (except in Appendix A: ( )s; the argument for the simulated trajectory)

$\nabla\lambda$ = The geographic longitude difference between two "momentarily synchronous" 24-hour satellite configurations

a_0, b_0 The major and minor equatorial radii of the "triaxial" earth $\left(R_0 = \frac{a_0 + b_0}{2}\right.$, according to the definition in Reference 10$\left.\right)$

w = The argument of perigee in a satellite orbit: The orbit angle (from the center of the earth) from the ascending node to perigee

M = The mean anomaly of the satellite in its orbit: The orbit angle (from the center of the earth) from perigee to a point M in the orbit, where $M = \frac{2\pi t}{T_p}$, t being the real time since perigee passage and T_p the period of the satellite's orbit

(e_n), (d_n) = Determinable coefficients in the drift and orbit-expansion equations (67) and (68)

T_0 = The time of "synchronism" from an arbitrary base time of reckoning T

$F(i)$ = The inclination factor in the triaxial driving function A_{22}

V_E = The gravity potential of the earth

g_0, g_s = The radial acceleration of the earth's gravity field at the earth's surface, and at the altitude of the "synchronous" satellite

m = A test mass

$F(k, \phi)$ = The elliptic integral of the first kind with argument (or amplitude) ϕ and modulus k

Λ = The longitude location of the vernal equinox

APPENDIX A

REDUCTION OF SIMULATED PARTICLE TRAJECTORIES FOR EARTH EQUATORIAL ELLIPTICITY

Tables A–1 and A–2 present data taken from a numerically integrated particle trajectory of a triaxial earth in the presence of the sun and moon's gravity field. Only perturbed equations of motion from a periodically rectified Keplerian reference orbit are actually integrated by the digital computer program (called ITEM at the Goddard Space Flight Center). For the 3 months' real orbit time of these trajectories, the accumulated truncation and roundoff error in the numerical integration is believed to be negligible for the purposes of this reduction. The initial position and velocity conditions for these simulated trajectories were the same as those reported for the "actual" Syncom II orbits 1–2 (for the trajectory of Table A–1) and 2–3 (for the trajectory of Table A–2). The program used the earth gaussian-gravity constant

$$\mu_E = 3.9862677 \times 10^5 \text{ km}^3/\text{sec}^2,$$

which is the gravity constant used by the GSFC Data and Tracking Systems Directorate in computing the elements of satellite orbits from radar and Minitrack observations. The best estimates (in the "least squares" sense) of the coefficients $(d)_{s,1}$ and $(e)_{s,1}$, obtained by fitting the drift and orbit expansion equations (67) and (68) to the data in Table A–1, have been found to be

$$(d_0)_{s,1} = 4.841 \pm .004 \text{ degrees}$$

$$(d_1)_{s,1} = -(1.22 \pm .03) \times 10^{-2} \text{ degrees/solar day}$$

$$(d_2)_{s,1} = (6.303 \pm .038) \times 10^{-4} \text{ degrees/solar day}^2$$
$$= (6.268 \pm .038) \times 10^{-4} \text{ degrees/sid. day}^2$$

$$(e_0)_{s,1} = 5.45 \pm 41 \text{ km}$$

$$(e_1)_{s,1} = (.091 \pm .010) \text{ km/solar day}$$
$$= (.091 \pm .010) \text{ km/sid. day.}$$

The mean value of the inclination during this first simulated trajectory period was

$$(i)_{s,1} = 33.005 \pm .003 \text{ degrees.}$$

From (70),

$$(T_0)_{s,1} = 9.68 \pm .30 \text{ days from 26.709 August 1963}$$

From (71),

$$(\lambda_0)_{s,1} = 4.782 \begin{matrix} +.008 \\ -.007 \end{matrix} \text{ degrees west of 50.0 degrees west longitude.}$$

From (72),

$$(\dot{\gamma}_0)_{s,1} = -(1.261 \pm .008) \times 10^{-3} \text{ degrees/solar day}^2$$
$$= -(2.188 \pm .013) \times 10^{-6} \text{ rad./sid. day}^2.$$

TABLE A-1.—*Data from Simulated Trajectory Beginning with the Elements of Syncom II Orbit 1-2.* ($J_{22} = -1.68 \times 10^{-6}$, $R_0 = 6378.388$ km, $\gamma_{22} = -108.0$: *Input into Trajectory Program*)

Time from 26.709 Aug. 1963: (Solar Days)	Ascending Equator Crossing: (Degrees West of 50.0° West Geog. Long.)	Semimajor Axis (42160.0+Data; km)	Inclination (32.0+Data: Degrees)
2.390	4.816	5.27	1.089
8.374	4.783	7.09	1.072
14.358	4.792	6.01	1.056
20.341	4.861	8.12	1.043
26.324	4.954	7.13	1.025
32.308	5.101	8.98	1.019
38.292	5.291	8.31	.997
44.276	5.537	9.67	.991
47.268	5.678	10.38	.983
50.260	5.821	10.03	.972
53.253	5.975	9.42	.967
56.245	6.144	9.74	.966
59.237	6.326	11.09	.960
62.229	6.522	11.94	.957

TABLE A-2.—*Data from Simulated Trajectory Beginning with the Elements of Syncom II Orbit 2-3.* ($J_{22} = -1.68 \times 10^{-6}$, $R_0 = 6378.388$ km, $\gamma_{22} = -108.0$: *Imput into Trajectory Program*)

Time from 10.0 Dec. 1963: (days)	Ascending Equator Crossing: (Degrees West of 50.0° West Geog. Long.)	Semimajor Axis (42160.0+Data; km)	Inclination (32.0+Data; Degrees)
0.823	9.243	6.88	.881
5.809	9.351	7.30	.881
10.796	9.495	9.41	.877
15.783	9.666	8.15	.864
20.769	9.885	9.85	.864
25.756	10.134	10.60	.850
30.743	10.401	9.95	.842
35.730	10.708	11.81	.841
40.717	11.044	12.18	.825
45.704	11.412	11.58	.816
50.692	11.830	13.93	.808
55.679	12.259	13.11	.790
58.672	12.534	13.07	.785
60.667	12.724	13.69	.784

From (74) and the above value of $(T_0)_{s,2}$,

$$(a_s)_{s,2} = 42166.3 \pm .4 \text{ km.}$$

The best estimates (in the "least squares" sense) of the coefficients $(d)_{s,2}$ and $(e)_{s,2}$, obtained by fitting the drift and orbit expansion equations (67) and (68) to the data in Table A-2, have been found to be

$$(d_0)_{s,2} = 9.224 \pm .004 \text{ degrees}$$

$$(d_1)_{s,2} = (1.830 \pm .028) \times 10^{-2} \text{ degrees/solar day}$$

$$(d_2)_{s,2} = (6.501 \pm .042) \times 10^{-4} \text{ degrees/solar day}^2$$

$$= (6.465 \pm .042) \times 10^{-4} \text{ degrees/sid. day}^2$$

$$(e_0)_{s,2} = 7.19 \pm .37 \text{ km}$$

$$(e_1)_{s,2} = (.111 \pm .010) \text{ km/solar day}$$

$$= (.111 \pm .010) \text{ km/sid. day.}$$

The mean value of the inclination during the second simulated trajectory period is

$$(i)_{s,2} = 32.836 \pm .003 \text{ degrees.}$$

From (70),

$$(T_0)_{s,2} = -(14.07 \pm .30) \text{ days from 10.0 December 1963.}$$

From (71),

$$(\lambda_0)_{s,2} = 9.095 \begin{matrix} +.009 \\ -.009 \end{matrix} \text{ degrees west of 50.0 degrees west longitude.}$$

From (72),

$$(\dot{\gamma}_0)_{s,2} = -(1.300 \pm .008) \times 10^{-3} \text{ degrees/solar day}^2$$

$$= -(2.257 \pm .015) \times 10^{-6} \text{ rad./sid. day}^2.$$

From (74) and the above value of $(T_0)_{s,2}$,

$$(a_s)_{s,2} = 42165.6 \pm .5 \text{ km.}$$

A graph of these trajectory simulations is seen in Figure A-1.

Combining the above results for the two simulated trajectories: from (61),

$$\frac{(A_{22})_{s,1}}{(A_{22})_{s,2}} = [(42165.6 \pm .5/42166.3 \pm .4)^2] \left[\frac{\cos^2 (33.005 \pm .003) + 1}{\cos^2 (32.836 \pm .003) + 1} \right]$$

$$= .99840 \pm .00007$$

$$\nabla\lambda = (\lambda_0)_{s,2} - (\lambda_0)_{s,1} = [-(59.095 \pm .009)] - [-(54.782 \pm .008)],$$

$$\therefore 2\nabla\lambda = -(8.626 \pm .034) \text{ degrees geographic longitude.}$$

Therefore, from (59), the location of the minor equatorial axis with respect to the "synchronous longitude" during the first simulated trajectory (54.782 ± .008 degrees west of Greenwich) is

$$(\gamma_0)_{s,1} = \frac{1}{2} \tan^{-1} \left\{ \frac{\sin [-(8.626 \pm .034)]}{\frac{(1.300 \pm .008}{(1.261 \pm .008} (.99840 \pm .00007) - \cos [-(8.626 \pm .034)]} \right.$$

$$= 52.5 \pm 2.5 \text{ degrees east of the minor equatorial axis.}$$

From (61A), the best estimate of the geographic location of the nearest extension of the equatorial minor axis from the simulated trajectory data is

$$(\gamma_{22})_s = -54.8 - (52.5 \pm 2.5) = -(107.3 \pm 2.5) \text{ degrees geographic longitude.}$$

This compares well with the input value of $(\gamma_{22})_s = -108.0°$ used to compute the simulated trajectories. From (60), the best estimate of the triaxial gravity coefficient J_{22} from the simulated data (according

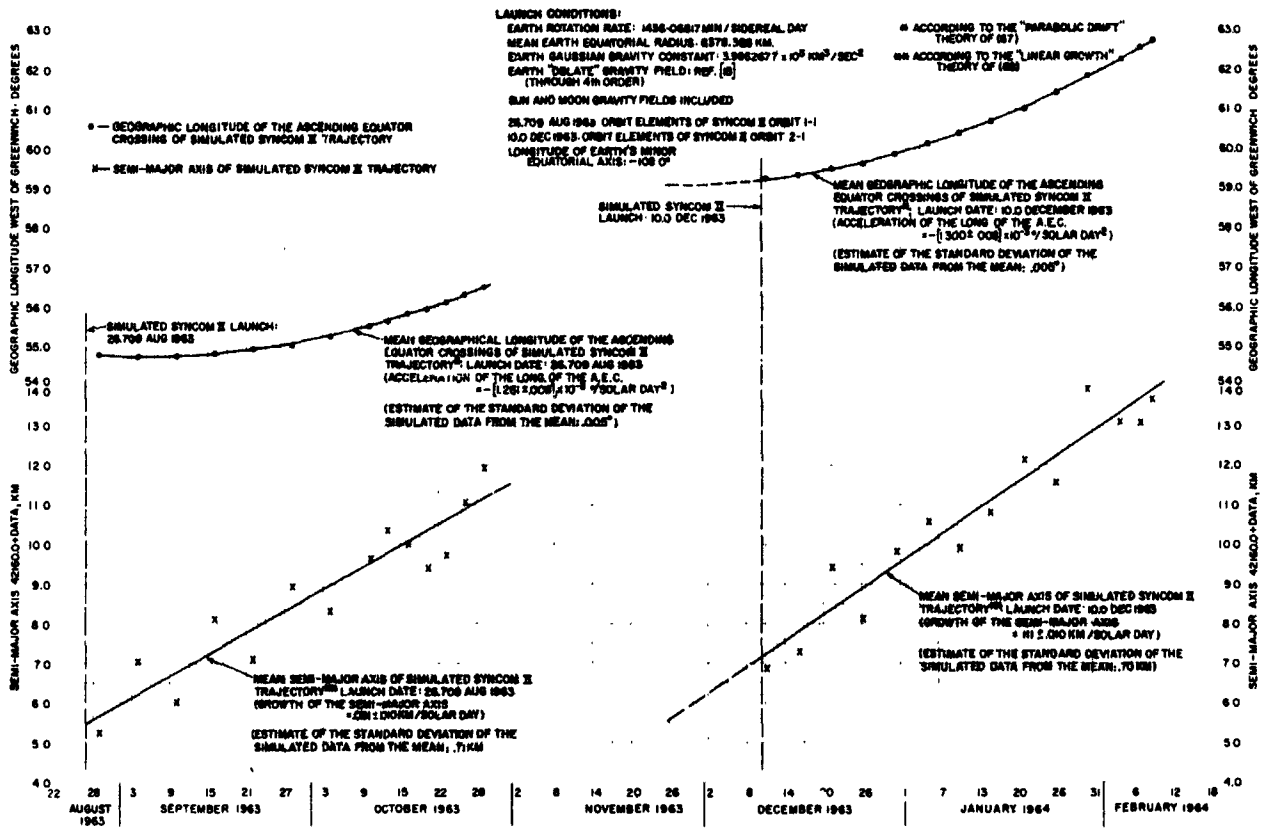

FIGURE A-1.—Drift of the ascending equator crossing and growth of the semimajor axis of simulated Syncom II trajectories.

to the theory of this report) is

$$(J_{22})_s = \left\{ \frac{-(2.188 \pm .013) \times 10^{-6}}{72\pi^2[\sin 2(52.5 \pm 2.5)](6378.388/42166.3 \pm .4)^2 \left[\frac{\cos^2 (33.005 \pm .003) + 1}{2}\right]} \right\}$$

$$= -(1.64 \pm .03) \times 10^{-6}.$$

The mean equatorial radius used in the simulation is $R_0 = 6378.388$ km, the same used to compute the "actual" Syncom II orbits from the radar and Minitrack observations.

The above value of $(J_{22})_s$ compares reasonably well with the input value of $(J_{22})_s = -(1.68) \times 10^{-6}$ used to compute the simulated trajectories.

The model error implicit in the difference between the reduced and inputed geodetic coefficients for the simulated trajectories warrants an adjustment of the J_{22} and λ_{22} reported in Section 7 from the reduction of the "actual" Syncom II orbits. The values below appear sufficient to cover all the *known* uncertainties of this reduction for a triaxial earth:

$$J_{22} \text{ (actual-adjusted)} = -(1.70 \pm .05) \times 10^{-6}$$

$$\lambda_{22} \text{ (actual-adjusted)} = -(19 \pm 6) \text{ degrees geographic longitude.}$$

As Appendix B will show, the principal *unknown* uncertainty of the reduction is the possible influence of higher order earth tesseral anomalies on the drift of Syncom II. When all relevant higher order anomalies in the earth's gravity potential are evaluated, the adjusted values above will probably remain

representative for an "average" triaxial potential field sufficient to consider for the future design of synchronous satellites. As a guess, the author would increase the upper limit of J_{22} to about $-(1.80)\times10^{-6}$ (based on some of the recent gravity potentials in Appendix B) for design purposes, based on an "average" triaxial geoid. A lower limit of $J_{22}=1.60\times10^{-6}$ for this purpose appears justifiable. The variance in the location of the major equatorial axis for the "average" triaxial geoid is not likely to change appreciably from the value quoted for the adjusted figure. The author is presently studying these higher order earth-gravity effects. The accumulated influence on synchronous satellites of all higher order earth anomalies, is believed to be small compared to the 2nd order anomaly. But it appears that close and continuing observations on the drift of these satellites will be rewarded in time by revelation of many of these "tesseral" anomalies to about 4th order with an absolute precision almost as good as that reported here for the 2nd order effect.

APPENDIX B

THE EARTH GRAVITY POTENTIAL AND FORCE FIELD USED IN THIS REPORT: COMPARISON WITH PREVIOUS INVESTIGATIONS

The gravity potential used as the basis for the data reduction in this study is the exterior potential of the earth derived in reference 10 for geocentric spherical coordinates referenced to the earth's spin axis and its center of mass. The infinite series of spherical harmonics is truncated after J_{44}. The nontesseral harmonic constants J_{20}, J_{30} and J_{40} are derived from reference 13.

The earth radius R_0 used in this study is:

$$R_0 = 6378.388 \text{ km.}$$

The earth's gaussian gravity constant used is:

$$\mu_E = 3.9862677 \times 10^5 \text{ km}^3/\text{sec}^2.$$

Neither of these values, taken from reference 14, nor the "zonal geoid" of Reference 13, is felt to be the most accurate known to date. They are the values used by the GSFC Tracking and Data Systems Directorate to calculate the orbit elements of Syncom II from radar and Minitrack observations. They were chosen to insure consistency between the data of this study and these published orbits, inasmuch as the "triaxial" reduction for which this study has been undertaken is not significantly affected by the probable errors in these values. The second-order tesseral harmonic constants used in the simulation studies were

$$J_{22} = -1.68 \times 10^{-6}$$

$$\lambda_{22} = -18°.$$

These are the values shown on the "tesseral geoid" below (for the J_{22} harmonic). At a later point in the analysis, the slightly different values reported in the abstract were estimated. The most accurate "zonal geoid" is probably that of Kozai (1962) [See Reference 6], with the following earth constants;

$$R_0 = 6.378.2 \text{ km}$$

$$\mu_E = 3.98603 \times 10^5 \text{ km}^3/\text{sec}^2.$$

The earth's gravity potential (to fourth order, probably sufficient to account for all significant perturbations on a 24-hour satellite) may be illustrated as follows (following Reference 6, Appendix B):

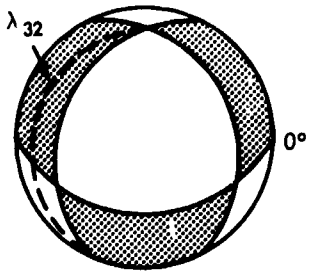

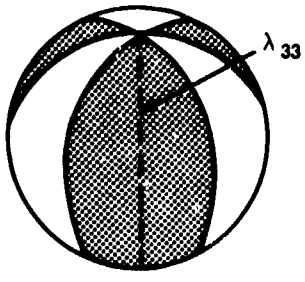

$$-15J_{32}\frac{R_0^3}{r^3}\cos^2\phi\sin\phi\cos 2(\lambda-\lambda_{32})-15J_{33}\frac{R_0^3}{r^3}\cos^3\phi\cos 3(\lambda-\lambda_{33})$$

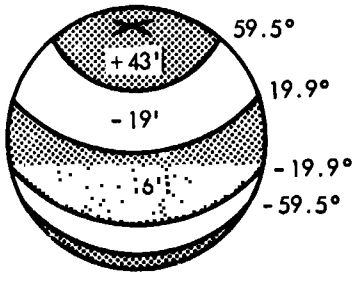

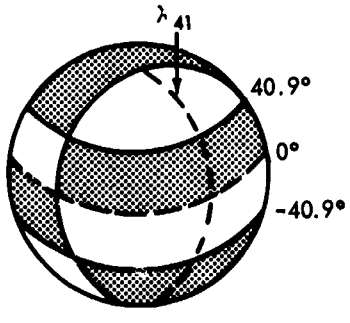

$$-\frac{J_{40}R_0^4}{8r^4}(35\sin^4\phi-30\sin^2\phi+3)-\frac{J_{41}R_0^4}{8r^4}[140\sin^3\phi-60\sin\phi]\cos\phi\cos(\lambda-\lambda_{41})$$

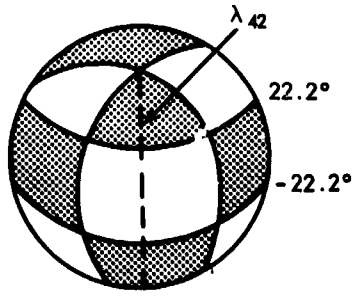

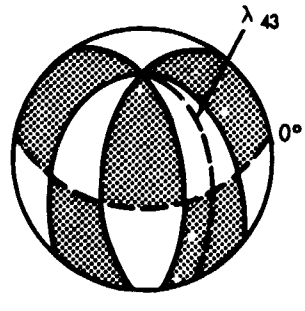

$$-\frac{J_{42}R_0^4}{8r^4}[420\sin^2\phi-60]\cos^2\phi\cos 2(\lambda-\lambda_{42})-\frac{J_{43}R_0^4}{8r^4}840\sin\phi\cos^3\phi\cos 3(\lambda-\lambda_{43})$$

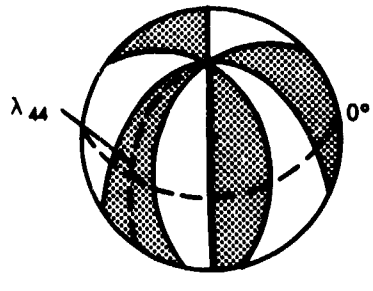

$$-\frac{J_{44}R_0^4}{8r^4}840\cos^4\phi\cos 4(\lambda-\lambda_{44})$$

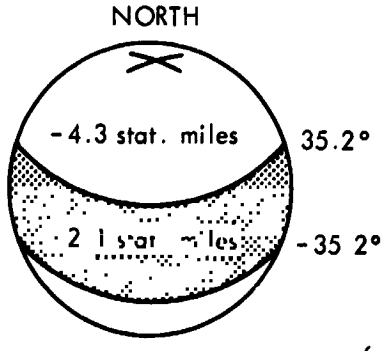

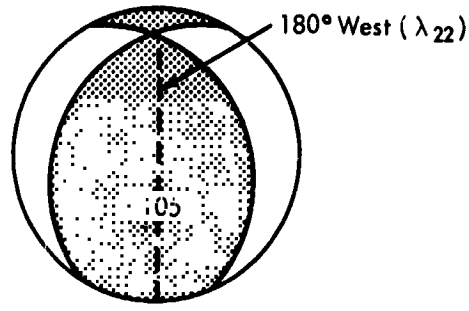

$$V_E=\frac{\mu_E}{r}\left\{1-\frac{\mu_{20}R_0^2}{2r^2}(3\sin^2\phi-1)-3J_{22}\frac{R_0^2}{r^2}\cos^2\phi\cos 2(\lambda-\lambda_{22})\right.$$

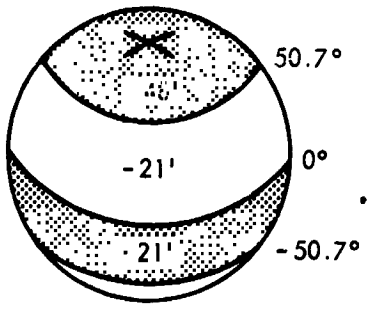

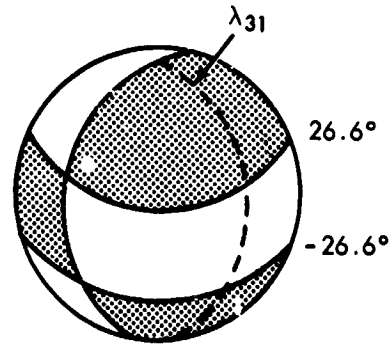

$$\left.-\frac{J_{30}R_0^3}{2r^3}(5\sin^3\phi-3\sin\phi)-\frac{J_{31}R_0^3}{2r^3}\cos\phi\cos(\lambda-\lambda_{31})(15\sin^2\phi-3)\right\} \qquad \text{(B-1)}$$

The earth-gravity field (per unit test mass) whose potential is (B-1) is given as the gradient of (B-1), or

$$\bar{F}=rF_r+\lambda F_\lambda+\phi F_\phi\pm\Delta V_E=r\frac{\partial V_E}{\partial r}+\frac{\lambda}{r\cos\phi}\frac{\partial V_E}{\partial\lambda}+\frac{\phi}{r}\frac{\partial V_E}{\partial\phi}, \qquad \text{(B-2)}$$

or

$$\begin{aligned}Fr=\frac{\mu_E}{r^2}\Big\{&-1+(R_0/)^2[3/2J_{20}(3\sin^2\phi-1)+9J_{22}\cos^2\phi\cos 2(\lambda-\lambda_{22})\\&+2(R_0/r)J_{30}(5\sin^2\phi-3)(\sin\phi)+6(R_0/r)J_{31}(5\sin^2\phi-1)\cos\phi\cos(\lambda-\lambda_{31})\\&+60(R_0/r)J_{32}\cos^2\phi\sin\phi\cos 2(\lambda-\lambda_{32})+60(R_0/r)J_{33}\cos^3\phi\cos 3(\lambda-\lambda_{33})\\&+5/8(R_0/r^2J_{40}(35\sin^4\phi-30\sin^2\phi+3)\\&+25/2(R_0/r)^2J_{41}(7\sin^2\phi-3)\cos\phi\sin\phi\cos(\lambda-\lambda_{41})\\&+75/2(R_0/r)^2J_{42}(7\sin^2-1)\cos^2\phi\cos 2(\lambda-\lambda_{42})\\&+525(R_0/r)^2J_{43}\cos^3\phi\sin\phi\cos 3(\lambda-\lambda_{43})+525(R_0/r)^2J_{44}\cos^4\phi\cos 4(\lambda-\lambda_{44})]\Big\}. \qquad \text{(B-3)}\end{aligned}$$

$$\begin{aligned}F_\lambda=\frac{\mu_E}{r^2}(R_0/r)^2\{&6J_{22}\cos\phi\sin 2(\lambda-\lambda_{22})+3/2(R_0/r)J_{31}[5\sin^2\phi-1]\sin(\lambda-\lambda_{31})\\&+30(R_0/r)J_{32}\cos\phi\sin\phi\sin 2(\lambda-\lambda_{32})+45(R_0/r)J_{33}\cos^2\phi\sin 3(\lambda-\lambda_{33})\\&+5/2(R_0/r)^2J_{41}[7\sin^2\phi-3]\sin\phi\sin(\lambda-\lambda_{41})+15(R_0/r)^2J_{42}(7\sin^2\phi-1)\cos\phi\sin 2(\lambda-\lambda_{42})\\&+315(R_0/r)^2J_{43}\cos^2\phi\sin\phi\sin 3(\lambda-\lambda_{43})\\&+420(R_0/r)^2J_{44}\cos^3\phi\sin 4(\lambda-\lambda_{44})\}. \qquad \text{(B-4)}\end{aligned}$$

Table B-1.—*Tesseral Coefficients in the Earth's Gravity Potential, To Fourth Order, As Reported 1916–1963.**

	J_{22}	λ_{22}	J_{21}	λ_{21}	J_{32}	λ_{32}	J_{31}	λ_{31}	J_{42}	λ_{42}	J_{41}	λ_{41}	J_{33}	λ_{33}	J_{43}	λ_{43}	J_{44}	λ_{44}
(1) Guier (Nov. 1963)	-1.80×10^{-6}	−10 4°	-1.77×10^{-6}	6.3°	$-.226\times10^{-6}$	− 2.6°	$-.304\times10^{-6}$	24.1°	$-.73\times10^{-6}$	219°	$-.273\times10^{-6}$	38.6°	$-.0791\times10^{-6}$	− .7°	$-.0102\times10^{-6}$	35.0°
(2) Kaula (Sept. 1963)	−1.51	−12.1	−1.65	+ 5.3	−.144	46.4	− .145	15.8	− .471	132	− 078	44.2	−.0265	22.6	−.0038	23.3
(3) Izsak (July 1963)	−1.05	−11.2	−1.1	+ 3.2	−.20	−21.8	− .14	20.0	− .43	−132.1	−.13	37.0	−.026	11.5	−.019	14.8
(4) Kaula (May 1963)	−1.4	−21.5	−1.6	− 1.9	−.15	35.8	− .12	18.5	− .53	+126.3	−.12	44.5	−.019	10.7	−.0038	23.3
(5) Cohen (May 1963)	−2.08	−14.1							− .775	201	−.288	34.6	− 162	−4.3		
(6) Kaula (Jan. 1963)	−1.62	−21.4	−1.81	− 3.57	−.145	6.6	− .112	37.6	− .479	114.5	−.072	47.7	−.0088	5.9	−.0132	28.4
(7) Kozai (Oct. 1962)	−1.2	−26.4	−1.9	+ 4.6	−.14	−16.8	− .10	42.6	− .52	−122.5	−.082	65.2	−.035	0.5	−.031	14.9
(8) Newton (April 1962)	−2.15	−10.9							−2.53	+170.9						
(9) Newton (Jan. 1962)	−6.16	−11.0														
(10) Kozai (June 1961)	−2.32	−27.5	−3.95	+22.0	−.41	+31.0	−1.91	51.3	− .264	+163.5	−.167	54.0	−.046	−13.0	−.056	50.3
(11) Kaula (June 1961)	− .55	−13.3	−2.30	20.6	−.06	− .9	− .46	22.6	−1.85	194	−.42	21.1	−.091	− .5	−.024	26.4
(12) Izsak (Jan. 1961)	−5.55	−33.15														
(13) Kaula (1961)	−1.68	−38.5							−1.15	−13.0						
(14) Kranowski (1961?)	−5.53	+15.0														
†(15) Kaula (1960)	− .62	−20 9	− 98	55 4	−	13.5	− .19	14.3	− .46	−132.3	−.081	48.6	−.01	−30.0	−.02	22.5
†(16) Jeffreys (1960)	−4.17	0														
†(17) Uotila (1957)	−3.5	− 6.0														
†(18) Zhongolovitch (1957)	−5.95	− 7.7	−2.21	−25.7	−.6	−26.4	− .54	13.0	− .78	−149.1	−.080	45.0	−.051	− 3.8	−.0224	15.9
†(19) Subbotin (1949)	−5.5															
†(20) Niskanen (1945)	−7.67	− 1 0														
†(21) Jeffreys (1942)	−4.1	J	−2 1	0	−.66	0	− .24	33.3								
†(12) Heiskanen (1938)	−6.34	0														
†(23) Heiskanen (1924)	−9.0	+18.0														
†(24) Helmert (1915)	−6.0	−17 6														

*The J_{nn} and λ_{nn} reported in this table except in one or two instances, have been converted from the original author's set of gravity coefficients of which there are all too many forms in the literature. The blanks indicate the author did not consider that particular tesseral harmonic in fitting an earth potential to the observed data.

†Gravimetric or astro-geodetic tesseral geoids. All other geoid's are either pure satellite geoids or use all three kinds of gravity observations.

COMMENTS

(17), (20), (22), (23), (24) Heiskanen and Meinesz: 1958, The Earth and Its Gravity Field (McGraw Hill, N.Y., p. 79).

(16) Jeffreys, H.: 1959, The Earth (Camb. Univ. Press, N.Y., 4th Ed. Ch. IV and V).

(18) Zongolovitch, D.: 1957, Bull. Inst. Theoret. Astron. 6,505.

(15) Kaula, W. M.: 1959, J. Geophys. Research 64, 2401.

(19) Subbotin, M. F.: 1959, Course in Celestial Mechanics III (Gostekhizdat, Moscow; p. 278).

(12) Izsak, I. G.: 1961, Smithsonian Astronomical Journal 66, #5, 1961 (June) p. 226–229. Uses 2 satellites of medium inclination

(6) Newton, R. R.: 1962, Paper Presented at the Symposium on the Use of Artificial Satellites for Geodesy, April 26–28, 1962, U.S. Naval Observatory, Wash. D.C. (In Press).

(13) Kaula, W. M.: 1961, in Rech. Astr. Van De Hulst, C. and De Jager and A. F. Moore, ed., ed., Space Research II, pp. 360–372, North Holland Publishing Co., Amsterdam.

(1), (5) In: "Non Zonal Harmonic Coefficients of the Geopotential from Satellite Doppler Data," W. H. Guier and R. R. Newton, Johns Hopkins [illegible] (NASA-GSFC), Nov. 1963

(3) Kaula, W. M.: "Tesseral Harmonics of the Gravitational Field and Datum Shifts Derived from Camera Observations of Satellites" *Journal of Geophysical Research*, Vol. 68 #2, Jan. 15, 1963.

(4) Kaula, W. M.: "Improved Geodetic Results from Camera Observations of Satellites" (NASA-GSFC) Paper in Press for the Journal of Geophysical Research—May 1963).

(2) Izsak, I. G.: "Tesseral Harmonics in the Geopotential:" (*Nature*; July 13, 1963; pp. 137–139). Uses 5 satellites, 1 of very high inclination: with Kaula, probably the most accurate satellite tesseral geoid to high order (through 1963).

(9) Newton, R. R.: "Ellipticity of the Earth's Equator Deduced from the Motion of Transit 4A" (*Journal of Geophysical Research*; Vol. 67 #1, Jan. 1962).

(14) In: "Passive Dynamics in Space Flight" A Bureau of Naval Weapons Paper by J. D. Nicolaides and M. M. [illegible] December—1962.

(7) Kozai, Y. (Oct. 1962): Private Communication to the Author.

(10) Kozai, Y. (June 1961: "Tesseral Harmonics of the Geopotential of the Earth as Derived from Satellite Motions" (The Astronomical Journal, 66, #7; Sept. 1961). Uses 2 satellites of medium inclination

(3) Kaula, W. M. (Sept. 1963): "Improved Geodetic Results from Camera Observations of Satellites" (In: *The Journal of Geophysical Research*; Vol. 68, #18, Sept. 1963). Uses 5 satellites of medium inclination

(11) Kaula, W. M. (June 1961): "A Geoid and World Geodetic System Based on a Combination of Gravimetric, Astro-geodetic and Satellite Data" (*Journal of Geophysical Research*; Vol. 66, #6, p. 1807). Probably the most comprehensive "Combined Geoid" to date

(21) Jeffreys, H. (1942): (In-Monthly Notices of the Royal Astronomical Society, Geophys. Supplements, Vol. 5, 55).

$$F_\phi = \frac{\mu}{r^2}(R_0/r)^2\{-3J_{20}\sin\phi\cos\phi + 6J_{22}\cos\phi\sin\phi\cos 2(\lambda-\lambda_{22}) \quad .$$

$$-3/2(R_0/r)J_{30}(5\sin^2\phi-1)\cos\phi + 3/2(R_0/r)J_{31}(15\sin^2\phi-11)\sin\phi\cos(\lambda-\lambda_{31})$$

$$+15(R_0/r)J_{32}(3\sin^2\phi-1)\cos\phi\cos 2(\lambda-\lambda_{32})$$

$$+45(R_0/r)J_{33}\cos^2\phi\sin\phi\cos 3(\lambda-\lambda_{33}) - 5/2(R_0/r)^2J_{40}(7\sin^2\phi-3)\sin\phi\cos\phi$$

$$+5/2(R_0/r)^2J_{41}(28\sin^4\phi-27\sin^2\phi+3)\cos(\lambda-\lambda_{41})$$

$$+30(R_0/r)^2J_{42}(7\sin^2\phi-4)\cos\phi\sin\phi\cos 2(\lambda-\lambda_{42})$$

$$+105(R_0/r)^2J_{43}(4\sin^2\phi-1)\cos^2\phi\cos 3(\lambda-\lambda_{43})$$

$$+420(R_0/r)^2J_{44}\cos^3\phi\sin\phi\cos 4(\lambda-\lambda_{44})\}. \qquad \text{(B-5)}$$

The actual sea-level surface of the earth is to be conceptualized through (B–1) as a sphere of radius 6378 km, around which are superimposed the sum of the separate spherical harmonic deviations illustrated. To these static gravity deviations, of course, must be added a centrifugal earth-rotation potential at the earth's surface, to get the true sea level surface (see Reference 10).

From Table B–1 and equation (B–3), the fourth-order tesseral geoids of Kaula (September 1963), Kozai (1962), Izsak (July 1963), and Zhongolovitch (1957) have been evaluated for the longitudinal perturbation force on a 24-hour satellite with zero inclination at $\lambda = -54.75°$ over the earth's surface (see Table B–2). The harmonics contributing to this perturbation are J_{22}, J_{31}, J_{33}, J_{42} and J_{44}. The results of this comparison are:

TABLE B–2.—*Comparison of Longitudinal Perturbation Forces on a 24-Hour Satellite, From Five Tesseral Geoids.*

	Full Field Longitude Acceleration [Units of 10^{-7} g_s*]	Ratio of Triaxial (J_{22}) Longitude Acceleration to Full Field Longitude Acceleration ($\lambda = -54.75°$)
Zhongolovitch (1957)	7.71	1.06
Kozai (1962)	1.08	1.28
Izsak (July 1963)	1.27	1.19
Kaula (Sept. 1963)	1.77	1.11
Wagner (this reduction: March 1964)	2.21	?

*g_s is the radial acceleration of earth gravity at the "synchronous" altitude ($g_s = 0.735$ ft/sec^2).

Judging from the consistency of the acceleration ratios among these investigators, the "actual" value of J_{22} (separated from higher order gravity effects) is probably somewhat higher than the -1.7×10^{-6} reported herein. All the geodesists reporting in Table B–2 agree that the next most influential earth tesseral at "synchronous" altitudes over most of the equator is J_{33}.

Appendix C

EXPRESSIONS FOR THE INCLINATION FACTOR

Equation (25) gives the inclination factor in the drift causing tangential perturbation (due to equatorial ellipticity) on a 24-hour satellite with a near-circular orbit, as

$$F(i) = \cos(i) + \frac{\Delta\lambda(\max)\,\sin^2(i)}{2} \tag{C-1}$$

$\Delta\lambda$(max.) is the absolute value of the maximum longitude excursion of the figure-8 ground track of the 24-hour satellite (with a near-circular orbit) from the geographic longitude of the nodes.

From (18), this longitude excursion function is

$$\Delta\lambda = \lambda - \lambda_0 = \tan^{-1}[\cos(i)\,\tan\theta] - \theta \tag{C-2}$$

Differentiating (C-2) with respect to the argument angle θ, the minimax excursion arguments are found from

$$\frac{d(\Delta\lambda)}{d\theta} = 0 = \frac{\cos(i)\,\sec^2\theta}{1+\cos^2(i)\,\tan^2\theta} - 1. \tag{C-3}$$

Solving (C-3) for sin θ at $\Delta\lambda$ (minimax),

$$\sin\theta_{\Delta\lambda(\text{minimax})} = [\cos(i)+1]^{-1/2}, \text{ from which}$$

$$\tan\theta_{\Delta\lambda(\text{minimax})} = \sec(i), \tag{C-4}$$

(C-4) in (C-2) gives

$$\Delta\lambda(\text{minimax}) = \tan^{-1}[\cos(i)\,\sec(i)] - \tan^{-1}\sec(i).$$

Thus, since only the absolute value of $\Delta\lambda$ (minimax) is required,

$$\Delta\lambda(\max) = \tan^{-1}[\sec(i)] - 45°, \tag{C-5}$$

where the $\tan^{-1}$ is to be taken in the first quadrant. For example: for $i = 30°$, (C-5) evaluates the maximum excursion as

$$\Delta\lambda(\max) = 49.1° - 45° = 4.1°.$$

The nodal argument angle at this maximum longitude excursion is

$$\theta[\text{at } \Delta\lambda(\max)] = \pm 49.1° \text{ from the nodes.}$$

The assumption in (20) that the excursion in longitude from the ascending node could be approximated by

$$\Delta\lambda - \Delta\lambda(\max)\,\sin 2\theta,$$

predicts the maximum excursion argument as

$$\theta[\text{at } \Delta\lambda(\max)] = \pm 45° \text{ from the nodes.}$$

This discrepancy in the assumed longitude excursion function is not serious until $i > 45°$, as simulated trajectories with variable inclination have borne out.

(C–5) can be written as

$$\Delta\lambda(\max) + 45° = \tan^{-1}[\sec(i)], \text{ from which}$$

$$\tan[\Delta\lambda(\max) + 45°] = \sec(i) \doteq \frac{1+\Delta\lambda(\max)}{1-\Delta\lambda(\max)}, \tag{C-6}$$

for $i < 45°$. Solving (C–6) for $\Delta\lambda$ (max),

$$\Delta\lambda(\max) = \frac{1-\cos(i)}{1+\cos(i)}, \tag{C-7}$$

approximately.

Thus the inclination factor becomes approximately

$$\begin{aligned} F(i) &= \cos(i) + \frac{\sin^2(i)[1-\cos(i)]}{2[1+\cos(i)]} \\ &= \cos(i) + \frac{[1-\cos(i)]^2}{2} = \frac{2\cos(i) + 1 - 2\cos(i) + \cos^2(i)}{2} \\ &= \frac{\cos^2(i)+1}{2} \end{aligned} \tag{C-8}$$

For example: For $i = 30°$,

$$F(i)_{\text{from (C-1)}} = .86603 + 4.1/8 \times 57.3 = .8750$$

$$F(i)_{\text{from (C-8)}} = .8750.$$

The agreement of $F(i)$ from forms (C–1) or (C–8) is good to the third decimal place as long as the inclination is less than 45 degrees. At inclinations higher than 45 degrees, however, the drift theory following (20) begins to break down because $\Delta\lambda(\max)$ is no longer a small angle.

Appendix D

DERIVATION OF THE EXACT ELLIPTIC INTEGRAL OF DRIFT MOTION FOR A 24-HOUR SATELLITE WITH A NEAR-CIRCULAR ORBIT: COMPARISON OF THE EXACT SOLUTION WITH THE APPROXIMATE SOLUTIONS FOR PERIODS VERY CLOSE TO SYNCHRONOUS

The differential equation (33) of 24-hour satellite drift is analogous to the equation describing the large-angle oscillations of a mathematical pendulum (see Reference 11), as in Figure D–1.

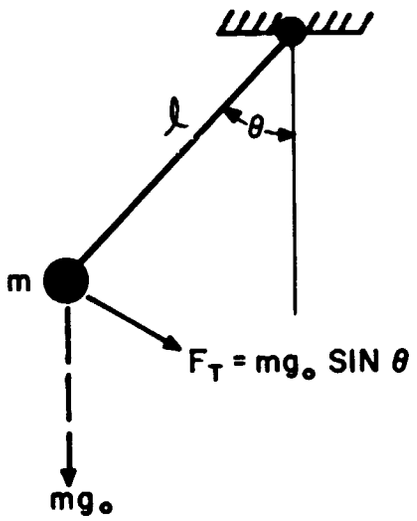

FIGURE D–1.—Configuration of a "mathematical pendulum."

The equation of angular motion of the mass m under the constant gravity force mg_0 is

$$F_T = \mathrm{mg}_0 \sin\theta = m(\dot{\ell}\dot{\theta}) = m\ell\ddot{\theta} \tag{D-1}$$

(D–1) can be rewritten as

$$\ddot{\theta} + (g_0/\ell)\sin\theta = 0. \tag{D-2}$$

From the theory developed in Reference 11 (pp. 327–335), (D–2) has an integral

$$t \text{ (time from } \theta = 0) = (\ell/g_0)^{1/2} F(k, \phi). \tag{D-3}$$

where $F(k, \phi)$ is the elliptic integral of the first kind with argument (or amplitude) $\phi = \sin^{-1}\left[\dfrac{\sin\theta/2}{\sin\theta\ (\max)/2}\right]$, and modulus $k = \sin\theta\ (\max)/2$.

Equation (33):

$$\ddot{\gamma}+A_{22}\sin 2\gamma=0,$$

with maximum libration angle γ_0, can be put in the form of (D–2) by the transformation of the dependent variable

$$\theta=2\gamma, \tag{D-4}$$

with the parameter identification

$$g_0/\ell=2A_{22}. \tag{D-4A}$$

(D–4) implies the identification

$$k=\sin\gamma_0, \qquad \phi=\sin^{-1}[\sin\gamma/\sin\gamma_0]. \tag{D-4B}$$

The pendulum solution (D–3), under the transformation (D–4) and identifications (D–4A) and (D–4B) becomes

$$t \text{ (time of drift libration from } \gamma=0)=(1/2A_{22})^{1/2}\,F(\sin\gamma_0,\,[\sin^{-1}\sin\gamma/\sin\gamma_0]), \tag{D-5}$$

$F(k, \phi)$, in its full integral form, is

$$F=\int_0^{\phi}\frac{d\phi}{(1-k^2\sin^2\phi)^{1/2}}, \tag{D-6}$$

(where $k^2=\sin^2\gamma_0$, $\sin^2\phi=\sin^2\gamma/\sin^2\gamma_0$) for the drift libration. In particular, when $\phi=\pi/2$; then $\gamma=\gamma_0;\dot{\gamma}_0=0$, and the pendulum-drift libration has completed a quarter-period.

Thus, from (D–5) and (D–6), the full period of the long-term drift libration of the 24-hour satellite ground track about the nearest minor equatorial axis longitude is

$$T(\gamma_0)=[8/A_{22}]^{1/2}\int_0^{\pi/2}\frac{d\psi}{(1-\sin^2\gamma_0\sin^2\psi)^{1/2}}. \tag{D-7}$$

The adequacy of the Taylor series expansion approximation of the drift motion in the neighborhood of γ_0, given in equation (51), may be tested against the exact drift solution implicit in (D–5). Table D–1 below gives the evaluation of F for arguments within 5° of $\gamma_0=60°$, using the integral tables in Reference 12.

TABLE D-1.—*Exact and Approximate Drifts of a 24-Hour Satellite from a Stationary Configuration 60° East of the Earth's Minor Equatorial Axis.*

$\gamma_0=60°$	γ (degrees)	γ' (degrees)	γ'' (degrees)	ϕ (degrees)	F (rad.)	ΔF (rad.)	Δt (days from $\gamma=60°$)
$A_{22}=23.2\times10^{-6}$ rad/day^2	60.0	60.0	60	90	2.1565	----------	----------
	59.0	59.003	59.000	81.7967	1.8730	.2835	41.619
	58.0	58.014	58.001	78.3056	1.7564	.4001	58.737
	57.0	57.029	56.999	75.5595	1.6671	.4894	71.846
	56.0	56.051	56.999	73.1938	1.5923	.5642	82.827
	55.0	55.077	54.996	71.0617	1.5265	.6300	92.487

In Table D–1, ΔF is the change in the elliptic integral from the "stationary" configuration at $\gamma=60°$ or $\phi=90°$. $\Delta t=(1/2A_{22})^{1-2}\Delta F$. A_{22} was computed from (30A) with the following gravity-earth

constants and for the inclination of Syncom II:

$$R_0 = 6378.2 \text{ km}$$

$$a_s = 42166 \text{ km}$$

$$J_{22} = -1.7 \times 10^{-6}$$

$$i = 33°.$$

γ' gives the drift position as calculated from the first righthand term of (51) alone (the $(\Delta t)^2$ term). γ'' gives the drift position as calculated from the first two righthand terms of (51). The "actual" Syncom II drift in mid-August 1963 began, apparently, at a γ_0 between 48° and 58° east of the minor axis. Thus, the 16 orbits chosen for the first drift period all should be well represented by the $(\Delta t)^2$-only theory, within the rms error of the longitude observations. Similar exact calculations for $\gamma_0 = 45°$, 50°, and 55° confirm the adequacy of the $(\Delta t)^2$-only theory to apply to the second drift-period orbits. They also prove the contention in section 5 that, for reasonably small excursions from "synchronism," the convergence of the Taylor series (51) is adequate if additional terms are included only when they become of a certain minimum significance to the total drift.

Appendix E

BASIC ORBIT DATA USED IN THIS REPORT

TABLE E-1.—*Syncom II Orbital Elements, August 1963 to Febrary 1964.*

Orbit #	Epoch (Universal Time) Year-Month-Day-Hour-Min	Semimajor Axis (km)	Eccentricity	Inclination (degrees)	Mean Anomaly (degrees)	Argument of Perigee (degrees)	Right Ascension of the Ascending Node (degrees)
1-1	63- 8-22- 6-12-14	42164.58	.00018	33.083	24.126	26.285	317.569
1-2	63- 8-26-17- 0	42164.52	.00016	33.090	190.841	26.099	317.454
1-3	63- 8-31- 0- 0	42166.02	.00018	33.062	296.125	30.073	317.475
1-4	63- 9- 5- 0-0	42166.39	.00012	33.064	333.521	357.756	317.362
1-5	63- 9- 9- 0-0	42166.35	.00015	33.048	326.207	9.077	317.272
1-6	63- 9-12- 2-0	42166.55	.00015	33.079	3.657	4.697	317.224
1-7	63- 9-17- 2-0	42166.70	.00018	33.043	12.694	0.581	317.165
1-8	63- 9-20- 2-0	42167.42	.00018	33.010	359.970	16.282	317.098
1-9	63- 9-27- 2-0	42167.51	.00022	33.046	38.922	344.162	316.996
1-10	63-10- 1- 2-0	42168.88	.00024	33.039	26.615	0.433	316.944
1-11	63-10 -8- 2-0	42169.14	.00020	33.013	42.889	350.866	316.780
1-12	63-10-14- 2-0	42169.78	.00028	32.982	36.727	2.673	316.813
1-13	63-10-22- 2-0	42171.51	.00026	32.993	62.833	344.246	316.603
1-14	63-10-30- 0-0	42171.09	.00028	32.948	29.865	354.548	316.570
1-15	63-11- 6- 0-0	42172.15	.00025	32.952	36.699	354.313	316.328
1-16	63-11-12- 0-0	42172.51	.00031	32.920	108.239	3.425	316.308
2-1	63-11-28- 1-0	42165.89	.00005	32.920	222.170	203.901	315.976
2-2	63-12- 4- 0-0	42167.20	.00009	32.892	39.435	17.564	315.919
2-3	63-12-10- 0-0	42167.18	.00010	32.881	51.942	10.958	315.877
2-4	63-12-16-17-0	42168.17	.00007	32.872	300.000	24.505	315.735
2-5	64- 1- 6-17-0	42168.01	.00013	32.867	332.997	11.625	315.544
2-6	64- 1- 9- 6-0	42169.90	.00015	32.857	165.031	16.992	315.469
2-7	64- 1-20- 0-0	42171.43	.00012	32.826	29.098	28.842	315.300
2-8	64- 1-29-20-0	42171.91	.00019	32.859	37.956	13.171	315.212
2-9	64- 2- 5-16-0	42172.89	.00019	32.800	321.168	36.275	315.075
2-10	64- 2-10-19-0	42173.31	.00014	32.833	32.517	14.553	314.982
2-11	64- 2-17- 0-0	42174.89	.00019	32.762	347.774	35.551	314.883

The Orbit elements for Syncom II in Table E-1 were calculated at the Goddard Space Flight Center from radar and Minitrack observations made during the slow drift periods from mid-August 1963 to February 1964.

As an example of the estimation of the ascending equator crossing nearest to epoch, consider the orbit geometry at epoch (Figure E-1).

6 January 1964 at 17.0 hours Universal Time (orbit 2-5).

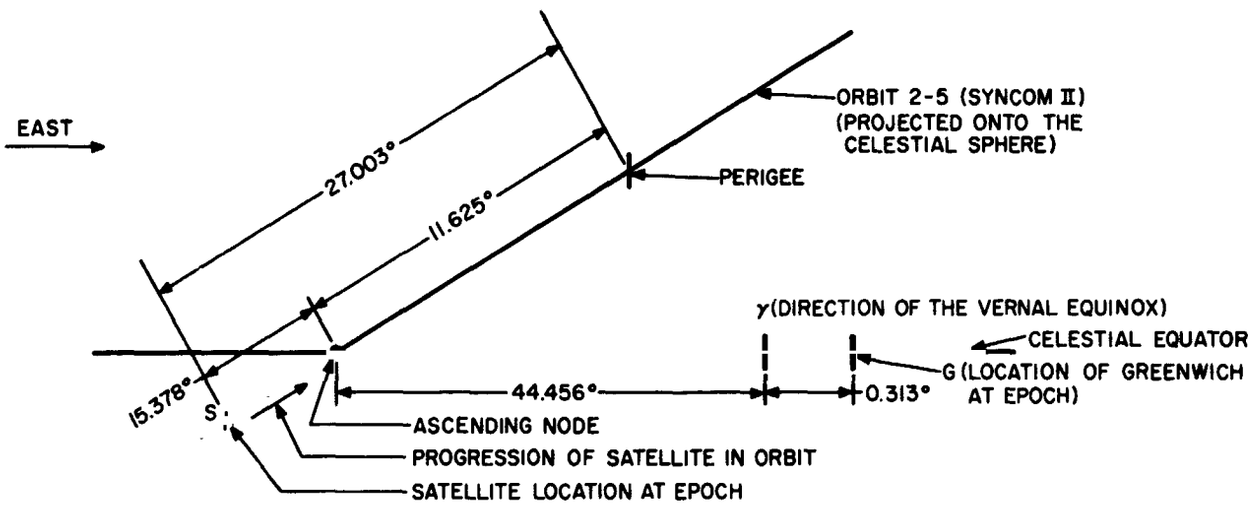

FIGURE E-1.—A portion of the celestial sphere at the epoch of orbit 2-5.

On 6.0 January 1964, the hour angle of the vernal equinox Λ *west* of Greenwich (expressed in hours, with 24 hours = 360°) was

6 hrs. 58 minutes 27.484 seconds (from the Nautical Almanac)

On 7.0 January 1964, the hour angle of Λ was

7 hrs. 2 min. 24.036 sec.

Interpolating, the hour angle of Λ on 6 January at 17 hours Universal Time was

0 hours 1 minute 15.042 seconds, or

0.313 degrees west of Greenwich.

In Figure E–1, the orbit angle 27.003° is taken directly as 360° − the mean anomaly, because the orbit is nearly circular. The reported period for this orbit was

$$T_p = 1436.21696 \text{ minutes.}$$

The earth's sidereal rotation period is taken to be

$$T_{\text{earth}} = 1436.06817 \text{ minutes.}$$

Thus, if the satellite is assumed to traverse orbit 2–5 at a nearly uniform rate, it will reach the celestial equator at a time when the Greenwich meridian has proceeded eastward from the epoch

$$15.378 \times 1436.21696/1436.06817 = 15.380°.$$

Thus, the estimated geographic longitude of the ascending equator crossing nearest to the epoch of orbit 2–5 is

$$\text{Ascending equator crossing longitude} = -(44.456+0.313+15.380)$$
$$= -60.149°.$$

The estimated time of this crossing is

$$15.380°/15°^{/hr.} = 1.025 \text{ hours after the epoch.}$$

The crossing time (Table 1) is thus estimated to be at

6.751 January 1964 (18.025/24+6.0, January 1964).

Appendix F

CALCULATION OF THE RADIATION PRESSURE ON SYMCOM II

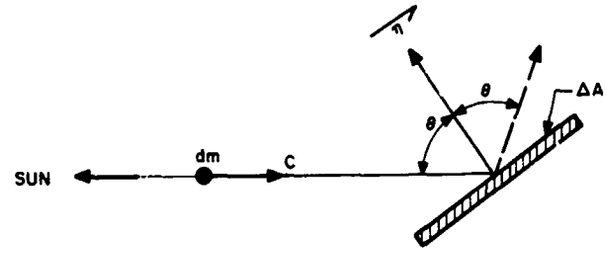

FIGURE F-1.—Flat plate ΔA of satellite surface, with normal η at angle θ with respect to sun's rays.

Consider a flat-plate element ΔA, of the surface of Syncom II, whose normal $\bar{n}$ is at angle θ with respect to the sun's rays (Figure F–1). The sun's radiant energy can be thought of as being made up of a stream of material particles such as dm, moving at the speed of light c. If the energy of each particle is dE, then from Einstein's classical energy-mass equivalence statement,

$$dm = dE/c^2 \tag{F-1}$$

Upon striking the surface, the incident radiation may:

- Reflect completely off the surface at an equal "reflection" angle, undegraded in energy
- Be absorbed into the body of the plate as thermal energy and partially reradiated in all directions from the surface at a reduced flux, depending on the surface and on the thermal properties of the plate and body of the spacecraft
- Be partially "reflected" and absorbed and reradiated, depending on the surface properties of the plate

An estimate of the radiation pressure on Syncom II will be calculated assuming complete light absorption with no reradiation. This is not the most conservative condition but will serve to show the order of magnitude of the effect.

Light-particle dm has $c\,dm$ momentum in the direction of the sun's rays before striking the plate element ΔA. Thus $(c)\,dm$ momentum is transferred to the plate with each light-particle collision. From Newton's second-law, the impulse transferred to the plate in the time of action dt, of dm alone, is;

$$\int_0^{dt} (dF)_{dm}\,dt = (c)dm, \tag{F-2}$$

dF acts on the plate element in the direction of the sun's rays. Assume that the discontinuous collision processes of (F–2) are so frequent as to amount to a smooth transfer of momentum between the stream of light particles and the plate; dt can then be replaced by Δt, a small but finite time interval; $(dF)_{dm}$ by ΔF, a smooth, constant small reactive force on the plate element ΔA; and dm can be replaced by Δm, a small but finite light particle mass impinging on the plate surface ΔA in Δt time. (F–2) then becomes

$$\Delta F(\text{radiation force})\ \Delta t = (c)\Delta m, \text{ or}$$

$$\Delta F(\text{radiation force}) = (c)\frac{\Delta m}{\Delta t}. \tag{F-3}$$

By the mass-energy equivalence relation (F–1) written for the finite small elements involved in the continuous momentum transfer,

$$\Delta m = \Delta E/c^2, \tag{F–4}$$

where ΔE is the energy flux falling on plate element ΔA in Δt time. Clearly,

$$\Delta E = \rho \Delta A \cos\theta(\Delta t), \tag{F–5}$$

where ρ is the sun's energy flux in units of energy/time-area, and $\Delta A \cos\theta$ is the projected area of the element in the direction of the sun's rays. Combining (F–3), (F–4) and (F–5);

$$\Delta F/\Delta A_p = \text{projected area-radiation pressure in the direction of the sun's rays} = p_s = \frac{\rho}{c}, \tag{F-6}$$

($\Delta A_p = \Delta A \cos\theta$ = projected area of the plate element in the direction of the sun's rays.)

The value of ρ outside the earth's atmosphere is estimated to be (see Reference 9)

$$\rho = 95.5 \text{ ft-pounds/ft.}^2\text{-sec.}$$

$$c = 9.835 \times 10^8 \text{ ft./sec.}$$

(F–6) thus becomes;

$$\rho_s \text{ (projected area-solar pressure against a fully absorbing surface in the direction of the sun's rays)} = .9725 \times 10^{-7} \text{ pounds/ft.}^2 \tag{F–7}$$

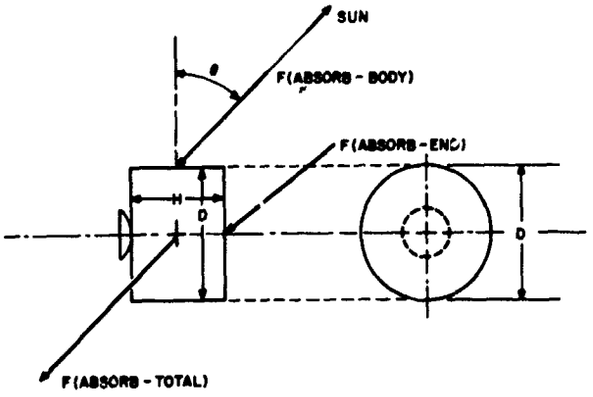

FIGURE F-2.—Configuration of Syncom II with respect to the sun during drift.

Figure F–2 shows the configuration of Syncom II with respect to the sun during the drift. For the cylindrical configuration in Figure F–2, from (F–7);

$$F(\text{absorb-total}) = F(\text{absorb-body}) + F(\text{absorb-end}) = .9725 \times 10^{-7}(HD\cos\theta + \pi D^2 \sin\theta/4) \tag{F–8}$$

The weight of Syncom II in the 24-hour orbit (including the apogee motor) is about 75 pounds. Other parameters are:

$$H = 15''$$

$$D = 28''$$

$$\theta = 21° \text{ (in late August 1963).}$$

INTRODUCTION TO THE APPLICATION OF VON ZEIPEL'S METHOD

WILLIAM J. WICKLESS, JR.

INTRODUCTION

To understand the application of Von Zeipel's method in the case of a satellite orbiting under the influence of a gravitational field plus small perturbating forces, it is first necessary to summarize the development of several concepts of classical mechanics. Therefore, the first portion of this paper will be a brief resume of material which may be found in greater detail and slightly modified form in Chapters 7–8 of *Classical Dynamics of Particles and Systems* by Jerry B. Marion, Dept. of Physics, University of Maryland. A good knowledge of ordinary differential and integral calculus is assumed.

1. AN INTRODUCTION TO THE CALCULUS OF VARIATIONS

The basic problem of the calculus of variations is determining the unknown function $y(x)$ describing a path between two fixed end points we call $y(x_1)$ and $y(x_2)$ such that

$$I=\int_{x_1}^{x_2} f[y(x), y'(x), x]dx$$

takes on a maximum or minimum. f is a given function of the functions $y(x)$, $y'(x)$ and the independent variable x and the limits of integration are fixed. That is, if we wish to minimize I (say), we wish to find a function $y(x)$ such that if $y_1(x)$ is any other continuous function such that $y_1(x_1)=y(x_1)$, $y_1(x_2)=y(x_2)$ – any other path between $y(x_1)$ and $y(x_2)$ – then:

$$\int_{x_1}^{x_2} f[y(x), y'(x), x]dx \leq \int_{x_1}^{x_2} f[y_1(x), y_1'(x), x]dx$$

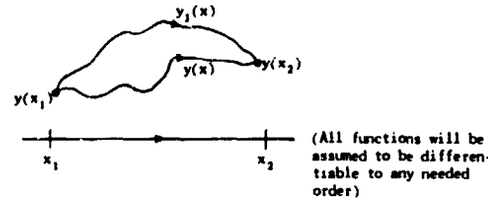

Two possible paths between $y(x_1)$ and $y(x_2)$ are sketched above.

Two possible paths between $y(x_1)$ and $y(x_2)$ are sketched above.

We will consider families of functions, giving possible paths between two fixed points $y(x_1)$, and $y(x_2)$, indexed by a parameter α, α running over a suitable segment of the real line. That is, we will consider families of the form

$$\{y(\alpha, x)\} \quad \begin{matrix} x\epsilon[x_1, x_2] \\ \alpha\epsilon[a, b] \end{matrix} \quad \text{with}$$

$$\left.\begin{matrix} y(\alpha, x_1)=y(x_1)=\text{constant} \\ y(\alpha, x_2)=y(x_2)=\text{constant} \end{matrix}\right\} \text{for all } \alpha\epsilon\,[a, b].$$

Then the integral I becomes a function of the parameter α:

$$I(\alpha)=\int_{x_1}^{x_2} f[y(\alpha, x), y'(\alpha,x), x]dx.$$

For example

$$I(\alpha)=\int_0^{2\pi} x(\alpha \sin x)dx \qquad \alpha\epsilon[1, 2]$$

where

$$y(\alpha, x)=\alpha \sin x$$
$$f[x, y(\alpha, x), y'(\alpha, x)]=xy(\alpha, x)$$
$$x_1=0,\ x_2=2\pi$$
$$y(x_1)=0\ y(x_2)=0$$

*Published as *Goddard Space Flight Center Document X-547-64-347*, September 1964

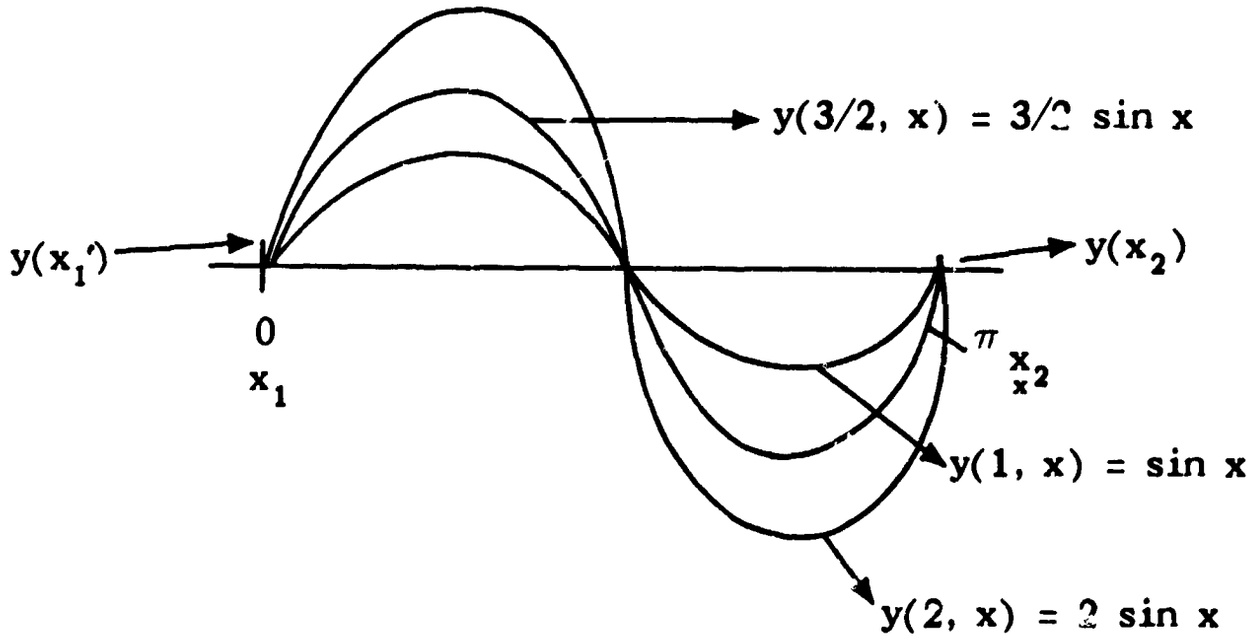

NOTE: $\alpha \sin(0) = 0$; $\alpha \sin 2\pi = 0$ for all $\alpha \epsilon [1, 2]$; $\{\alpha \sin x\}$ represents the family of paths between the pts $(0, 0) \equiv y(x_1)$, $(2\pi, 0) \equiv y(x_2)$ shown at top.

Now if the integral so written is to have an extremum along some path $y(\alpha_0, x)$

$$\alpha_0 \epsilon [a, b]$$

then

$$\left.\frac{\partial I(\alpha)}{\partial \alpha}\right|_{\alpha=\alpha_0} = 0.$$

This means

$$\left.\frac{\partial}{\partial \alpha}\int_{x_1}^{x_2} f[y(\alpha, x), y'(\alpha, y), x]dx\right|_{\alpha=\alpha_0} = 0.$$

since x is independent of α, the partial may be taken under the integral sign:

$$\left.\int_{x_1}^{x_2} \left[\frac{\partial f}{\partial y}\frac{\partial y}{\partial \alpha} + \frac{\partial f}{\partial y'}\frac{\partial y'}{\partial \alpha}\right]dx\right|_{\alpha=\alpha_0} = 0.$$

Now the above equation may be integrated by parts (see (1), Sec. 7-3) to obtain

$$\left.\int_{x_1}^{x_2} \left[\frac{\partial f}{\partial y} - \frac{d}{dx}\frac{\partial f}{\partial y'}\right]\frac{\partial y}{\partial \alpha}dx\right|_{\alpha=\alpha_0} = 0.$$

As f is assumed to be an arbitrary function of $y(\alpha, x)y'(\alpha, x)x$, the integrand itself must vanish:

$$\left[\frac{\partial f}{\partial y} - \frac{d}{dx}\frac{\partial f}{\partial y'}\right]\left.\frac{\partial y}{\partial \alpha}\right|_{\alpha=\alpha_0} = 0$$

for all $x \epsilon [x_1, x_2]$.

Also since $\{y(\alpha, x)\}$ is an arbitrary family of paths, in general

$$\left.\frac{\partial y(\alpha, x)}{\partial \alpha}\right|_{\alpha=\alpha_0} \neq 0 \text{ along the curve}$$

$$y = y(\alpha_0, x)$$
$$x \epsilon [x_1, x_2]$$

therefore

$$\frac{\partial f}{\partial y)\alpha_0, x)} - \frac{d}{dx}\frac{\partial f}{\partial y'(\alpha_0, x)} = 0$$

for all $x \epsilon [x_1, x_2]$.

This is known as the Euler-Lagrange equation.

II. APPLICATION OF THE EULER-LAGRANGE EQUATION TO PHYSICAL SYSTEMS

It is known that if a particle is allowed to move between two fixed pts in the plane $x(t_1)$ and $x(t_2)$ in the time interval $[t_1, t_2]$ in any of the possible paths given by the family of curves $\{x(\alpha, t)\}$

$$t \epsilon [t_1, t_2] \quad \alpha \epsilon [a, b]$$

it will actually move in the path $x=x(\alpha_0, t)$ for which

$\int_{t_1}^{t_2}(T-U)dt$ is a relative extreme. (Note that this is a local condition.)

(see (1), Sec. 8.3)

Here T is the kinetic energy of the particle at the point $x(\alpha, t)-T=\frac{1}{2}m\dot{x}^2(\alpha, t)$—and U is the potential energy at the same pt $U=U(x(\alpha, t))$.

$\therefore$ along the path of the particle's motion $\bar{x}(t)=x(\alpha_0, t)$, the Euler-Lagrange equation must be satisfied by the quantity $L=(T-U)$. L is called the *Lagrangian* of the system.

Thus we have

$$\frac{\partial L}{\partial \bar{x}(t)}-\frac{d}{dt}\frac{\partial L}{\partial \bar{x}'(t)}=0.$$

If the Lagrangian of a system is known, the above equation may be integrated giving the path of the particles motion $x=\bar{x}(t)$.

EXAMPLE: Determination of the Equation of Motion for a Harmonic Oscillator

Let a particle of mass m be attached to a spring with spring constant K and relaxed length 0. Choose a co-ordinate system such that the point of equilibrium of the spring is at $x=0$. Let the mass be pulled to a distance h above the $x=0$ level and released at a time $t=0$. Find $x(t)$ (the bar is hereafter dropped for convenience)

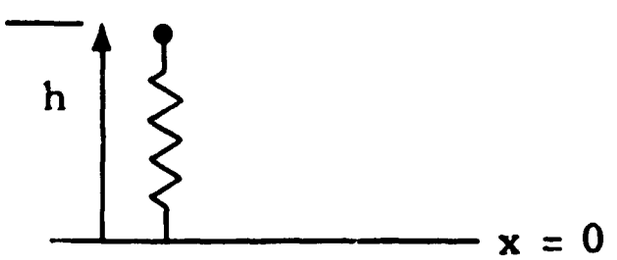

Now for any time t, we have $T=\frac{1}{2}m\dot{x}^2(t)$ and $U=\frac{1}{2}Kx^2(t)$.

so $L=T-U=\frac{1}{2}m\dot{x}^2(t)-\frac{1}{2}Kx^2(t)$.

Now if $x(t)$ is the path followed by the particle, the Euler-Lagrange equation must be satisfied, i.e.

$$\frac{\partial L}{\partial x(t)}-\frac{d}{dt}\frac{\partial L}{\partial \dot{x}(t)}=0.$$

Now

$$\frac{\partial L}{\partial x(t)}=-Kx(t);\ \frac{\partial L}{\partial \dot{x}(t)}=m\dot{x}(t)$$

$$\therefore -Kx(t)=\frac{d}{dt}[m\dot{x}(t)]$$

or

$$\ddot{x}(t)+w_0^2x(t)=0 \text{ with } w_0\equiv\sqrt{K/m}.$$

This differential equation may be solved (see any elementary text) to obtain

$$x(t)=A\sin(w_0t+\delta)$$

where $A+\delta$ are constants of integration to be fitted to the initial data—in this case $A=h$, $\delta=\pi/2$.

Now an important thing to notice is that the Lagrangian is a scalar function (being the difference of kinetic and potential energies—both scalar functions). Thus we can, if desired, transform one co-ordinate variable $x(t)$ to a new variable $q(t)$ under some co-ordinate transformation ϕ and we have

$$L(x(t), \dot{x}(t), t)=\bar{L}(q(t), \dot{q}(t), t).$$

(This is actually the defining property of a scalar function).

The Euler-Lagrange equation is still valid:

$$\frac{\partial \bar{L}}{\partial q(t)}-\frac{d}{dt}\frac{\partial \bar{L}}{\partial \dot{q}(t)}=0.$$

Now as one final generalization, it is clear the original analysis could have been carried out to treat the case of a particle with more than one degree of freedom. The Lagrangian then would have been a function of several co-ordinate variables, their derivatives, and possibly the time, i.e.

$$L=L(x_1(t)\cdots x_n(t), \dot{x}_1(t)\cdots\dot{x}_n(t), t).$$

We then could proceed in a similar fashion [see (1), Sec. 7-7] to obtain, instead of the single equation

$$\frac{\partial L}{\partial x}-\frac{d}{dt}\frac{\partial L}{\partial \dot{x}}=0$$

the system of equations:

$$\frac{\partial L}{\partial xj}-\frac{d}{dt}\frac{\partial L}{\partial \dot{x}j}=0$$

$$j=1, 2\cdots N.$$

Now as this Lagrangian is still a scalar function, we may make if desired, a co-ordinate transformation ϕ from the position variables $\{x_1(t)\cdots x_n(t)\}$ to some new set of variables $\{q_1(t)\cdots q_n(t)\}$ and we still have:

$$\bar{L}(q_1\cdots q_n, \dot{q}_1\cdots\dot{q}_n, t)=L(x_1\cdots x_n, \dot{x}_1\cdots\dot{x}_n, t)$$

And also

$$\frac{\partial \bar{L}}{\partial qj}-\frac{d}{dt}\frac{\partial \bar{L}}{\partial \dot{q}j}=0. \quad j=1\cdots n(a)$$

It is important to note that the new variables may be chosen as a set of *any N functions* $q_1(t)\cdots q_n(t)$ at all as long as the Lagrangian may be expressed as $L=L(q_1(t)\cdots q_n(t), q_1(t)\cdots\dot{q}_n(t)t)$. In a real problem, a set of variables $q_1(t)\cdots q_n(t)$ are usually chosen so that L may be easily expressed as $\bar{L}(q_1\cdots q_n\dot{q}_1\cdots\dot{q}_n\, t)$. Then the system (a) is integrated, giving $qj=qj(t,$ constants of integration$)$ $j=1\cdots n(b)$.

Finally the transformation ϕ is inverted and ϕ^{-1} is applied to (b), yielding

$$xj=xj(t) \quad j=1\cdots N.$$

The vector $\vec{r}(t)=(x_1(t)\cdots x_n(t))$ is then the position vector of the particle under consideration.

III. CONSTRUCTION OF THE HAMILTONIAN; THE CANONICAL EQUATIONS OF MOTION

Now let us consider a system in which (1) the Lagrangian is not an explicit function of the time, i.e. $L=L(q_1(t)\cdots q_n(t), \dot{q}_1(t)\cdots\dot{q}_n(t))$ and (2) the q_j's have been obtained from the x_j's by some transformation ϕ that does not explicitly involve the time.

Let us define N new quantities:

$$Pj\equiv\frac{\partial L}{\partial \dot{q}_j} j=1, 2\cdots N. \quad (I)$$

P_j is called the *conjugate momentum* associated with q_j.

Using this definition, the Euler-Lagrange equations for our system may be rewritten in the form

$$\dot{P}j=\frac{\partial L}{\partial q_j} j=1, 2\cdots N. \quad (II)$$

Now let us define a new quantity

$$H\equiv \Sigma P_j\dot{q}_j-L.$$

H is called the *Hamiltonian* of the system, and under assumptions (1) and (2) above, it can be shown that H is equal to the total energy of the particle under consideration. $H=T+U$. (See (1), Sec. 8–8).

Now if H is considered to be a function of q_j, P_j $j=1\cdots N$, then

$$dH=\sum_j\frac{\partial H}{\partial q_j}dq_j+\frac{\partial H}{\partial P_j}dP_j \quad (A)$$

also since

$$H=\sum_j P_j\dot{q}_j-L$$

$$dH=\sum_j P_j\, d\dot{q}_j+\dot{q}_j\, dP_j-\frac{\partial L}{\partial q_j}dq_j-\frac{\partial L}{\partial \dot{q}_j}dq_j$$

using (I) and (II), the above becomes

$$dH=\sum_j[P_j\, d\dot{q}_j-P_j\, d\dot{q}_j]+\dot{q}_j dP_j-\dot{P}_j dq_j$$
$$=\sum_j\dot{q}_j\, dP_j-\dot{P}_j\, dq_j. \quad (B)$$

Now identifying the coefficients of dP_j & dq_j in (A) and (B) we have

$$-\dot{P}_j=\frac{\partial H}{\partial q_j}\dot{q}_j=\frac{\partial H}{\partial P_j} \quad j=1, 2\cdots N.$$

These are called the *cyclic equations of motion.* As in the case of the Euler-Lagrange equations, they may be integrated to obtain the equations of motion of the particle under consideration.

We will now consider our problem—determination of the equations of motion for a satellite orbiting under the influence of a gravitational field plus small perturbations (e.g. the effects of the earth's oblateness.) The following (sec. IV) is a summary of a portion of the material found in the paper "Notes on Von Zeipel's Method" by Giorgio E. O. Giacaglia, published at the Goddard Space Flight Center.

IV. VON ZEIPEL'S METHOD

In the case we are considering, the Hamiltonian may be expressed as a function of six variables (L, G, H, ℓ, g, h) where L, G, H are the conjugate momenta associated with ℓ, g, h respectively. These six variables are called the *Delaunay variables.*

The equations to be integrated for our problem then are:

$$\dot{\ell}=\frac{\partial H}{\partial L}\ \dot{g}=\frac{\partial H}{\partial G}\ \dot{h}=\frac{\partial H}{\partial H}\quad -\dot{L}=\frac{\partial H}{\partial \ell}-\dot{G}=\frac{\partial H}{\partial g}-\dot{H}=\frac{\partial H}{\partial h}$$

here we have just taken the cyclic equations of motion and set $L=P_1$, $G=P_2$, $H=P_3$, $\ell=q_1$, $g=q_2$, $h=q_3$.

In many cases the negative of the Hamiltonian $F=-H$ is introduced; the cyclic equations of motion for our system then become:

$$\dot{\ell}=-\frac{\partial F}{\partial L}\quad \dot{g}=-\frac{\partial F}{\partial G}\quad \dot{h}=-\frac{\partial F}{\partial H}$$

$$\dot{L}=\frac{\partial F}{\partial \ell}\quad \dot{G}=\frac{\partial F}{\partial g}\quad \dot{H}=\frac{\partial F}{\partial h}.$$

Now in solving the above system, it would greatly simplify our problem if we could transform our variables (L, G, H, ℓ, g, h) to a new set of variables $(L', G', H', \ell', g', h')$ in which the new function F could be expressed in a form not explicitly containing one of the new variables (ℓ' say), i.e.

$$F'=F'(L', G', H'-g', h')$$

then

$$\dot{L}'=\frac{\partial F'}{\partial \ell'}=0;\qquad L'=\text{constant}.$$

Here we must remember that, for the cyclic equations of motion to be valid, the new variables must satisfy

$$L'=\frac{\partial L}{\partial \dot{\ell}'}\quad G'=\frac{\partial L}{\partial \dot{g}'}\quad H'=\frac{\partial L}{\partial \dot{h}'}$$

i.e. L', G', H' must be the conjugate momenta with respect to ℓ', g', h'. (This assumption was used to derive the cyclic equations of motion).

If the above equations are satisfied, then $(L', G', H', \ell', g', h')$ are said to be a *canonical set* of variables, and the transformation connecting the primed and unprimed variables is called a *canonical transformation* [assuming $F(L, G, H, \ell, g, h)=F'(L', G', H', -g', h')$ for all times t].

Now finding the desired canonical transformation connecting (L, G, H, ℓ, g, h) to a new set of variables $(L', G', H', \ell', g', h')$ for which $\partial F'/\partial \ell'=0$ is equivalent to finding a function $S=S(\ell, g, h, L', G', H')$, called a *generating function*, satisfying:

$$L=\frac{\partial S}{\partial \ell}\quad G=\frac{\partial S}{\partial g}\quad H=\frac{\partial S}{\partial h}$$

$$\ell'=\frac{\partial S}{\partial L'}\quad g'=\frac{\partial S}{\partial G'}\quad h'=\frac{\partial S}{\partial H'}.$$

This function S will determine an implicit transformation connecting (L, G, H, ℓ, g, h) and $(L', G', H', \ell', g', h')$ and it is known that the new set of variables will be canonical. (See *Planetary Theory* by Brown and Shook, sec. 5–3.)

We now shall give explicit formulas for determining S and F'. Here we first employ the assumption that our satellite is orbiting in a gravitational field, subject to small perturbing forces. We assume the function $F(L, G, H, \ell, g, h)$ can be expanded in a series

$$F=F_0+\sum_{j=1}^{\infty}F_j\lambda$$

where F_0 is the negative of the Hamiltonian calculated in the case of a body orbiting under the influence of gravity alone and λ is a small parameter. (For the calculation of $F_0=\mu^2/2L^2$ where $\mu=K^2M$, with K the Gaussian constant and M the mass of the orbited body; see any intermediate textbook in celestial mechanics.)

We assume similarly:

$$F=F_0'+\sum_{j=1}^{\infty}F_j\lambda^j$$

$$S=S_0+\sum_{j=1}^{\infty}S_j\lambda^j$$

where S_0 is the generating function determining the identity transformation, $S_0=L'\ell+G'g+H'h$. (In the Keplerian case the original set of variables are the ones desired; no transformation is necessary.)

Now to any order in λ, $F(L, G, H, \ell, g, h)=F'(L', G', H'-g', h')$. (Remember F' is not to be an explicit function of ℓ'.)

Look at this equation up to second order in λ, i.e.

$$F_0+\lambda F_1+\lambda^2F_2=F_0'+\lambda F_1'+\lambda^2F_2' \qquad (A)$$

now

$$L=\frac{\partial S}{\partial \ell}=\frac{\partial S_0}{\partial \ell}+\sum_{j=1}^{\infty}\lambda^j\frac{\partial S_j}{\partial \ell}=L'+\sum_{j=1}^{\infty}\lambda^j\frac{\partial S_j}{\partial \ell}.$$

$$g'=\frac{\partial S}{\partial G'}=\frac{\partial S_0}{\partial G'}+\sum_{j=1}^{\infty}\lambda^j\frac{\partial S_j}{\partial G'}=g+\sum_{j=1}^{\infty}\lambda^j\frac{\partial S_j}{\partial G}$$

with similar expressions for G, H, h'.

Substituting the above into (A), we have

$$F_0\left(L'+\sum_{j=1}^{\infty}\lambda^j\frac{\partial S_j}{\partial \ell}\right)+\lambda F_1\left(L'+\sum_{j=1}^{\infty}\lambda^j\frac{\partial S_j}{\partial \ell},\right.$$

$$\left.G'+\sum_{j=1}^{\infty}\lambda^j\frac{\partial S_j}{\partial g},\ H'+\sum_{j=1}^{\infty}\lambda^j\frac{\partial S_j}{\partial h},\ \ell,\ g,\ h\right)$$

$$+\lambda^2F_2\left(L'+\sum,\ G'+\sum,\ H'+\sum,\ \ell,\ g,\ h\right)$$

$$=F_0'L',\ G',\ H'-,\ g+\sum_{j=1}^{\infty}\lambda^j\frac{\partial S_j}{\partial G'}h'+\sum_{j=1}^{\infty}\lambda^j\frac{\partial S_j}{\partial H'}$$

$$+\lambda F_1'(L',\ G',\ H'-g+\Sigma,\ h+\Sigma)+\lambda^2F_2'(L',$$

$$G',\ H'-g+\Sigma,\ h+\Sigma.) \quad \text{(B)}$$

Now expanding the left side of (B) in a Taylor series around L, G, H and F'_1 and F'_2 on the right hand side in a Taylor series around g', h' and keeping only terms up to and including the second order in λ, we have

$$F_0(L')+\frac{\partial F_0}{\partial L}\left[\frac{\partial S_1}{\partial \ell}\lambda+\frac{\partial S_2}{\partial \ell}\lambda^2\right]+\lambda^2F_1(L',\ G',\ H',$$

$$\ell,\ g,\ h)+\lambda^2\left[\frac{\partial F_1}{\partial L}\frac{\partial S_1}{\partial \ell}+\frac{\partial F_1}{\partial G}\frac{\partial S_1}{\partial g}+\frac{\partial F_1}{\partial H}\frac{\partial S_1}{\partial h}\right]$$

$$+\lambda^2F_2[L',\ G',\ H',\ \ell,\ g,\ h]=F_0'(L',\ G',\ H'-g',\ h')$$

$$+\lambda F_1'(L',\ G',\ H'-g,\ h)+\lambda^2\left[\frac{\partial F_1'}{\partial g'}\frac{\partial S_1}{\partial G'}+\frac{\partial F_1}{\partial h'}\frac{\partial S_1}{\partial H'}\right]$$

$$+\lambda^2F_1'[L',\ G',\ H'-g,\ h] \quad \text{(C)}$$

Now equating the coefficients of like powers of λ in (C) we obtain

$$F_0'(L',\ G',\ H'-g',\ l')=F_0(L')=\frac{U^2}{2L'^2} \quad \text{(D)}$$

$$F_1(L',\ G',\ H',\ \ell,\ g,\ h)+\frac{\partial F_0}{\partial L}\frac{\partial S_1}{\partial \ell}$$

$$=F_1'(L',\ G',\ H'-g,\ h) \quad \text{(E)}$$

$$\frac{\partial F_0}{\partial L}\frac{\partial S_2}{F\ell}+\frac{\partial F_1}{\partial L}\frac{\partial S_1}{\partial \ell}+\frac{\partial F_1}{\partial G}\frac{\partial S_1}{\partial G'}+\frac{\partial F_1}{\partial H}\frac{\partial S_1}{\partial h}$$

$$+F_2(L',\ G',\ H',\ \ell,\ g,\ h)=\frac{\partial F_1}{\partial g'}\frac{\partial S_1}{\partial G'}+\frac{\partial F_1}{\partial h}\frac{\partial S_1}{\partial H'}$$

$$+F_2(L',\ G',\ H'-g,\ h). \quad \text{(F)}$$

Now F'_0 is determined by (D) so (E) may be solved by putting F'_1 = part of F_1 independent of ℓ. This means $(\partial F_0/\partial L)(\partial S_1/\partial \ell)=-(F_1-F'_1)$ $=-$(part of F_1 dependent on ℓ). Now F'_1 and S_1 are determined with the desired properties, and therefore (F) may be solved for S_2 by putting F'_2 = part of F_2 independent of ℓ.

This determines F'_2 and S_2 with the required properties. This process may be continued to determine F'_n and S_n to any desired order.

REFERENCES

1. Classical Dynamics of Particles and Systems; JERRY B. MARION; University of Maryland.
2. Planetary Theory; BROWN and SHOOK; Cambridge University Press.
3. Notes on Von Zeipel's Method; GIORGIO E. O. GIACAGLIA; GSFC—X-547-64-161.

III. SOLAR PHYSICS

COMMENTS ON HIGH ENERGY X-RAYS BURSTS OBSERVED BY OSO-1*

KENNETH J. FROST

Instrumentation aboard the first Orbiting Solar Observatory observed five separate instances of high energy X-ray bursts accompanying solar flares. The X-ray bursts were observed in the 20 to 100 Kev range. Data on the types of flares producing the X-ray bursts and the associated microwave radio bursts are presented.

INTRODUCTION

Among the experiments carried by OSO–1 in the pointed section was a scintillation counter designed to detect hard solar X-ray bursts in the 20 to 100 Kev energy range. The scintillation counter consisted of a cylindrical NaI(Tl) crystal 0.3 cm high and 2.24 cm in diameter and an R.C.A. C-7151 photomultiplier tube. The photomultiplier tube and crystal assembly was placed in a cylindrical copper shield which through an opening in the front end provided a field of view of 0.3 steradian. The copper shield had a wall thickness of 1 cm. The 3.8 cm^2 area of the front surface of the crystal was held normal to the solar direction by the pointing of the satellite. An aluminum disc of 0.08 cm thickness was placed over the front surface of the crystal. The efficiency of the detector in the 20 to 100 Kev interval was approximately 0.90.

The electronics associated with the detector consisted of lower and upper level discriminator circuits and a logarithmic ratemeter. The lower and upper level discriminator circuits were set to select only those pulses from the photomultitube which correspond to an energy loss of between 20 and 100 Kev. in the crystal. The pulses accepted by the discriminator circuits where then passed on to the logarithmic ratemeter. The output of the ratemeter was a voltage level between zero and five volts which corresponded to an input count rate between 10 and 10^4 counts per second. The output of the ratemeter was able to respond to changes in count rate that occurred in a time longer than 10 milliseconds.

The satellite telemetry system sampled the voltage level at the output of the ratemeter continuously for two seconds once every twenty seconds. This sampling format was operative during the entire daylight part of an orbit.

DATA

With the return of the first hundred orbits of reduced data the response of the detector to the general spacecraft X-ray background and the response to the regions ot trapped radiation was determined. In addition it was found that the experiment responded to the electron warm spots detected by an electron-proton spectrometer placed aboard the spacecraft by Schrader et al[1]. When passing through regions not including trapped radiation or electron warm spots the detector was found to produce a count rate for a 2 second sample that consistently fell between limits of 10.5 to 14.5 counts per second.

Only 17 March 1962 a short lived increase in count rate occurred while the satellite was passing through a region where the count rate normally fell in the background range of 10.5 to 14.5 counts per second. The increase in count rate started at 19:39:49 U.T. and ended at 19:40:08 U.T. A record of the satellite telemetry signal for the orbit containing this time period indicated conclusively that the fluctuation in count rate was real and could not be attributed to telemetry noise that

*Published as *Goddard Space Flight Center Document X-610-64-60*, May 1964.

This paper is an abridged version of the paper published in the proceedings of the 5th International Space Science Symposium, Florence, Italy, 1964.

had been erroneously digitized by the automatic data reduction system. Reference to the available solar data revealed that a solar flare had been observed by the McMath-Hulbert and Lockheed Observatories between the times of 1934 to 1959 U.T. and 1936 to 2003 U.T. respectively. The flare was observed on the east limb of the sun and was classified by McMath-Hulbert as an importance 1 flare and by Lockheed as an importance 2 flare. Also at this time an impulsive radio burst of three minutes duration beginning at 19:39 U.T. and reaching maximum at 19:40:12 U.T. was observed at 2800 Mc/sec by Ottawa. Furthermore an SID accompanied the flare beginning at 19:40 U.T. and reaching maximum at 19:44 U.T. The very close correlation in the time of these events and the fluctuation of the 20 to 100 Kev count rate suggested that the most plausible explanation of the fluctuation was a burst of energetic X-rays produced by the flare.

During succeeding orbits of the spacecraft four more instances of rapid excursions in count rate were observed during the presence of a flare on the sun which produced an impulsive radio burst in the microwave range and an SID. These excursions in count rate were also interpreted as solar flare X-ray bursts. The history of these five events is presented graphically in Figures 1 through 5[2].

DISCUSSION

Prior to the launch of OSO-1 eight occurrences of high energy X-ray bursts accompanying solar

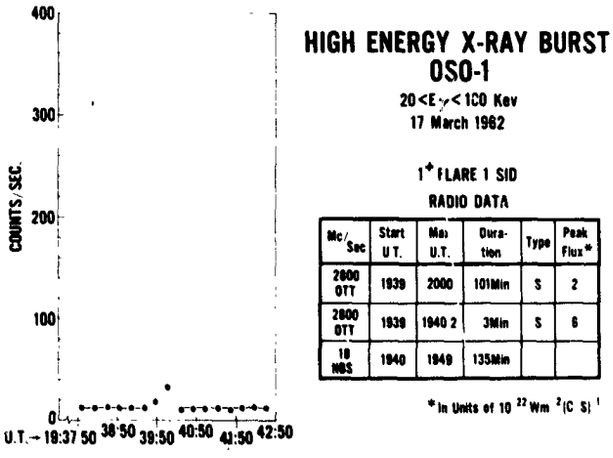

FIGURE 1.—High energy x-ray burst, OSO1; $20 < E_\gamma < 100$ kev, March 17, 1962.

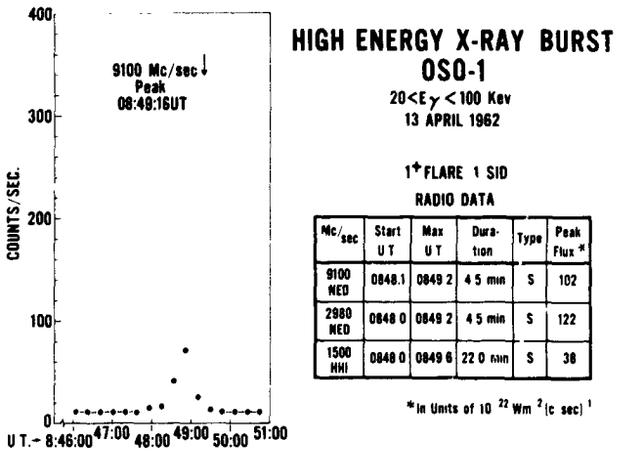

FIGURE 2.—High energy x-ray burst, OSO I; $20 < E_\gamma < 100$ kev, April 13, 1962.

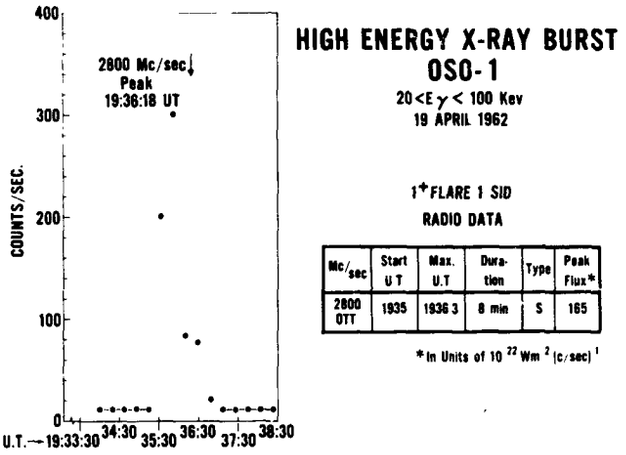

FIGURE 3.—High energy x-ray burst, OSO I; $20 < E_\gamma < 100$ kev, April 19, 1962.

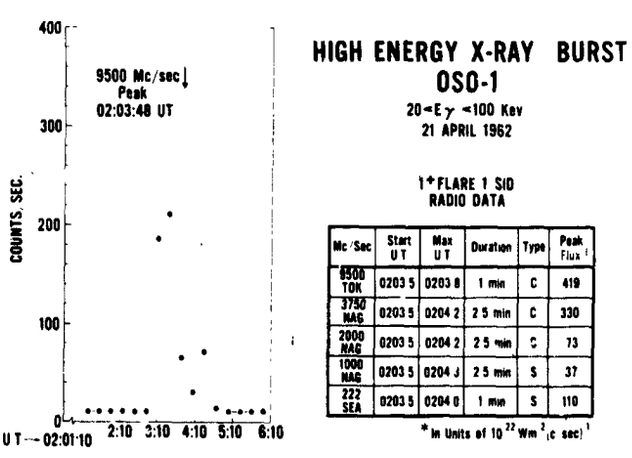

FIGURE 4.—High energy x-ray burst, OSO I; $20 < E_\gamma < 100$ kev, April 21, 1962.

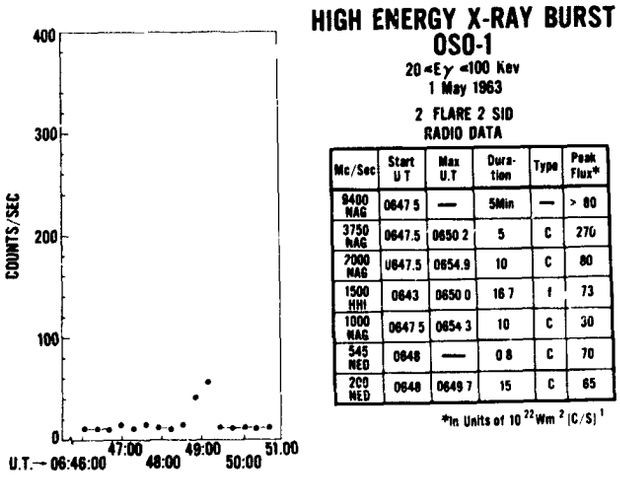

2 FLARE 2 SID
RADIO DATA

Mc/Sec	Start U T	Max U.T	Duration	Type	Peak Flux*
9400 NAG	0647 5	—	5Min	—	> 80
3750 NAG	0647.5	0650 2	5	C	270
2000 NAG	0647.5	0654.9	10	C	80
1500 HM	0643	0650 0	16 7	f	73
1000 NAG	0647 5	0654 3	10	C	30
545 NED	0648	—	0 8	C	70
200 NED	0648	0649 7	15	C	65

*In Units of 10^{22} Wm^{-2} (C/S)$^{-1}$

FIGURE 5.—High energy x-ray burst, OSO I; $20 < E_\gamma < 100$ kev, May 1, 1963.

flares had been observed[3–7]. Kundu has analyzed the radio data associated with each of these events[8]. He has found that an impulsive microwave burst was associated with every X-ray burst whereas type III bursts and other meter wave events did not show as strong a correlation. Furthermore the general character of the microwave spectrum was found to be such that the peak flux observed at wavelengths in the 3 to 10 cm range was stronger than that observed at wavelengths in the 10 to 20 cm range. The radio data associated with the OSO-1 X-ray bursts as indicated in Fig. 1 through 5 appears to lend strong support to Kundu's analysis. Additional information of interest to this analysis is the fact that as far as can be determined from spectral observations in the meter wave range no type III bursts occurred during the X-ray events.

REFERENCES

1. SCHRADER, C., KAIFER, R. C., WAGNER, J. A., ZINGER, J. H., and BLOOM, S., University of California, Lawrence Radiation Laboratory—"Proton, Electron Fluxes (75 Kev) from OSO"—Presented at AGU Spring Meeting, April 1963.
2. Flare, SID, and Radio Data taken from Quarterly Bulletin on Solar Activity No. 137, January/March 1962 and No. 138, April/June 1962.
3. PETERSON, L. E., and WINCKLER, J. R.—J. Geophys. Research, 64, 697, 1959.
4. CHUBB, T. A., FRIEDMAN, and KREPLIN, R. W.—International Space Science Symposium, Nice, p. 695, 1960.
5. WINCKLER, J. R., MAY, T. C. and MASLEY, A. J.—J. Geophys. Research, 66, 316, 1961.
6. VETTE, J. I. and CASAL, F. G.—Phys. Rev. Letters, 6, 334, 1961.
7. Anderson, K. A., and WINCKLER, J. R.—J. Geophys. Res. 67, 4103, 1962.
8. KUNDA, M. R.—Space Science Reviews 2 (1963) 438-469.

N64-27061

TEMPERATURE OF A GRAY BODY MOST CLOSELY FITTING THE SOLAR EXTRATERRESTRIAL SPECTRUM*

WILLIAM B. FUSSELL AND JOHN B. SCHUTT

A definition of "closeness" of fit of a gray body curve to the sun's extraterrestrial spectrum is presented. F. S. Johnson's data are used for the solar spectrum. For the wavelength interval 0.3 to 2.4 microns (pertinent to thermal design), the magnitude of C_1 calculated for use in Planck's black body formula is 8.6504×10^{-17} watt-cm² at a temperature of 5742 ± 0.5 °K.

INTRODUCTION

The problem of simulating the extraterrestrial solar illumination for testing the thermal design of satellites has recently become of wide interest. If the materials for the satellite surface have been selected, the problem reduces to one of matching the absorbed energy from the simulating source—for each material composing the surface—to the absorbed solar energy for that material. However, many materials have spectral absorptivity curves which vary slowly with wavelength between wavelength limits including most of the sun's energy. A solar simulator which matches the sun's spectrum fairly well on a finely resolved basis, and which matches the total energy exactly, will automatically match the solar absorptivities and the simulated absorptivities closely for these materials. To this end, the black body function was used in constructing a gray body curve for which a solar fit was obtained by parametrically varying the temperature.

METHOD

In establishing a closeness of fit criterion for approximating the sun's extraterrestrial spectrum by that of a black body, it seems pertinent at this point to recall the geometric interpretation of the quantities in the black body equation which can be treated as parameters. Consequently, any criterion which is established by means of parametric variations can only be defined as ultimate when it is the most valid one from geometric considerations.

From the black body definition

$$J_\lambda(T;\, C_1,\, C_2) = C_1\, J_\lambda(T;\, C_2) = \frac{C_1}{\lambda^5\, e^{C_2/\lambda T} - 1}, \qquad (1)$$

where λ is the wavelength in cm, T is the temperature in °K, and C_1 and C_2 are constants (or parameters). Any of the quantities T, C_1, and C_2 may be chosen as a parameter. First consider variations in C_1. It is clear that any change in the magnitude of C_1 shifts the spectral distribution up or down along the ordinate depending on the sign of the chosen change for C_1. Since the parameters C_2 and T are geometrically equivalent (in a reciprocal manner), only one of them need be considered; T was chosen because of its experimental accessibility. Variations in T affect the shape of the black body distribution and, of course, the wavelength at which the maximum spectral intensity occurs. Therefore, any criterion which is to be established for fitting the sun's extraterrestrial spectral distribution to Equation 1 can be determined by means of parametric variations in T and C_1, or a gray body fit.

The most straightforward approach is to find the temperature at which the black body maximum matches the sun's maximum, 0.475 micron. This temperature is readily found to be 6060°K. But this method gives a black body curve which contains a greater integrated energy than the sun's integrated spectral distribution, since by

*Published as *NASA Technical Note* D-1845, August 1964

definition the black body distribution gives an upper limit to the emissive ability of any body at a given temperature. Consequently, an upper bound on the required temperature has been established from this matching process. Next, an estimate of the lower bound can be found. To accomplish this, C_1 and T may be varied in an effort to minimize the residual

$$R = \int |J_\lambda(T;\ C_1,\ C_2) - H_\lambda| d\lambda \quad , \qquad (2)$$

where H_λ and the vertical lines represent the sun's spectral distribution and absolute magnitude, respectively. From Equation 2 the lower bound is found to be approximately 5738°K. It is apparent that Equation 2 alone cannot give the required closeness of fit to the desired accuracy because one criterion cannot be used to minimize a bivariant distribution. The final criterion, the one defined as geometrically ultimate and, consequently, most pertinent from the thermal design viewpoint, is the system:

$$R_{Min} = \text{Min} \int |J_\lambda(T;\ C_1,\ C_2) - H_\lambda| d\lambda \qquad (3)$$

and

$$\int J_\lambda(T;\ C_1,\ C_2) d\lambda = \int H_\lambda \, d\lambda \quad . \qquad (4)$$

The addition of Equation 4, to establish the most meaningful criterion, allows a temperature to be found by using matched areas as the basis. The absolute magnitude in Equation 3 is necessary in order to insure that the total deviation between the two curves is minimized. From Equation 1 it is clear that C_1 can be eliminated in Equation 3 by means of Equation 4, which gives a single relation for the determination of T. These equations give a temperature of 5742 ± 0.5°K and a value of 8.65040×10^{-17} watt-cm² for C_1 for the 0.3 to 2.4 micron (μ) region.

It remains to show that Equation 2 should give results identical to Equations 3 and 4, indicating therefore that 5742°K is the desired temperature. If the spectral region of interest is broken into intervals of $J_\lambda(T;\ C_1) > H_\lambda$ and $J_\lambda(T;\ C_1) < H_\lambda$, where the intervals of the first kind are designated by $\Delta_{1,1}$ and those of the second kind by $\Delta_{2,1}$, then Equations 2 and 3 may be rewritten:

$$\int_{\Delta_{1,1}} |J_\lambda(T;\ C_1) - H_\lambda| d\lambda + \int_{\Delta_{2,1}} |J_\lambda(T;\ C_1) - H_\lambda| d\lambda$$

$$= \int_{\Delta_{1,1}} C_1 \bar{J}_\lambda(T) d\lambda - \int_{\Delta_{1,1}} H_\lambda \, d\lambda - \int_{\Delta_{2,1}} C_1 \bar{J}_\lambda(T) d\lambda + \int_{\Delta_{2,1}} H_\lambda \, d\lambda \quad . \qquad (5)$$

where the first subscript of Δ refers to the interval type and the second is an index which enumerates subintervals. When the derivatives of the right-hand side of Equation 5 (ignore Equation 4) are taken with respect to C_1 and T in an effort to obtain simultaneous equations for C_1 and T, the following results are obtained:

$$\int_{\Delta_{1,1} \cdot \Delta_{2,1}} \bar{J}_\lambda(T) d\lambda = 0$$

and

$$C_1 \int_{\Delta_{1,1} \cdot \Delta_{2,1}} \frac{\partial}{\partial T} \bar{J}_\lambda(T) = 0 \quad .$$

Consequently, Equation 4 must be included in order to define C_1 and obtain the desired results. This implies the equivalence of Equation 2 and the system of Equations 3 and 4. By taking the derivative of the right-hand side of Equation 5 with respect to T and equating the result to zero in order to obtain a minimum (make use of Equation 4), Equation 5 may be rewritten:

$$\int_{\Delta_{1,1}} |J_\lambda(T;\ C_1) - H_\lambda| d\lambda + \int_{\Delta_{2,1}} |J_\lambda(T;\ C_1) - H_\lambda| d\lambda \leq \epsilon \quad . \qquad (6)$$

where ϵ is a number characterizing the fit of the black body curve to the sun's distribution and $\Delta_{1,i}$ and $\Delta_{2,i}$ become the sets $\{\Delta_{1,i}\}$ and $\{\Delta_{2,j}\}$, respectively, with $1 \leq i \leq N$ and $1 \leq j \leq M$. If the fit is exact, $\epsilon = 0$ and the equality sign holds; however, if the fit is not exact, the left-hand side of Equation 5 gives the best fit, which means that Equations 3 and 4 give the desired temperature.

RESULTS

The results given after each method of calculation described in the previous section are for the wavelength range of $0.3-2.4\ \mu$. Calculations were also made for the intervals $0.4-1.2$ and $0.220-7.0\mu$; the former region is of interest for purposes of solar cell illumination, and the latter is a complete cover of Johnson's data.* All results are given in Table 1. The auxiliary range of $0.3-2.0\mu$ is included for comparison purposes.

It is apparent that the best fit (2.97 percent) was obtained for the $0.4-1.2\mu$ region, which indicates that the adjusted black body curve conforms reasonably well to Johnson's data throughout the visible and into the near infrared. Less satisfactory agreement (6.08 percent) was obtained for the region of $0.3-2.0\mu$ because a single black body formula cannot be made to fit the steep rise in emissiveness characteristic of the sun's radiation in the region of $0.34-0.4\mu$. Agreement is enhanced, however, when the region is extended to 2.4μ because the additional $2.0-2.4\mu$ region, where the fit is good, makes the subvisible region ($0.34-0.4\mu$) of somewhat less weight. The fit for the complete range covered by Johnson's data, $0.220-7.0\mu$, is least satisfactory. The black body curve (with only two adjustable parameters) cannot be made to fit the steep rise in the $0.220-0.4\mu$ region as well as the tail of the sun's spectral distribution in the infrared.

Table 1

Results of Gray Body Fit to Solar Extraterrestrial Spectrum.

Range (microns)	T (°K)	C_1 (watt-cm^2)	$\int H_\lambda d\lambda$ (watt/cm^2)	$\int \lvert J_\lambda - H_\lambda \rvert d\lambda$ (watt/cm^2)	$\frac{\int \lvert J_\lambda - H_\lambda \rvert d\lambda}{\int H_\lambda d\lambda} \times 100$
0.4 - 1.2	6142 ± 0.5	6.76111×10^{-17}	9.86137×10^{-2}	2.92699×10^{-3}	2.97
0.3 - 2.0	5730 ± 0.5	8.72019×10^{-17}	1.29419×10^{-1}	7.86669×10^{-3}	6.08
0.3 - 2.4	5742 ± 0.5	8.65040×10^{-17}	1.32629×10^{-1}	7.88560×10^{-3}	5.94
0.220 - 7.0	5693 ± 0.5	8.80334×10^{-17}	1.39424×10^{-1}	1.03376×10^{-2}	7.41

In order to clarify the fit to the solar extraterrestrial spectrum by the above gray body matching technique, a gray body curve was calculated for the $0.3-2.4\mu$ region. The gray body curve of this region for a temperature of 5742°K is compared with the solar data in Figure 1. According to column 6 of Table 1 the areal mismatch of these curves is 5.94 percent when computed relative to the solar constant. It can be concluded that a gray body curve agrees well with the solar data

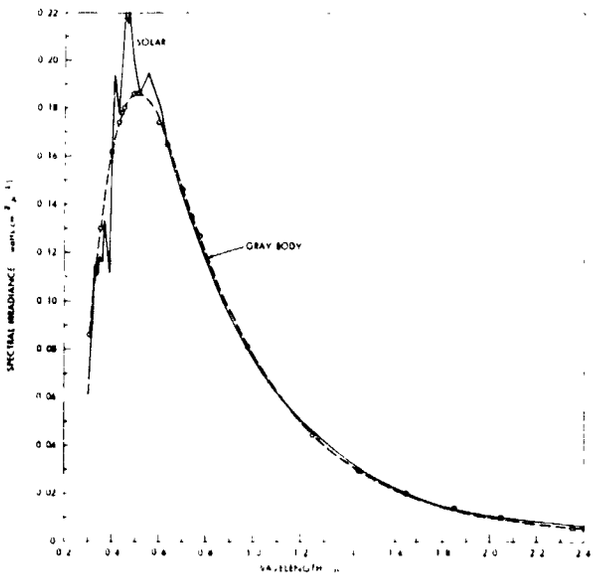

FIGURE 1.—Comparison of a 5742° K gray body curve with the solar extra terrestrial spectrum.

*Johnson, F. S., "The Solar Constant," *J. Meteorology* 11(6): 431–439, December 1954.

curve, except forthe irregular region of 0.41–0.55μ. What has happened is that virtually exact fits occurred at 0.43 and 0.52μ, and the intermediate irregularities could not be fit by a single gray body curve.

DISCUSSION

If the black body approximation to the solar spectrum is to be useful from the thermal design viewpoint, the average absorptance of a spacecraft coating material, as calculated from the black body spectrum, should be fairly close in value to the average solar absorptance of the material. Mathematically expressed, it is desirable that $\bar{a}_{BB} \approx \bar{a}_s$ where

$$\bar{a}_{BB} = \frac{\int_0^\infty a_\lambda J_\lambda(T)d\lambda}{\int_0^\infty J_\lambda(T)d\lambda} , \qquad (7)$$

and

$$\bar{a}_s = \frac{\int_0^\infty a_\lambda H_\lambda d\lambda}{\int_0^\infty H_\lambda d\lambda} , \qquad (8)$$

with

$\bar{a}_{BB}$ = the average absorptance for a black body,
$\bar{a}_s$ = the average solar absorptance,
H_λ = the solar spectral intensity per unit wavelength bandwidth, as given by Johnson,
$J_\lambda(T)$ = the Planck black body spectral intensity for absolute temperature T,
a_λ = the absorptance of the material at wavelength λ.

For simplicity, it is desirable to normalize H_λ and J_λ to H'_λ and J'_λ:

$$H'_\lambda = \frac{H_\lambda}{\int_0^\infty H_\lambda \, d\lambda} ,$$

$$J'_\lambda = \frac{J_\lambda}{\int_0^\infty J_\lambda \, d\lambda} .$$

Equations 7 and 8 now become

$$\bar{a}_{BB} = \int_0^\infty a_\lambda J'_\lambda(T)d\lambda , \qquad (9)$$

and

$$\bar{a}_s = \int_0^\infty a_\lambda H'_\lambda d\lambda . \qquad (10)$$

Arbitrarily, a 10 percent proportional difference in $\bar{a}_{BB}$ and $\bar{a}_s$ will be chosen as the criterion of usefulness; that is, if

$$\frac{|\bar{a}_{BB} - \bar{a}_s|}{\bar{a}_s} = E_p \leq 0.1 , \qquad (11)$$

the black body approximation will be considered useful. Equation 11 is actually

$$\frac{\left|\int_0^\infty \left[J'_\lambda(T)d\lambda - H'_\lambda\right] a_\lambda d\lambda\right|}{\int_0^\infty a_\lambda H'_\lambda \, d\lambda} \leq 0.1 . \qquad (12)$$

It can be seen that the results given in column 5, Table 1 for the quantity

$$\int |J'_\lambda(T) - H'_\lambda| d\lambda = \Delta_p \qquad (13)$$

do not indicate the magnitude of E_p (Equation 11). Consider now the following two cases:

1. If a_λ is approximately constant, then the proportional error E_p becomes

$$E_p = \frac{a_\lambda \left|\int_0^\infty \left[J'_\lambda(T) - H'_\lambda\right] d\lambda\right|}{a_\lambda \int_0^\infty H'_\lambda d\lambda} , \qquad (14)$$

and, since

$$\int_0^\infty J'_\lambda(T)d\lambda = \int_0^\infty H'_\lambda d\lambda = 1 , \qquad (15)$$

it is clear that

$$\int_0^\infty \left[J'_\lambda(T) - H'_\lambda\right] d\lambda = 0 \qquad (16)$$

and $E_p = 0$.

2. If a_λ can be represented by a power series in λ, that is,

$$a_\lambda = (a_\lambda)_0 + (\lambda - \lambda_0)\left(\frac{da_\lambda}{d\lambda}\right)_0 + \frac{(\lambda - \lambda_0)^2}{2!}\left(\frac{d^2 a_\lambda}{d\lambda^2}\right)_0 + \cdots , \tag{17}$$

then

$$E_p = \frac{\left| \int_0^\infty \left[J'_\lambda(T) - H_\lambda \right] \lambda \left(\frac{da_\lambda}{d\lambda}\right)_{0,1} d\lambda \right|}{\int_0^\infty H'_\lambda a_\lambda d\lambda} , \tag{18}$$

in which the error is now weighted by the slope.

See N64-33628

DISTRIBUTION IN HELIOGRAPHIC LONGITUDE OF FLARES WHICH PRODUCE ENERGETIC SOLAR PARTICLES*

DONALD E. GUSS

A number of evidences have been found in the past which point to the longitudinal persistence of solar phenomena. The life of active regions on the sun extends over several solar rotations and centers of sunspot formation exist which seem to outlive individual spot groups.[1,2] Also, there are 27-day recurrences of geomagnetic disturbances[3] and neutron-monitor counting-rate data,[4] which sometimes last for as long as 10 solar rotations. More recently Bryant *et al.*[5] and Simpson[6] have found 27-day recurrences in the enhancement of low-energy proton intensity in free space as measured on satellites. It is the purpose of this Letter to point out a similar longitudinal persistence in the occurrence of solar flares which result in solar particle events. In particular, flares from a single 10° interval in heliographic longitude caused most of the large solar particle events over the last solar cycle. This indicates the existence of a center for the formation of active regions which has persisted for more than 73 solar rotations.

Figure 1 shows the heliographic longitude for flares which produced solar-particle events between 16 January 1955 and 23 October 1962 during the last solar cycle. The list of 56 events used is from that compiled by Malitson[7] plus the 23 October 1962 event. The series of flares between 80° and 90° in Fig. 1 produced the largest particle events of the last solar cycle, the event of 23 February 1956, the multiple events of July 1959, the multiple events of November 1960, and the multiple events of July 1961. Using the integrated particle intensities calculated by Malitson and Webber,[8] these events contributed about 75 percent of the integrated particle intensity with energy greater than 30 MeV and about 90 percent of that with kinetic energy >100 MeV detected at the earth during the last solar cycle. In addition, of the ten solar particle events which produced neutron-monitor increases, indicating the presence of significant numbers of particles with kinetic energy greater than about 500 MeV, seven are in this narrow longitude region.

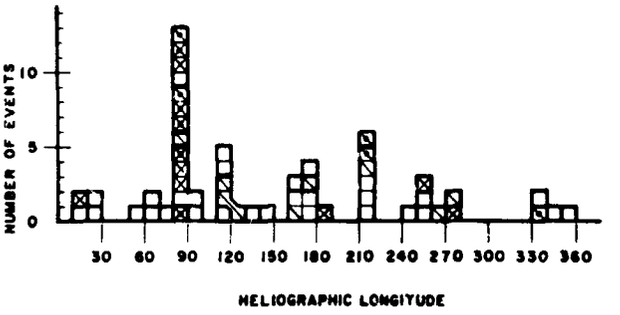

FIGURE 1.—Number of solar particles events vs heliographic longitude with the central meridian during the 23 February 1956 event set to 0°, and assuming a rotation period of 27.04 days. The particle intensity with kinetic energy >30 MeV detected at the earth[8] integrated over the particle event is ⊠, $I \geq 10^8$p/cm²; ⊡, $I \geq 5\times10^6$p/cm²; open squares, $I < 5\times10^6$p/cm². A dot in a square signifies that there was a neutron-monitor rate increase, indicating the presence of a significant number of particles with kinetic energy greater than about 500 MeV. Light lines are used to separate individual events and heavy lines to separate individual active regions.

Trotter and Roberts[9] have noted that the vicinity of the sun where the 23 February 1956 flare occurred had had a prior history of active regions lasting for several rotations, dying out, and returning in new bursts of activity. Hence, this center of activity existed prior to the 23 February 1956 event and persisted beyond the event of 20 July 1961, a period of more than 5.5 years. In his theory of the sun's field Babcock[10] proposes a mechanism to explain the longitudinal

*Published in *Physical Review Letters*, 13(12):363-364, September 21, 1964.

persistence whereby new active regions are likely to arise near old regions. However, it is not clear whether this mechanism is sufficient to explain an active site of such long duration.

The remainder of the events during the last solar cycle also fall into longitude bands, but not so sharply defined. The events between 240° and 280° with one exception occurred between 20 January 1957 and 23 March 1958, indicating the existence of an active site which lasted for more than a year. The events between 210° and 220° are those of March through September 1960, two of which caused ground-level neutron-monitor increases. The interval between 160° and 190° contains events which occurred between 9 August 1957 and 10 May 1959. The large event is that of 10 May 1959. The interval between 110° and 140° includes events from 6 June 1958 to 22 August 1958 and the two small events of 10 September and 28 September 1961.

Finally, there is a dearth of events in the longitude interval between 280° and 80°. Of the 26 larger particle events during the last solar cycle only two, the events of 31 August 1956 and 7 July 1958, resulted from flares in this 160° interval.

In conclusion, flares which produce energetic particles arise predominantly in narrow longitudinal regions which outlive visible active regions. This points to the existence of long-lived active centers beneath the photosphere which periodically manifest themselves on the surface as active regions which produce flares that accelerate solar particles. A single well-defined longitude region was responsible for the most intense particle events of the last solar cycle. The fact that this region can be compressed into a 10° band of longitude with a suitable choice of the period of solar rotation would indicate that this site rotated at constant rate as opposed to the variable rotation of the photosphere. The shorter lived regions, responsible for the smaller events, in general show a wider spread in longitude which could indicate a drift of the producing centers. A study of the meridional distribution of a larger body of data such as solar flares would perhaps result in a further definition of the active centers.

---

[1] K. O. KIEPENHEUER, *The Sun*, edited by G. P. Kuiper (University of Chicago Press, Chicago, Illinois, 1953), p. 338.

[2] H. M. LOSH, Publ. Obs. Univ. Mich. **7**, 127 (1938).

[3] J. BARTELS, Terrest. Magnetism Atmospheric Elec. **37**, 48 (1932).

[4] J. A. SIMPSON, W. FONGER, and L. WILCOX, Phys. Rev. **85**, 366 (1952).

[5] D. A. BRYANT, T. L. CLINE, U. D. DESAI, and F. B. MCDONALD, Phys. Rev. Letters **11**, 144 (1963).

[6] J. A. SIMPSON, IMP Symposium, Goddard Space Flight Center, Greenbelt, Maryland, March 1964 (unpublished).

[7] H. H. MALITSON, National Aeronautics and Space Administration Technical Report No. R-169, edited by F. B. McDonald, 1963, p. 109 (unpublished).

[8] H. H. MALITSON and W. R. WEBBER, National Aeronautics and Space Administration Technical Report No. R-169, edited by F. B. McDonald, 1963, pp. 12, 13 (unpublished).

[9] D. E. TROTTER and W. O. ROBERTS, Solar Activity Summary I, High Altitude Observatory (1956) p. 8.

[10] H. W. BABCOCK, Astrophys. J. **133**, 581 (1961).